# INFORMATION TO USERS

# THE ROLE OF HEAT SHOCK PROTEINS (Hsp70 AND Hsp27)

# IN PROTECTION AGAINST ISCHEMIC INJURY

# IN THE MYOCARDIUM AND CEREBRAL CORTEX.

by Jean-Christophe L. Plumier

Canada

# DALHOUSIE UNIVERSITY

# FACULTY OF GRADUATE STUDIES


The undersigned hereby certify that they have read and recommend to the Faculty of

Graduate Studies acceptance of a thesis entitled "The Role of Heat Shock Proteins (Hsp70

and Hsp27) in Protection against Ischemic Injury in the Myocardium and Cerebral Cortex"


by _____ Jean-Christophe Plumier _____


in partial fulfillment of the requirements for the degree of Doctor of Philosophy.


External Examiner

Research Supervisor

Examining Committee

ii
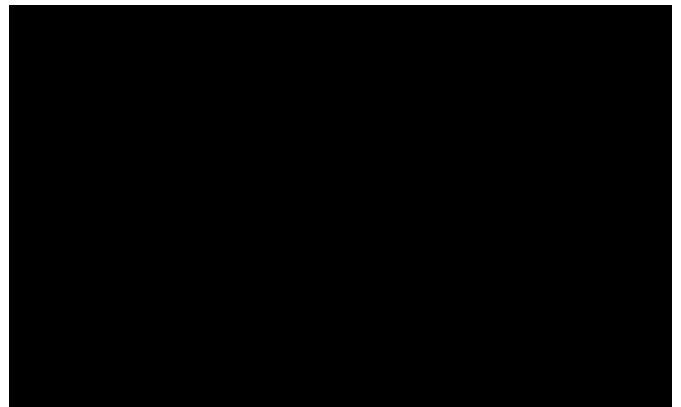
DALHOUSIE UNIVERSITY

DATE:  12 September 1996
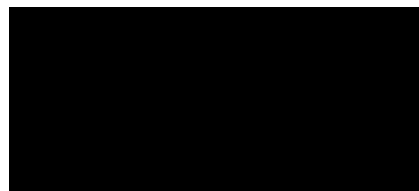
AUTHOR:     Jean-Christophe L. Plumier

TITLE:      The role of heat shock proteins (Hsp70 and Hsp27) in protection against

ischemic injury in the myocardium and cerebral cortex.

DEPARTMENT OR SCHOOL:      Department of Anatomy and Neurobiology

DEGREE:  Doctor of Philosophy      CONVOCATION:  November 25      YEAR: 1996

Permission is herewith granted to Dalhousie University to circulate and have to

copied for non-commercial purposes, at its discretion, the above title upon request of

individuals or institutions.



Signature of Author

The author reserves other publication rights, and neither the thesis nor extensive

extracts from it may be printed or otherwise reproduced without the author's written

permission.

The author attests that permission has been obtained for the use of any copyrighted

material appearing in this thesis (other than brief excerpts requiring only proper

acknowledgement in scholarly writing), and that all such use is clearly acknowledged.

Cette thèse n'aurait jamais pu être réalisée sans les nombreux sacrifices et l'aide d'Emmanuelle. Tout au long de mon travail, Emmanuelle m'a écouté, encouragé dans les moments de doutes et soutenu dans les épreuves. Emmanuelle parvient aussi à maintenir une excellent qualité de vie familiale grâce à son attention et son amour de chaque instant. Je dédie donc ma thèse a ma petite femme adorée, Emmanuelle, et au tout nouveau membre de ma famille, ma mignonne petite fille, Charline, qui m'apportent tant de joie chaque jour.

# TABLE OF CONTENTS

# LIST OF FIGURES AND TABLES

**List of figures**

## List of tables

# ABSTRACT

Ischemic injury induces expression of heat shock proteins (Hsp70 and Hsp27). After ischemia and reperfusion, mRNA for *Hsp70* progressively accumulated in the ischemic area of isolated and perfused hearts but not in the necrotic area of the ischemic zone, suggesting that Hsp70 expression in the area at risk may play a role in myocardial recovery after ischemia. The protective role of Hsp70 was examined in transgenic mice over-expressing the human Hsp70. After ischemia, upon reperfusion, transgenic hearts compared to non-transgenic hearts had significantly improved recovery of contractile force and showed less cellular injury. These results demonstrate that constitutive expression of the human Hsp70 protects the mouse myocardium from ischemic injury. In the brain, no significant difference in infarct areas was observed between transgenic and non-transgenic mice following 24 hour-occlusion of the middle cerebral artery. However, non-transgenic mice showed ipsilateral hippocampal injury while no injury was detected in the hippocampus of transgenic mice. This suggests that Hsp70 did not protect against severe ischemic injury induced in the cerebral cortex but protected hippocampal neurons from injury.

While Hsp27 was constitutively expressed in select populations of brain stem and spinal cord neurons of the adult rat, Hsp27 was not present in the cerebral cortex. However, focal cortical ischemia induced Hsp27 in most astrocytes of the ipsilateral cerebral cortex. Different distributions of Hsp27 and Hsp70 suggested that Hsp70 was expressed in the penumbra and that ischemic injury induced changes in gene expression that vary according to cell type and brain region. Cortical spreading depression triggered by cortical application of potassium chloride induced Hsp27 in GFAP-positive astrocytes of the ipsilateral cortex. Blockade of spreading depression by systemic administration of MK-801 significantly reduced Hsp27 expression in the parietal cortex. These results suggest that spreading depression can trigger Hsp27 astrocytic expression. It may be that Hsp27 plays a role in spreading depression-induced ischemic tolerance in neurons through protection of astrocyte functions.

# LIST OF ABBREVIATIONS AND SYMBOLS

°C          Celsius degree

µg          microgram

µl          microliter

µm          micrometer

Amb         nucleus ambiguus

AP          area postrema

BiP         Binding-immunoglobulin protein

c           compact formation of the nucleus ambiguus

CA1         (cornu ammonis) hippocampal pyramidal cell layer sector 1

CA1/2       (cornu ammonis) hippocampal pyramidal cell layer, sectors 1 and 2

CA3         (cornu ammonis) hippocampal pyramidal cell layer, sector 3

cen         central subnucleus of the nucleus of the tractus solitarius

Ci          Curie

com         commissural subnucleus of the nucleus of the tractus solitarius

cpm         counts per minute

CU          cuneate nucleus

Dm-Hsp22    Drosophila 22-kDa heat shock protein

Dm-Hsp23    Drosophila 23-kDa heat shock protein

Dm-Hsp26    Drosophila 26-kDa heat shock protein

| | |
|---|---|
| Dm-Hsp27 | Drosophila 27-kDa heat shock protein |
| DMV | dorsal motor nucleus of the vagus nerve |
| f | fornix/fimbria |
| g. gVII | genu of the facial nerve |
| GFAP | glial fibrillary acidic protein |
| GR | gracile nucleus |
| Hg | mercury |
| Hsc70 | the constitutive 70-kDa heat shock protein |
| HSF | heat shock transcription factor |
| Hsp | heat shock protein |
| Hsp25 | the murine 25-kDa heat shock protein |
| Hsp27 | the 27-kDa heat shock protein |
| Hsp70 | the inducible 70-kDa heat shock protein |
| IgG | immunoglobulin G |
| ip | intraperitoneally |
| is | interstitial subnucleus of the tractus solitarius |
| KCl | potassium chloride |
| kDa | kiloDalton |
| kg | kilogram |
| l | loose formation of the nucleus ambiguus |
| M | molar |

| | |
|---|---|
| mA | milliampere |
| mCi | milliCurie |
| MeV | mesencephalic nucleus of the trigeminal nerve |
| mg | milligram |
| ml | milliliter |
| mlf | medial longitudinal fasciculus |
| mm | millimeter |
| mM | millimolar |
| MoV | trigeminal motor nucleus |
| Mtp70 | the mitochondrial 70-kDa heat shock protein |
| n | number of animals |
| N | Newton |
| NMDA | N-methyl-D-aspartate |
| PBS | 100 mM phosphate-buffered saline |
| Pi | orthophosphate (inorganic) |
| PrV | principal sensory nucleus of the trigeminal nerve |
| sc | semicompact formation of the nucleus ambiguus |
| SD | standard deviation |
| SDS | sodium dodecyl sulfate |
| SDS-PAGE | sodium dodecyl sulfate polyacrylamide gel electrophoresis |
| SEM | standard error on the mean |

| | |
|---|---|
| SG | substantia gelatinosa |
| SpV | spinal trigeminal nucleus |
| spV | spinal trigeminal tract |
| SpVc | spinal trigeminal nucleus part caudalis |
| SpVo | spinal trigeminal nucleus, pars oralis |
| ts | tractus solitarius |
| VC | vestibular complex |
| III | third ventricle |
| VI | abducens nucleus |
| VII | facial nucleus |
| VIIn | facial nerve root |
| XII | hypoglossal nucleus |
| XIIn | hypoglossal nerve root |

# ACKNOWLEDGEMENTS

# CHAPTER 1:

# INTRODUCTION

## Overview

All living organisms respond to stresses due to changes in the environmental conditions by synthesizing new proteins called Heat Shock Proteins (Hsps). The role of these proteins during stress is still obscure although recent evidences suggest that most Hsps can act as molecular chaperones and regulate protein folding and translocation (Pelham, 1986, 1990; Hartl, 1996). Interestingly, expression of several Hsps have been shown to protect *in vitro* against cell death induced by various means such as heat shock, oxidative injury, or cytokines (Landry et al., 1989; Angelidis et al., 1991; Li et al., 1991; Williams et al., 1993; Mestril et al., 1994; Mehlen et al., 1995, 1996a, 1996b). It was further suggested that these Hsps could also be protective *in vivo* in pathological conditions such as ischemia (Currie et al., 1988). In this context, my work examines the expression of two major Hsps (Hsp70 and Hsp27) after ischemia and their relationship with cellular protection against ischemic injury.

## Heat shock proteins

The name of "Heat Shock" proteins comes from their initial discovery following heat shock treatment. Ritossa (1962) observed that a brief exposure of *Drosophila* larvae raised normally at 25°C to the elevated temperature of 30-32°C induced changes in the salivary gland chromosomes with the appearance of new chromosomal puffs. This observation was not restricted to the salivary glands but occurred in other tissues of the *Drosophila* larvae. Additional experiments demonstrated that the new puffs corresponded

to new RNA transcription sites. The discovery of the first "heat shock proteins" *per se* came with the work of Tissières et al. (1974). Seven new proteins were detected in the salivary glands of *Drosophila* larvae following heat shock treatment, while seven new puffs were observed on the chromosomes. Examination of other tissues confirmed the generality of the phenomenon. Similar results were reported for other organisms, from prokaryotes and yeast to mammals including man (see Heat shock: From bacteria to man, Schlesinger et al. (eds) 1982). Since then, more proteins have been discovered and classified in several Hsp families according to their molecular weight (see Table 1.1): the 110-kDa Hsp family, the 90-kDa Hsp family, the 70-kDa Hsp family, the 60-kDa Hsp family, the 27-kDa Hsp family, and ubiquitin (Lindquist, 1986; Welch, 1990, 1992).

**The 70-kDa family of heat shock proteins**

In mammals, the 70-kDa family of Hsps consists of at least four members of specific molecular weight and subcellular location (Table 1.1). These proteins include Hsp70, Hsc70, BiP (immunoglobulin-binding protein) and Mtp70 (the 70-kDa mitochondrial protein). Among these heat shock proteins, Hsp70 is highly inducible by heat shock as well as other stresses, has a molecular weight of 71 kDa in rats and 72 kDa in humans, and has been referred to as P71, SP71 and Hsp71 in rats and Hsp72 in humans. Hsc70 is a constitutive protein, has an apparent molecular weight of 73 kDa and has been referred to as P73 and Hsp73 in rats and Hsp73 and Hsc73 in humans.

Table 1. Classification of the heat shock proteins (modified from Welch, 1990;

Morimoto et al., 1994).

| heat shock protein | intracellular localization | functions |
| --- | --- | --- |
| Hsp110 | nucleolus | -help the recovery of nucleolar transcription after stress. |
| Hsp90 | cytoplasm and nucleus | - regulate glucocorticoid receptor function; <br> - escort polypeptides to their cellular compartment. |
| Hsc70 (constitutive Hsp70; human Hsp73) | cytoplasm, nucleus and nucleolus | - uncoating and/or reformation of clathrin-coated vesicles; <br> - translocation of proteins across intracellular membranes. |
| Hsp70 (inducible Hsp70; human Hsp72; rat Hsp71, SP71, P71) | cytoplasm, nucleus and nucleolus | - similar to HSC70; <br> - maintain the solubility of cytosolic and nuclear proteins; <br> - facilitate the removal or refolding of denatured proteins |
| BiP Grp78 | endoplasmic reticulum | -facilitate the assembly of monomeric proteins into larger complexes |
| Grp75 Mtp70 | mitochondrial matrix | -similar to BiP in the mitochondria: facilitate the proper assembly of monomeric proteins into larger macromolecules |
| Hsp60 | mitochondria | - maintain polypeptides in unfolded state to facilitate their translocation <br> - accelerate proper folding and assembly |
| Hsp32 (heme oxygenase-1) | cytoplasm | -facilitate the turnover of heme-containing protein |
| Hsp27 murine Hsp25 | cytoplasm and nucleus | - help refolding of denatured protein <br> - regulation of actin dynamics |
| ubiquitin | cytoplasm | -tag unfolded polypeptides destined to be destroyed |

The immunoglobulin-binding protein, BiP, has an apparent molecular weight of 78 kDa

and has also been referred to as the 78-kDa glucose-regulated protein (Grp78). Mtp70 is

a mitochondrial Hsp and is also a glucose-regulated protein with an apparent molecular

weight of 75 kDa. These Hsps can be found in most compartments of the eukaryotic cell

including cytoplasm (Hsp70 and Hsc70), nuclei (Hsp70 and Hsc70), endoplasmic

reticulum (BiP) and mitochondria (Mtp70). More than 50% identity of amino acid

sequence exists between the 70-kDa family of Hsps (Boorstein et al., 1994; Craig et al.;

1994; McKay et al., 1994). An ATP binding activity has been identified in the N-

terminal two thirds and a protein binding domain has been found in the C-terminal portion

of these Hsps (Chappell et al. 1987; DeLuca-Flaherty et al., 1990). The presence of such

highly conserved domains among the 70-kDa family of Hsps suggested the idea of

similarities in the biochemical functions.

*Molecular chaperones*

The first evidence that protein folding *in vivo* was not spontaneous and that

protein folding required the assistance of specific cellular proteins came from the

observation that mutations in GroEL, mitochondrial Hsp60 homologue, prevented the

assembly of bacteriophage particles (Coppo et al., 1973; Georgopoulos et al., 1973).

These proteins involved in folding of other proteins become known as molecular

chaperones. Evidence that members of the 70-kDa family of Hsps might participate in

protein folding came from the study of protein translation in the endoplasmic reticulum.

Haas and Wabl (1983) identified in the endoplasmic reticulum, BiP, a homologue Hsp70

that formed complexes with unassembled immunoglobulin heavy chains. Hsc70, another

homologue of Hsp70, was also found to interact with newly synthesized proteins. Hsc70

was found to bind nascent or precursor polypeptides in a ATP-dependent manner, to

stabilize them and to facilitate translocation (Chirico et al., 1988; Deshaies et al., 1988;

Zimmermann et al., 1988; Beckmann et al., 1990; Flynn et al., 1991). In the

mitochondrial matrix, Mtp70, another member of the 70-kDa family of Hsps, binds to

protein passing through the mitochondrial membrane into the matrix, helping in the

translocation process (Becker and Craig, 1994; Ryan and Jensen, 1995; Brodsky, 1996).

Interestingly the yeast Hsc70 was not capable of replacing the function of the endoplasmic

BiP (Brodsky et al., 1993; Brodsky, 1996). This result suggested that each member of

the 70-kDa family of Hsps has specific chaperoning functions and is probably needed for

the normal functioning of the cell.

The highly inducible member of the 70-kDa family of Hsps, Hsp70, shares more

than 90% sequence identity with Hsc70. Hsp70 is thought to have the same functional

properties as Hsc70, mainly binding to proteins that are unfolded or denatured by stress

and facilitating protein translocation into cellular organelles (mitochondria, nucleus and

lysosomes) (reviewed by Schatz and Dobberstein, 1996). Cytosolic Hsp70s seem to

recognize compartment-specific sequences of proteins and present these sequences to the

appropriate receptors (Chiang et al., 1989; Dingwall and Laskey, 1992; Becker and

Craig, 1994; Schatz and Dobberstein, 1996).

Recently, Hartl (1996) proposed that: "Molecular chaperones are [...] proteins

that mediate the correct assembly of other proteins, but are not themselves components of

the final functional structures. [...] Molecular chaperones do not contain steric

information specifying the correct folding: instead, they prevent incorrect interactions

within and between non-native polypeptides."

The mechanism of protein folding is probably best described for the bacterial

Hsp70 homologue (DnaK) (reviewed by Hartl, 1996) (Figure 1.1). The bacterial Hsp40

homologue (DnaJ) binds to an unfolded polypeptide and presents it to Hsp70. Hsp70 in

association with ATP binds to the polypeptide. Hsp40-Hsp70 interaction induces the

hydrolysis of ATP by Hsp70 and the formation of a stable complex between Hsp70-ADP,

Hsp40 and the polypeptide. Then ADP is released from Hsp70 by the nucleotide-

exchange factor (GrpE), destabilizing the complex Hsp70-Hsp40. Hsp40 dissociates from

Hsp70 and the polypeptide is released from Hsp70. Hsp70 binds to ATP and re-enters

the cycle while the released polypeptide may be transferred into the proper folding cycle

involving in the mitochondrion, Hsp60 and Hsp10 homologues (GroEL and GroES,

respectively) or in the cytoplasm, the chaperonin containing t-complex polypeptide (CCT

also known as TriC, TCP(tail complex protein)-1 ring complex).

Although some steps in the chaperonin cycle remain uncertain, the current view,

based on bacterial Hsp60-Hsp10 (GroEL-GroES) interaction, is well accepted (Becker

and Craig, 1994; Hartl, 1996) (Figure 1.1). These chaperonins are made of two rings

containing seven Hsp60 molecules. In the central cavity of the cylinder is the binding site

for the unfolded polypeptide when one ring is interacting with Hsp10. Polypeptide and ATP binding to the ring and ATP hydrolysis promote the release of ADP and Hsp10 from the second ring. Hsp10 and ATP bind a ring and enclose the polypeptide that starts folding in the Hsp60-Hsp10 cylinder cavity. ATP hydrolysis in the Hsp10-bound ring tightens the interactions. ATP binding and hydrolysis of the opposite ring promote the opening of the complex and the release of the folded polypeptide (Figure 1.1).

In summary, it is apparent that protein folding involves cooperation of several Hsps. Members of the 70-kDa family of Hsps interact with Hsp40 and probably other co-chaperones (Höhfeld et al., 1995) to maintain unfolded polypeptides in a soluble conformation that can be transferred to chaperonins for folding into the native state. Several Hsps from other Hsp families have also been reported to share molecular chaperone functions. Hsp90 and small Hsps (Hsp27 and αB-crystallin) have been shown to bind to denatured proteins and assist in the protein folding process *in vitro* (Horwitz, 1992; Jakob et al., 1993; Jakob and Buchner, 1994).

Figure 1.1 Participation of heat shock proteins in protein folding (modified from Hartl,

1996).
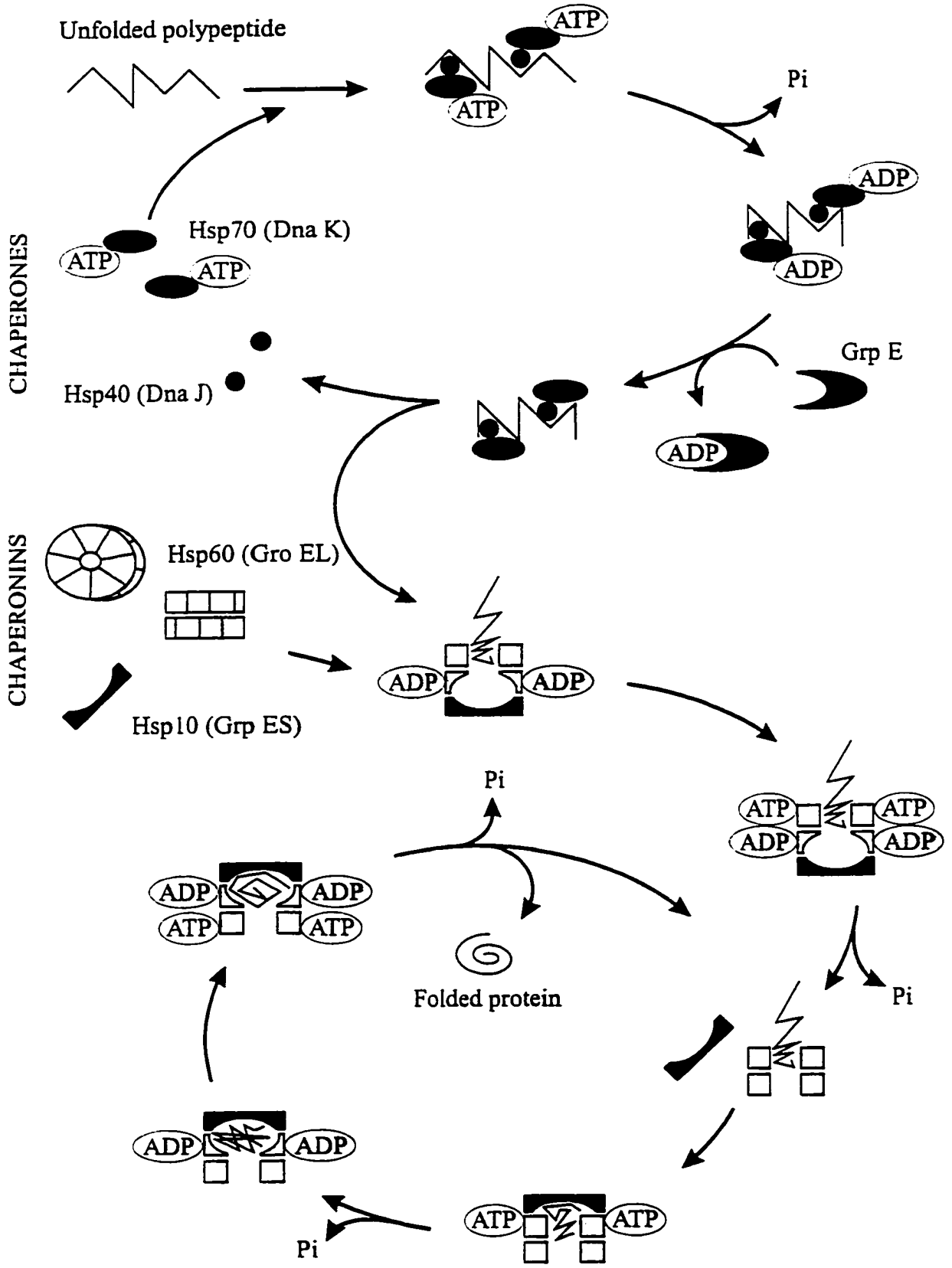
Figure 1.1

Figure 1.2  Overview of the functions and the induction of Hsp70 (modified from

Hightower and Li, 1994; Morimoto et al., 1994).
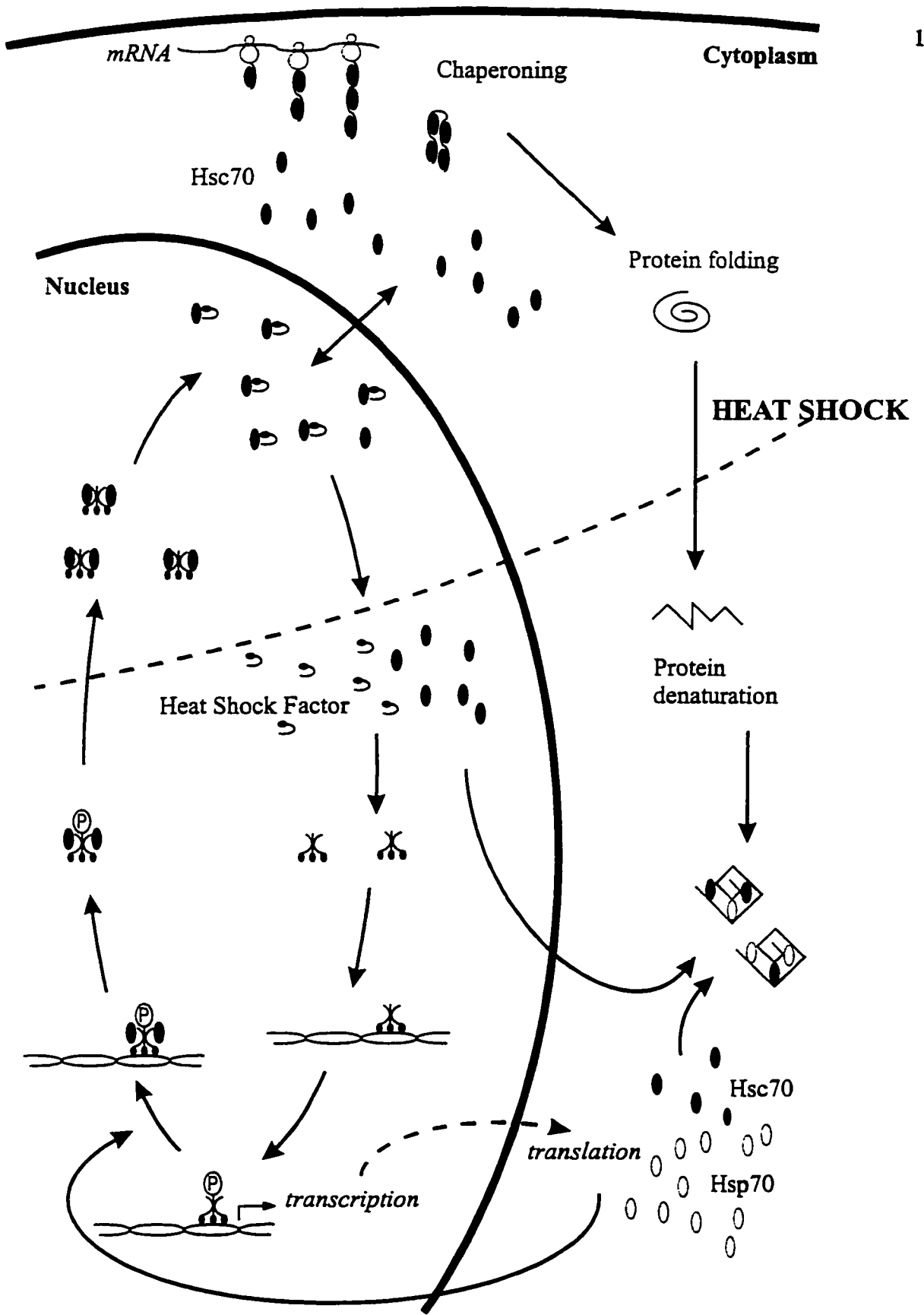
**Figure 1.2**

*Transcription of Hsp70*

Hightower (1980) observed that heat shock or amino acid analogue treatment

induced accumulation of denatured proteins and protein aggregation and that both

treatments induced the synthesis of Hsps. He suggested that intracellular accumulation of

abnormally folded protein induced by heat shock or other stresses could be the

intracellular mechanism that triggers synthesis of Hsps. This hypothesis has been tested

by examining the mechanisms of induction of Hsp70 expression (Morimoto et al., 1992;

Morimoto 1993; Hightower and Li, 1994; Morimoto et al., 1994) (Figure 1.2).

Transcription of *Hsp70*, *Hsc70* and probably other *Hsps* is regulated by a specific heat

shock transcription factor (HSF) that binds a specific DNA sequence (inverted repeats of

the pentameric sequence 5'-nGAAn-3') in the promoter region of the *Hsp70* gene. *Hsp70*

may regulate its own expression via a negative feedback loop (DiDomenico et al., 1982).

In normal conditions, Hsc70 forms complexes with HSF, preventing the interaction of the

transcription factor with DNA. Under stress, Hsc70 releases HSF and binds to denatured

proteins. Free HSFs form trimeric complexes that possess DNA-binding properties

(Morimoto, 1993) and migrate into the nucleus. Two trimers bind to the promoter region

of *Hsc70* and *Hsp70* and after phosphorylation, activate their transcription (Morimoto et

al., 1994). *De novo* synthesis of Hsc70 and Hsp70 increases the concentration of free

Hsc70 and Hsp70 that bind again to HSF, ending the transcription of *Hsc70* and *Hsp70*

(Morimoto et al., 1992).

Similarly to Hsps, homology of sequences has been observed among HSFs from different organisms (Wu et al, 1994). HSFs from different organisms show two highly conserved domains (Morimoto et al., 1994): one hundred amino acids at the amino-terminal, containing the DNA binding domain and a motif of hydrophobic heptad repeats that is involved in the oligomerization. This observation suggests that similar mechanisms might regulate *Hsp70* transcription in different organisms. Interestingly, there are at least two different HSFs (called HSF1 and HSF2) within a given cell type (Sarge et al., 1991; Schuetz et al., 1991). HSF1 regulates transcription of *Hsp70* in response to heat shock, heavy metals and amino acid analogues while HSF2 is not activated following these stressors (Morimoto et al., 1994). HSF2 seems to be activated by non-stressful conditions such as cell differentiation or development (Mezger et al., 1989; Morimoto et al., 1992; Sistonen et al., 1992; Morimoto et al., 1994; Sarge et al., 1994). Recently, a third HSF, HSF3, was described in chicken embryos (Nakai and Morimoto, 1993). Although HSF3 bears identical sequences of amino acids with HSF1 and HSF2, HSF3 shows different induction properties. In addition to differences in the mechanisms of activation of HSF1 and HSF2, HSF1 and HSF2 do not drive *Hsp70* transcription with the same intensity. HSF1 appears to be a stronger activator of *Hsp70* transcription (Sistonen et al., 1992). Interestingly, HSF1 and HSF2 can act synergistically and increase the transcription of *Hsp70* obtained by either HSF action alone (Sistonen et al., 1994). Therefore, the presence of multiple transcription factors regulating *Hsp70* expression may represent a complex mechanism of regulation, involving

homo- and hetero-dimers as described for other transcription factor families, i.e., fos/jun

family (Morimoto et al., 1992).

*Ischemic induction of Hsp70*

In addition to heat shock, anoxia, oxidative stress and other changes in cell

homeostasis can induce Hsp70 expression. *In vivo*, ischemia causes hypoxia or anoxia,

oxidative stress and other metabolic stresses. In hearts, a short period of ischemia was

sufficient to induce Hsp70 expression (Currie and White, 1981). Occlusion of the left

descending coronary artery in dog or rabbit activated the expression of *Hsp70* gene as

revealed by analyses of *Hsp70* mRNA (Northern analysis) and Hsp70 protein (Western

analysis) (Dillmann et al., 1986; Mehta et al., 1988). Semi-quantitative Northern analysis

demonstrated that 5 minute-ischemia increased *Hsp70* mRNA levels by two fold

(Knowlton et al., 1991). Changes in the amount of Hsp70 were detected two hours after

the ischemic insult. In rat hearts, similar results were obtained *in vitro* (Currie, 1987,

1988) and *in vivo* (Currie et al., 1987; Das et al., 1993). These experiments

demonstrated that Hsp70 expression was rapid and could be triggered by brief ischemic

episodes. Similar Hsp70 activation occurred after cerebral ischemia. Cerebral ischemia

induced increased amounts of Hsp70 in rat brain (Currie and White, 1981; Dienel et al.,

1986; Nowak, 1985). *In situ* hybridization studies further characterized the Hsp70

induction in ischemic brains. In global ischemia, *Hsp70* mRNA accumulation occurred in

the hippocampus. Three hours after 5 minute-occlusion of both carotid arteries, *Hsp70*

mRNA was observed in the dentate granule neurons and in the pyramidal neurons of

gerbils (Nowak, 1990, 1991). Only CA1 hippocampal neurons showed *Hsp70* mRNA

accumulation at 48 hours (Nowak, 1991). This neuronal population is the most

susceptible to ischemia-induced cell death. Therefore, Hsp70 expression has been

suggested to be a useful marker for neuronal injury after ischemia (Nowak, 1990, 1991).

Immunohistological studies demonstrated that Hsp70 immunoreactivity could be detected

in dentate granule cells and in CA3 hippocampal neurons but not in CA1 hippocampal

neurons that will eventually die (Vass et al., 1988; Gonzalez et al., 1991). Similar results

have been reported in transient global cerebral ischemia in the rat. After 20 minutes of

ischemia, no Hsp70 immunoreactivity was observed in CA1 hippocampal cells (Simon et

al., 1991). However, when ischemia was brief and no CA1 neuronal death was detected,

Hsp70 immunoreactivity was observed in CA1 neurons (Simon et al., 1991). Therefore,

it was suggested that neurons that are destined to survive express Hsp70 (Tomoika et al.,

1993). Interestingly, in focal ischemia, infarcted areas showed Hsp70 immunoreactivity

in neurons, endothelial cells and glial cells (Gonzalez et al., 1989; Sharp et al., 1991b;

Kinouchi et al., 1993). However, in the penumbra, area that surrounds the necrotic area

and undergoes a delayed cell death after focal ischemia, only neurons were

immunoreactive for Hsp70 (Gonzalez et al., 1989; Kinouchi et al., 1993).

*Protective role of Hsp70*

Hsp70 has been reported to play a role in protection against cell injury (Welch and

Feramisco, 1984; Sanchez et al., 1993). Intracellular injection of antibodies against

Hsp70 increased the susceptibility of fibroblasts to heat shock-induced cell death

(Riabowol et al., 1988). In addition, *Hsp70* transfection protected cultured cells against thermal stress (Angelidis et al., 1991; Li et al., 1991; Heads et al., 1994). Moreover, in *in vitro* conditions mimicking ischemia, increase in cell survival has been reported in *Hsp70*-transfected myogenic cells (Mestril et al., 1994).

While the protective role of Hsp70 seems well established in *in vitro* studies, evidence of Hsp70 protection against ischemic injury *in vivo* is circumstantial. Heat shock pre-treatment enhanced post-ischemic myocardial contractile recovery of isolated and perfused hearts (Currie et al., 1988; Yellon et al., 1992). Although heat shock treatment (42°C for 15 minutes) could not reduce the infarct size induced by 45 minutes of coronary occlusion (Yellon et al., 1992), the same treatment did decrease the infarct size following 30 minutes of ischemia (Currie et al., 1993), suggesting that heat shock only delayed the onset of irreversible ischemic injury. Heat shock also reduced arrhythmia due to reperfusion injury in the rat (Steare and Yellon, 1993). All these effects have been suggested to be related to the synthesis of heat shock proteins, and especially Hsp70. Following this idea, Marber et al. (1993) compared myocardial resistance to ischemic infarction in rabbits pre-treated by hyperthermia or by short periods of ischemia. Since a similar protection was observed following both treatments and that both treatments induced Hsp70 expression, they concluded that the increase in heat shock protein, rather than non-specific effects of thermal or ischemic pre-treatment, seemed responsible for the induction of ischemic tolerance. In further studies, Marber et al. (1994) demonstrated that heat shock-induced protection was related to the amount of

Hsp70 but not Hsp60. Similarly, Hutter et al. (1994) examined the infarct size after 35 minutes of left coronary artery occlusion in rats pre-treated with different degrees of hyperthermia. Reduction of the infarct size was observed in 42°C pre-treated rats and to a lesser extent, in 41°C pre-treated rats. However, no difference was detected between control and 40°C pre-treated rats. Since the amount of Hsp70 was proportional to the intensity of the hyperthermic treatment, a direct correlation was suggested between myocardial Hsp70 amount and degree of protection (Hutter et al., 1994).

Hyperthermia has also been reported to protect against cerebral ischemia. In rats or gerbils pre-treated by heat shock, a reduction in the number of injured cells has been shown after global ischemia (Chopp et al., 1989; Kitagawa et al., 1991b). Additional evidence arose from the study of the so-called "ischemic tolerance". A mild ischemic insult could reduce the extent of damage of a subsequent severe ischemic episode in gerbils (Kitagawa et al., 1990) and in rats (Liu et al., 1992). Further studies reported that Hsp70 synthesis after ischemic pre-treatment correlated to the amount of protection conferred against subsequent ischemic injury (Kitagawa et al., 1991b; Nishi et al., 1993). In addition, pre-treatment with Hsp70 antibody inhibited the acquisition of ischemic tolerance in gerbils (Nakata et al., 1993). Therefore, it has been suggested that Hsp70 could play a role in protecting neurons against ischemic damage (Nakata et al., 1993).

## The 27-kDa heat shock protein

The 27-kDa heat shock protein (Hsp27; also known as the mouse Hsp25), αA-
and αB-crystallins share highly conserved sequences and have been grouped in the
mammalian small heat shock protein family (Wistow, 1985; de Jong et al., 1993;
Arrigo and Landry, 1994). In addition, Hsp27 and αB-crystallin share other features
such induction by heat shock, phosphorylation sites, translocation during stress (Arrigo et
al., 1988; Klemenz et al., 1991; Voorter et al., 1992; Arrigo and Landry, 1994).
During heat shock, both Hsp27 and αB-crystallin migrate into the nucleus and slowly
return in the cytoplasm during recovery (Arrigo et al., 1988; Voorter et al., 1992).
Moreover, Hsp27 and αB-crystallin form complexes that dissociate during heat shock and
progressively reform during the recovery period (Zantema et al., 1992). Finally, like
Hsp70 or Hsp90, both Hsp27 and αB-crystallin act as molecular chaperones and bind
unfolded proteins after heat shock, preventing unspecific aggregation (Horwitz, 1992;
Jakob et al., 1993; Merck et al., 1994).

### Protective functions of Hsp27

Small Hsps seem to be involved in the mechanisms of protection against cell
stress, such as heat shock. For example, the steroid hormone ecdysone induces the small
Hsps and leads to thermoresistance in Drosophila cells (Berger and Woodward, 1983).
On the other hand, Dictyoselium mutants that are unable to synthesize small Hsps fail to
develop thermotolerance despite the accumulation of other Hsps (Loomis and Wheeler,

1982). Interestingly, tomato cells, which constitutively synthesize Hsp70, are thermosensitive but become thermotolerant when given a mild heat treatment that induces the small Hsps (Nover and Scharf, 1984). Chinese hamster cells that express Hsp27 constitutively are thermotolerant (Chrétien and Landry, 1988). Finally, Hsp27 transfection confers a thermoresistant phenotype to NIH/3T3 cells (Landry et al., 1989; Lavoie et al., 1993a) and increases resistance to oxidative stress and cytotoxicity induced by tumor necrosis factor-α treatment (Mehlen et al., 1995).

Although the mechanism of thermotolerance is still unclear, it has been suggested that induction of thermotolerance could be caused by a transient accumulation of small Hsps. However, the kinetics of development and decay of thermotolerance induced by a mild heat shock, differs from accumulation and decay of Hsp27. Firstly, maximal thermotolerance is reached 5 hours after the induction whereas Hsp27 levels attain a maximum level at 14 hours (Landry et al., 1991). Secondly, thermotolerance decays between 5 and 14 hours (half-life=10 hours) while Hsp27 decay is slower (half-life=13 hours) (Landry et al., 1991). Therefore, although expression of Hsp27 appears to be important in the acquisition of thermotolerance, thermotolerance cannot be explained by the concentration of Hsp27 alone. Since Hsp27 can be phosphorylated, it has also been suggested that phosphorylation of Hsp27 might be involved in thermotolerance (Crête and Landry, 1990). Although there was no direct relationship between the amount of any Hsp27 isoforms and the level of thermotolerance which develops after heat shock (Landry et al., 1991), it was demonstrated that phosphorylated isoforms of Hsp27 increased cell

survival against lethal heat shock or cell death induced by hydrogen peroxide (Lavoie et al., 1995; Huot et al., 1996).

*Intracellular mechanisms of action of Hsp27*

Like many Hsps, Hsp27 is a molecular chaperone. Hsp27 has been reported to bind denatured proteins and participate to protein folding in an ATP-independent manner (Jakob et al., 1993; Jakob and Buchner, 1994). Other functions for Hsp27 have also been suggested.

Hsp27 might regulate actin filament organization. This hypothesis came from the studies of Miron et al. (1988, 1991). In turkey smooth muscle, a member of the small Hsp family that showed 80% sequence homology with Hsp27, bound with high affinity to F-actin barbed-end cap and with lower affinity to monomeric actin. This Hsp27-like binding protein inhibited actin polymerization and induced F-actin disassembly (Miron et al., 1988, 1991). In thermotolerant cells or in Hsp27-transfected cells, heat shock-induced disassembly of actin filaments is prevented or is repaired more rapidly. The protection of microfilament organization appears as a consequence of interaction between Hsp27 and actin components, since Hsp27 overexpression also protects against cytotoxicity induced by actin polymerization inhibitor cytochalasin D (Lavoie et al., 1993a) and stabilizes actin filament during oxidative stress (Huot et al., 1996). In addition, expression of phosphorylated Hsp27 increases concentration of actin filament in the cell cortex and elevates pinocytotic activity (Lavoie et al., 1993b). It seems therefore that Hsp27 regulates actin filament dynamics.

Hsp27 has also been suggested to be involved in cell proliferation (Pechan, 1991).

Hsp27 might participate in the transduction signal from mitogen-activated receptors to

actin filament (Arrigo and Landry, 1994).

Two other functions for Hsp27 and small Hsps have recently been suggested

(Mehlen et al., 1996a; 1996b). Firstly, overexpression of *Drosophila* Hsp27, human

Hsp27 or αB-crystallin reduced the intracellular generation of reactive oxygen species

induced by treatment with tumor necrosis factor-α (Mehlen et al., 1996a). This

protective effect of small Hsps was related to an increase in glutathione levels in all three

transfected cell lines. This suggested that small Hsps might regulate the level of

antioxidative enzymes, and thus, the cellular resistance to oxidative stress. Secondly,

Hsp27 or αB-crystallin overexpression inhibited apoptosis induced by Fas/APO-1

receptor activation or treatment with staurosporine, a protein kinase C inhibitor (Mehlen

et al., 1996b). These results suggested that Hsp27 and αB-crystallin might regulate

mechanisms leading to apoptosis.

*Transcriptional regulation of Hsp27*

Little is known about the exact mechanisms involved in the transcription of

Hsp27. The presence of a heat shock element in the promoter region of Hsp27 suggests

that Hsp27 expression is regulated via a similar negative feedback loop involving heat

shock transcription factors, similar to that regulating Hsp70 expression (Arrigo and

Landry, 1994). In addition to heat shock activation, increase in estrogen level has been

reported to induce Hsp27 expression (Ciocca et al., 1983; Fuqua et al., 1989; Seymour

et al., 1990). Finally, several cytokines such as tumor necrosis factor, interleukins and transforming growth factor have been showed to regulate Hsp27 phosphorylation as well as synthesis (Arrigo, 1990; Shibanuma et al., 1992; Löw-Friedrich et al., 1992; Graeme et al., 1993).

## Distribution of the small heat shock proteins

Most of the work on the distribution of small Hsps has been reported in *Drosophila* (for review, see Arrigo and Landry, 1994). In *Drosophila*, small Hsps accumulated at specific developmental stages (Sirokin and Davison, 1982; Cheney and Shearn, 1983). Expression of small Hsps correlated with high levels of the molting hormone β-ecdysterone (Handler, 1982; Mason et al., 1984). In addition, treatment of cultured cells with β-ecdysterone induced synthesis of small Hsps (Ireland and Berger, 1982; Ireland et al., 1982; Vitek and Berger, 1984). Steroid-binding sequences were found upstream of the coding sequence of small Hsps, suggesting possible regulatory activity of steroid hormones on Hsp27 expression (Mestril et al., 1986; Riddihough and Pelham, 1986, 1987).

In *Drosophila*, four small Hsps were described and have specific tissue distribution during development (for review see Arrigo and Landry, 1994). Expression of two small Hsps (Dm-Hsp26 and Dm-Hsp27) was detected in the female reproductive system (Zimmerman et al., 1983). In addition, Dm-Hsp26 was detected in neurons using a reporter gene construct (Glaser et al., 1986). Dm-Hsp23 expression during development was restricted to midline precursor cells in the central nervous system

(Tanguay, 1989; Hass et al., 1990). Adult *Drosophila* expressed Dm-Hsp23 in the

gonads, in neurocytes and glial cells of the central nervous system and in nerves of the leg

(Hass et al., 1990, Marin et al., 1993). The fourth Dm-Hsp, Dm-Hsp22, was not

observed during development but following teratogenic drug treatment inducing cellular

differentiation (Buzin and Bounias-Vardiabasis, 1982).

In mammals, Hsp27 and αB-crystallin have been detected in several organs

(Tanguay et al., 1993; Klemenz et al., 1993). In fact, both proteins can reach

considerable levels in unstressed organs such as skeletal muscle or the heart. αB-

crystallin constitutes about 5 % of the total soluble protein of rat hearts composed of type

I fibers (Longoni et al., 1990a). Similarly, in skeletal muscles, oxidative type I fibers

have high levels, type IIA fibers have moderate levels and glycolytic type IIB fibers have

low levels of αB-crystallin (Iwaki et al., 1989; 1990). αB-crystallin is localized in the

central region (the Z-line) of the I-band (Longoni et al., 1990b; Bennardini et al., 1992)

and is not found associated with F-actin in preparations of rat heart myofibrils. Since αB-

crystallin is not found in white muscle, it seems that αB-crystallin is not a basic ingredient

in the formation of cytoskeletal lattice nor of the contractile machinery. The distribution

of Hsp27 in skeletal muscle or in the heart is unknown.

In the developing mouse nervous system, Hsp27 was observed in Purkinje

neurons of the cerebellum and in large neurons of the spinal cord in the rat (Gernold et

al., 1993). Similarly, in human brains, Hsp27 expression was detected around the

seventeenth week of gestation (Aquino et al., 1996). In the adult mammalian brain,

Hsp27 was not detected (Tanguay et al., 1993; Klemenz et al., 1993; Wilkinson and

Pollard, 1993). However, αB-crystallin is expressed in the adult mammalian brain (Iwaki

et al., 1990; Klemenz et al., 1993). Immunoreactivity for αB-crystallin was found in

some small round, oligodendrocyte-like cells. A few astrocytes were also labeled,

principally those near the subpial glial limitans (Iwaki et al., 1990).

**Distribution of small heat shock proteins in pathological conditions**

Hsp27 was detected in various forms of cancer such as breast or endometrial

carcinomas (Têtu et al., 1992; Ciocca et al., 1993). The presence of Hsp27 has been

suggested to be a useful diagnostic tool for malignant fibrous histiocytoma (Têtu et al.,

1992). Similarly, Hsp27 has been detected in several types of brain tumors (Kato et

al., 1992a; Kato et al., 1993; Khalid et al., 1995; Hitotsumatsu et al., 1996) and

seemed to correlate with the anaplasia of the tumors (Hitotsumatsu et al., 1996). Other

pathological conditions also induced Hsp27 in the brain. Abnormal neurons in

Creutzfeldt-Jakob disease and in Pick's disease showed immunoreactivity for Hsp27

and αB-crystallin but no Hsp27 or αB-crystallin immunoreactivity was detected in

neurons in amyotrophic lateral sclerosis (Kato et al., 1993). Hsp27 and αB-crystallin

have also been reported to accumulate in astrocytes in various disorders, including

Alzheimer's disease (Renhawek et al., 1994), Alexander's disease (Iwaki et al., 1992,

1993; Head et al., 1993) and chronic infarct (Iwaki et al., 1993).

Ischemia also induces upregulation of *Hsp27* transcription in rat hearts. Isolated and perfused rat hearts showed *Hsp27* mRNA expression following repetitive periods of short ischemia (Das et al., 1993). As little as 10 minutes of left descending artery occlusion caused a significant increase in *Hsp27* mRNA (Das et al., 1993). *In vivo* experiments on pigs showed a similar increase in *Hsp27* mRNA in the heart following brief repetitive ischemic insults (Andres et al., 1993).

## Rationale

Although there seems to be a strong relationship between Hsp70 induction and ischemic protection in the heart and the brain following heat shock treatment, the evidence is circumstantial. Indeed, heat shock induces a variety of changes, not only at the cellular level but also at the organ and whole animal level. Therefore, it seems reasonable to suggest that other proteins, including other Hsps could play a role in heat shock-induced cellular protection against ischemia.

1. It appears therefore that a better description of the distribution of Hsp70 after ischemia in the heart could bring some insights into the cell types involved in the protective effect.

2. Examination of ischemic resistance of hearts of transgenic mice constitutively expressing Hsp70 could determine whether ischemic protection could be obtained by the sole expression of Hsp70 independent from other mechanisms triggered by heat

shock treatment. This will demonstrate the role of Hsp70 in myocardial protection against ischemia.

3. Similarly, resistance of Hsp70-transgenic mice against cerebral ischemia might reveal a function for Hsp70 in cerebral ischemic tolerance.

4. Alternatively, description of constitutive expression and induction of other Hsps such as Hsp27 that is induced following ischemia and that has been shown to protect against oxidative stress *in vitro*, might reveal new mechanisms of ischemic protection, independent from Hsp70.


## Overview of the research work

In this thesis, I am reporting on the expression and role of two heat shock proteins in the heart and the brain after ischemic injury. Following 30 minutes of ischemic injury, as shown by *in situ* hybridization, *Hsp70* was expressed in the ischemic area but not the necrotic area of hearts (chapter 2). Expression of Hsp70 in the ischemic area suggested that Hsp70 might play a role in protection or repair of the ischemic myocardium. A role for Hsp70 in protection against ischemia was then examined using transgenic mice expressing the human Hsp70 (chapter 3). Isolated hearts expressing the transgene Hsp70 had resistance to ischemic injury and had improved contractile recovery following 30 minutes of global ischemia. These results suggest that Hsp70 plays a role in protection of the myocardium against ischemic injury.

To determine whether Hsp70 played a role in cellular resistance to ischemic injury in organs other than the heart, the effects of focal cerebral ischemia was examined in the Hsp70-transgenic mice (chapter 4). Although infarct areas were not different between non-transgenic and transgenic mice, the hippocampal neurons in the Hsp70-transgenic mice were resistant to this ischemia-related injury. This result suggested that Hsp70 protected the hippocampal neurons from injury induced by ischemia and the associated excitotoxicity.

Considerable evidence suggests that Hsp27 also protects cells from oxidative stress and possibly ischemic injury. Using immunohistochemistry, the distribution of Hsp27 was examined in the brain before and after ischemic injury. Hsp27 was found normally, in select neurons of the brain stem and spinal cord, but not in the cerebral cortex (chapter 5). After focal ischemic injury to the cerebral cortex, Hsp27 was expressed throughout the ipsilateral cortex in astrocytes (chapter 6). Interestingly, Hsp70 was expressed only adjacent to the area of necrosis and not throughout the ipsilateral cortex. I considered whether the expression of Hsp27 in astrocytes was induced in reactive astrocytes by cortical spreading depression associated with focal cerebral ischemia (chapter 7). Thus expression of Hsp27 was examined in a model of astrogliosis in the cerebral cortex. Application of potassium chloride to the cortex induced expression of Hsp27 in astrocytes and revealed that Hsp27 could be induced in astrocytes by multiple pathways, one being cortical spreading depression. This result

raised the intriguing possibility that Hsp27 might be involved in cortical spreading

depression-induced protection against cerebral ischemic injury.

# CHAPTER 2:

## EXPRESSION OF Hsp70 IN THE ISCHEMIC MYOCARDIUM.

**Introduction**

In the last several years, considerable interest has developed in the heat shock response and myocardial protection (Currie et al., 1993; Donnelly et al., 1992; for review see Mestril and Dillmann, 1995; Knowlton, 1995). In fact, several reviews have suggested a link between induction of the heat shock response and improved recovery of the myocardium from ischemic injury (Thorne et al., 1992; Yellon and Latchman, 1992; Yellon et al., 1993). Interruption of blood flow to the heart or other organs causes the affected area to become ischemic and the consequences are usually devastating. Ischemia undoubtedly induces a heat shock response (Currie, 1987; Mehta et al., 1988), but whether dying and necrotic cells in the middle of an infarcted area synthesize Hsps or other new protein is a matter of speculation. Cells on the periphery of an ischemic area in brain synthesize heat shock proteins in abundance (Gonzalez et al., 1989). In the rabbit heart, coronary artery occlusion for only 5 minutes induces *Hsp70* mRNA accumulation in the ischemic area during a 1 hour reflow period as revealed by Northern analysis. Although a single 5-minute episode of coronary artery occlusion did not increase the level of *Hsp70* mRNA in the non-ischemic area, repetitive (4 times) occlusions induce a two fold elevation of *Hsp70* mRNA in the non-ischemic area, as detected by Northern analysis (Knowlton et al., 1991).

Ischemic injury also induces the expression of a number of immediate early genes that are transcription factors and regulate the expression of other genes (for review, see Das et al., 1995). Transcriptional activity of immediate early genes (FOS-

JUN) has been shown to depend upon the formation of a dimer between two members of FOS-JUN. It is likely that combination of immediate early gene products might be required in the recovery and repair process following ischemia as well as in trigger of cell death genes. These immediate early gene products accumulate in the ischemic area of the pig heart (Brand et al., 1992). Immediately after 10 minutes of coronary artery occlusion mRNA for *c-fos*, *Egr-1* (also called *ngfi-a, Knox 24, or zif 268*), *c-jun* and *jun-B* accumulate in the ischemic area and this accumulation of mRNA increases during the reperfusion period. *c-jun* was only slightly increased while *c-fos*, *erg-1*, and *jun-B* genes were all highly induced in the ischemia region as shown by Northern analysis (Brand et al., 1992). In these experiments, the expression of *c-myc* was unchanged and expression of *fos-B* was not detected. In addition, *jun-B* mRNA was also detected in the non-ischemic area of the pig heart.

To explore further the effect of ischemia on the induction of immediate early genes and heat shock genes, isolated and perfused hearts were examined by *in situ* hybridization after 30 minutes of coronary artery occlusion. The purpose of the present work is to locate more precisely the site of heat shock and immediate early gene expression within the ischemic heart.

## Materials and methods

Rats were cared for in accordance with the *Guide to the Care and Use of Experimental animals* of the Canadian Council on Animal Care.

## *Langendorff perfusion protocol*

Male Sprague-Dawley rats (250-300 grams, Charles River, Montreal) were anesthetized with sodium pentobarbital (50 mg/kg body weight, ip). Hearts were excised rapidly, immersed in ice-cold buffer and hung on an aortic cannula in a Langendorff apparatus (Currie et al., 1988). Hearts were perfused retrogradely with Krebs-Henseleit buffer consisting of (mM) NaCl 120, NaHCO$_3$ 20, KCl 4.63, KH$_2$PO$_4$ 1.17, MgCl$_2$ 1.2, CaCl$_2$ 1.25, and glucose 8. The pH of the buffer was 7.4 and the temperature of perfusion system was regulated at 37°C using a water-jacketed chamber and coil. The hearts were electrically paced at 300 stimulations/minute with a Grass S44 stimulator (Grass Instruments, Quincy, Massachusetts) at twice threshold voltage. Buffer flow was controlled with a peristaltic pump at 10 ml/minute. A 5-0 nylon suture was put around the left anterior descending coronary artery near to its origin.

After 15 minutes of equilibration, the coronary artery was occluded for 30 minutes. After the 30 minute-ischemic injury, some hearts were processed for *in situ* analysis, while other hearts were reperfused. The occluding suture was then loosened and the ischemic area was reperfused for 30, 60, or 90 minutes. Mechanical activity was measured throughout each perfusion experiment according to previously described methods (Currie et al., 1988; Karmazyn et al., 1990). Briefly, apicobasal displacement was obtained by attaching a Grass FT.03 strain gauge transducer to the heart apex. This measurement was proportional to the contractile force of the perfused heart. The transducer was positioned to yield an initial resting tension of 2 grams. Recordings of

mechanical activity were made on a Grass Model 7 polygraph. The contractile force

was obtained by measuring the height of the trace above baseline for each contraction.

At the end of the reperfusion period, hearts were sliced in 2 mm thick sections. Slices

were incubated in 1% 2,3,5-triphenyl tetrazolium chloride in perfusion buffer in order

to determine the necrotic area. After 30 minutes at 37 °C, slices were immersed in 4%

paraformaldehyde in phosphate-buffered saline (PBS; mM, NaCl 136, KCl 2.6,

$Na_2HPO_4$ 1, $KH_2PO_4$ 1.75). Slices were kept at 4°C until paraffin-embedding. At the

end of some experiments, the (loose) occluding suture was re-tightened. Evans Blue (1

ml) was injected through the aorta to delineate firstly the normally perfused zone of the

heart and secondly, the under-perfused zone, the area at risk. Hearts were rinsed,

chilled on ice and frozen at -80 °C. Frozen sections of each heart were cut at 14 μm on

a LKB freezing microtome and mounted on glass slides. Tissue sections were stored at

-80 °C for later analysis. Some hearts were immersed in 4% paraformaldehyde-PBS

overnight, cut at 50 μm on a vibratome or further processed for paraffin embedding and

cut at 10 μm.

*Creatine kinase analysis*

Creatine kinase release from hearts was measured in the effluent buffer to assess

the level of cellular injury induced by ischemia. Buffer samples were collected during

the last minute of ischemic period, and at 1, 5, 10, 15, 20 and 30 minutes of

reperfusion. Creatine kinase content was determined by the spectrophotometric method

of Rosalki (1967) using CK kits from Sigma Chemical, St. Louis, MO.

*Statistical analysis*

Statistical analysis of variance for repeated measures was used to compare

physiological data. Data are means ± standard deviations. Significant F-tests were

followed up using Duncan's for *post hoc a posteriori* multiple comparisons.

*Oligonucleotide probes*

Oligonucleotide probes were synthesized at the Marine Gene Probe Lab,

Dalhousie University. Probes for *Hsp70* (inducible) and *Hsc70* (cognate) have been

shown to hybridize to their respective mRNA by Northern analysis (David et al.,

1994). Similarly, probes for *c-fos*, *c-jun*, *jun-B*, *jun-D* and *erg-1* were specific (Paul et

al., 1995). Sequences of oligonucleotide probes for Hsps, immediate early genes and

*β-actin* are listed in table 2. All the probes were 3'end labeled with [$\alpha$-$^{35}$S]dATP using

a 3'end labeling kit (Amersham). Unincorporated label was removed from the [$\alpha$-

$^{35}$S]dATP labeled oligonucleotides with a NENSORB 20 nucleic acid purification

cartridge (Dupont, Wilmington). The oligonucleotide probes were labeled to a specific

activity of 1-4 x $10^6$ cpm/µg DNA.

*In situ analysis*

*In situ* hybridization was done according to the method of Wisden et al. (1991)

and with minor modifications. Briefly, heart sections were thawed and immersed 5

minutes in 4% paraformaldehyde in PBS. Paraffin sections were treated with

proteinase K. Either slides were rinsed twice in PBS for 3 minutes and in a buffer

containing 300 mM NaCl and 30 mM sodium citrate (pH 7.2). The heart sections on

the slides were then dried at room temperature for 30 minutes. The [$\alpha$-$^{35}$S]dATP-

oligonucleotide probes were diluted to 5 x 10$^6$ cpm/ml of hybridization buffer consisting

of deionized formamide 50%, NaCl 600 mM, sodium citrate 60 mM, sodium phosphate

25 mM (pH 7.0), acid alkali hydrolyzed salmon sperm DNA 0.02 mg/ml , heparin 0.12

mg/ml, dextran sulfate 0.1 g/ml, sodium pyrophosphate 1 mM, dithiothreitol 1.5

mg/ml, and Denhardts reagent (bovine serum albumin 0.02%, polyvinylpyrrolidone

0.02%, and Ficoll 0.02%). Heart sections were incubated with 0.1 ml of hybridization

buffer overnight at 37°C. The sections on the slides were washed at 58°C in increasing

dilutions (1:1, 1:2 and 1:4 in distilled water) of the rinse buffer for 30 minutes, each

rinse. After a final wash in the same buffer at room temperature for 1 hour, the heart

sections were dried at room temperature overnight. Autoradiographic film (Hyperfilm,

Kodak) was exposed to the sections for 1 week at -80°C. Following development the

autoradiographs were used directly to print the figures. *In situ* autoradiography was

also performed using Kodak autoradiography emulsion NTB2 on paraffin-embedded

sections.

Table 2. Sequences of oligonucleotide probes for *Hsp70*, *Hsc70*, *c-fos*, *c-jun*, *jun-B*,

*jun-D*, *erg-1* and *β-actin*.

| Probe | oligonucleotide sequence |
|-------|--------------------------|
| *Hsp70* | 5'- cga tct cct tca tct tgg tca gca cca tgg -3' |
| *Hsc70* | 5'- atg cct gtg agc tca aac ttc cca agc agc -3' |
| *c-fos* | 5'- cag cgg gag gat gac gcc tcg tag tcc gcg ttg aaa ccc gag aac -3' |
| *c-jun* | 5'-gca act gct gcg tta gca tga ctt ggc acc cac tgt taa cgt ggt tca tga ctt tct gtt-3' |
| *jun-B* | 5'- gaa ggc gtg tcc ctt gac ccc tag cag caa ctg gca gcc gtt gct gac atg ggt cat gac -3' |
| *erg-1* | 5'- ccg ttg ctc agc agc atc atc tcc tcc agt ttg ggg tag ttg tcc -3' |
| *β-actin* | 5'- gcc gga gcc gtt gtc gac gac gag cgc agc gat atc gtc atc cat-3' |

## Results

### *Contractile force*

Occlusion of the left anterior descending coronary artery for 30 minutes significantly [$F_{(11,77)} = 51.6$, $p < 0.05$] decreased the contractile force of the hearts (Figure 2.1A). Contractile force significantly decreased from $79.5 \pm 13.6 \; 10^{-3}N$ (end of pre-occlusion period) to $35.7 \pm 12.2 \; 10^{-3}N$ at the end of the 30 minute-occlusion (Duncan's statistical analysis; $p < 0.05$) (n=16). Upon reperfusion of the ischemic area, contractile force of the heart significantly increased to $51.0 \pm 8.7 \; 10^{-3}N$ at 5 minutes of reperfusion (n=12). During the remainder of the reperfusion period, there was a slow, progressive decline in contractile force.

### *Creatine kinase analysis*

Creatine kinase release (Figure 2.1B) during the reperfusion period was determined. Upon reperfusion, even the initial effluent buffer sample contained detectable levels of creatine kinase. The amount of creatine kinase in the effluent buffer significantly [$F_{(8,39)} = 7.9$, $p < 0.05$] increased at 1 minute of reperfusion and appeared to peak at 5 to 10 minutes of reperfusion (n=12).

### *In situ analysis*

*In situ* hybridization analysis revealed accumulation of *Hsp70* mRNA in the ischemic zone of the hearts after 30 minutes of coronary artery occlusion followed by 90 minutes of reperfusion (Figure 2.2a). Minimal hybridization signal was detected in hearts perfused for a total of 135 minutes (same duration as 15 minutes of pre-ischemic

perfusion, 30 minutes of coronary artery occlusion, and 90 minutes of reperfusion) with no ischemic insult (Figure 2.2b). Similarly, there was minimal or no mRNA accumulation for *c-fos*, *c-jun*, or *Hsc70* in hearts perfused for 135 minutes with no ischemic episode (data not shown). Interestingly, little or no accumulation of mRNA for *Hsp70* was detected in the ischemic zone, and minimal accumulation of *Hsp70* mRNA was detected in the normally perfused area of hearts with coronary artery occlusion for 120 minutes (with no reflow) (Figure 2.2c).

2,3,5-triphenyl tetrazolium chloride staining of hearts with 30 minutes of coronary artery occlusion and 90 minutes of reflow revealed the area of necrosis (Figure 2.3a). On a serial section of the same heart, *Hsp70* mRNA was localized around the border of the necrotic region. Only a small portion of the underperfused area was labeled by *Hsp70* oligonucleotide probe (Figure 2.3b). Another heart subjected to 30 minutes of coronary artery occlusion and 90 minutes of reflow revealed a similar labeling pattern for *Hsp70* mRNA (Figure 2.4a). After this film autoradiogram was developed, the heart sections were coated with Kodak NTB2 emulsion. Light microscopic examination of the NTB2 autoradiogram revealed that most of the silver grains were over the identical region as observed with autoradiographic film. Light microscopic examination revealed accumulation of the silver grains over cardiomyocytes (Figure 2.4b) as well as other cell types (endothelial cells, fibroblasts, smooth muscle cells) in the region around the necrotic area while no

specific accumulation was detected in the non-ischemic area (Figure 2.4c) or in the necrotic area (Figure 2.4d).

On serial sections of another heart, *Hsp70* mRNA was localized again to ischemic zone (Figure 2.5a) and probe specific for *β-actin* mRNA was localized throughout the heart (Figure 2.5b).

Immediate early gene products (*c-fos* and *c-jun* mRNA) and heat shock gene products (*Hsc70* and *Hsp70* mRNA) were detectable with same pattern of accumulation in the hearts (4 hearts / group) examined by *in situ* hybridization using specific [α-$^{35}$S]dATP 3' end labeled oligonucleotide probes (Figure 2.6). Immediately after 30 minutes of coronary artery occlusion (0 minute of reperfusion) there was little or no hybridization of probes to *c-fos*, *c-jun*, *Hsc70*, and *Hsp70* mRNA (Figure 2.6 a - d, respectively) in the ischemic area or in the normally perfused area of the hearts. After 30 minutes of reperfusion, the ischemic area had detectable accumulation of mRNA for *c-fos*, *c-jun*, *Hsc70*, and *Hsp70* (Figure 2.6 e - h, respectively), while there continued to be little or no detectable labeling in the non-ischemic part of the heart. In general, the accumulated *c-fos*, *c-jun*, *Hsc70*, and *Hsp70* mRNA appeared to be increased at 60 minutes (Figure 2.6 i - l) and 90 minutes of reperfusion (Figure 2.6 m - p). An exception to this was that *c-fos* mRNA appeared to peak at 60 minutes of reperfusion (Figure 2.6 i). It should be noted that Figure 2.6 a - d, e - h, i - l, and m - p are serial sections of 4 hearts. Each of these 4 hearts is a typical example of 4 hearts analyzed at each time point of reperfusion. Comparison of the 4 sections at 30, 60, and 90 minutes

of reperfusion reveals that the labeling of the 4 probes is coincident. The accumulated

*Hsp70* mRNA appears to be localized to a larger area than the accumulated *c-fos*, *c-jun*

or *Hsc70* mRNA.

The highly inducible nature of *Hsp70* mRNA is illustrated by comparison with

*Hsc70*. Careful examination of the *c-fos*, *c-jun* and *Hsc70* labeled areas at 90 minutes

of reperfusion (Figure 2.6 m, n, and o, respectively) reveals a small unlabeled area in

the centre of the labeled area. This central unlabeled area was observed also for *Hsp70*

mRNA.

Serial sections of hearts were examined for *erg-1* and *jun-B* mRNA after 30

minutes of coronary artery occlusion and 0, 30, 60 and 90 minutes of reperfusion.

There was a progressive increase in labeling intensity with reperfusion. Results for the

90 minute-reperfusion period are shown (Figure 2.7). *Hsc70* and *Hsp70* mRNA-

labeled sections (Figure 2.7 a and b, respectively) serve as positive controls to delineate

the ischemic area and again reveals the highly inducible nature of *Hsp70*. While

detectable levels of *erg-1* and *jun-B* mRNA (Figure 2.7 c and d, respectively) were seen

in the ischemic area as indicated by *Hsp70* labeling (Figure 2.7 b), there also appears to

be considerable *jun-B* mRNA (Figure 2.7 d) throughout the non-ischemic part of the

heart.

Figure 2.1. Contractile force and creatine kinase release of isolated and perfused hearts during coronary artery occlusion and reperfusion. A. The 30 minute-occlusion of the left anterior descending coronary artery is indicated by the horizontal bar (ischemia). The data points are mean ± SD (n = 16, for pre-ischemic and ischemic points; n = 12, for 1, 5, 10, 15, 20, and 30 minutes of reperfusion (46, 50, 55, 60, 65 and 75 minutes, respectively); n = 8, for 45 and 60 minutes of reperfusion (90 and 105 minutes, respectively); and n = 4, for 90 minutes of reperfusion (135 minutes)). B. Creatine kinase release during the reperfusion period. The data points are mean ± SD (n = 12). Asterisks represent significant differences between selected time points using Duncan's test for post hoc a posteriori multiple comparison.
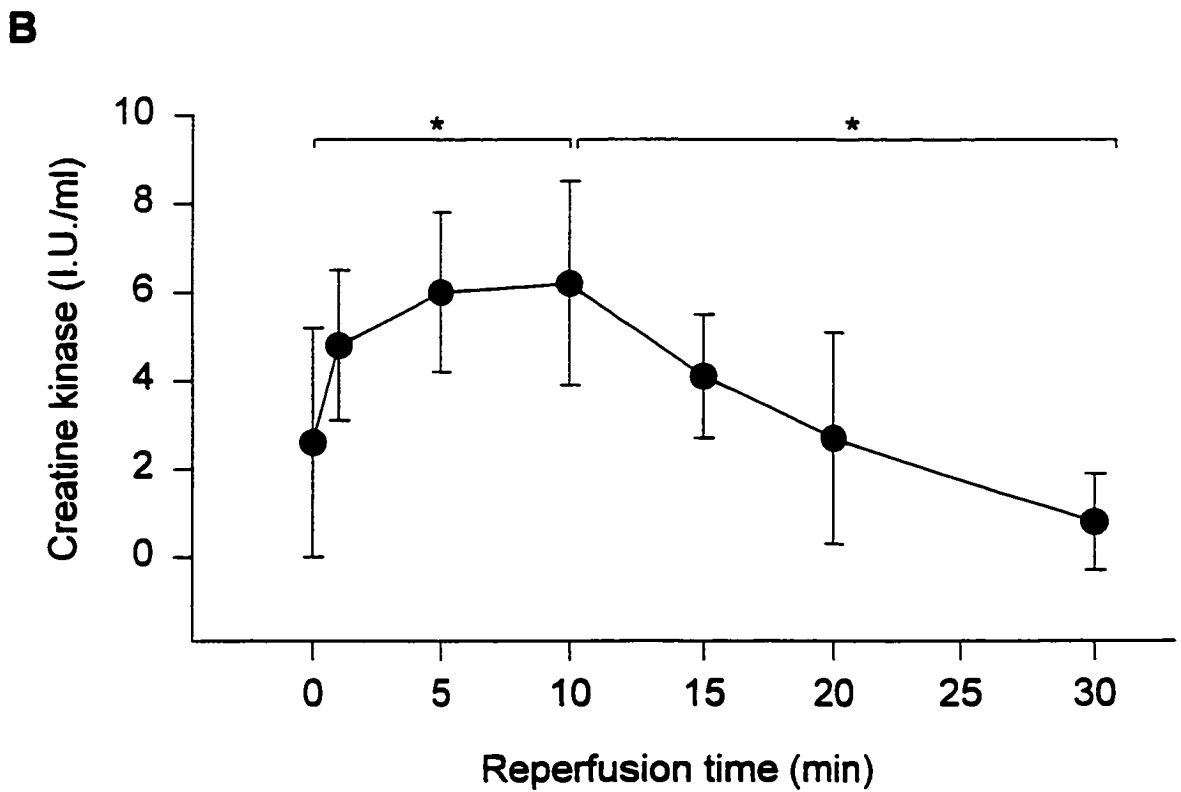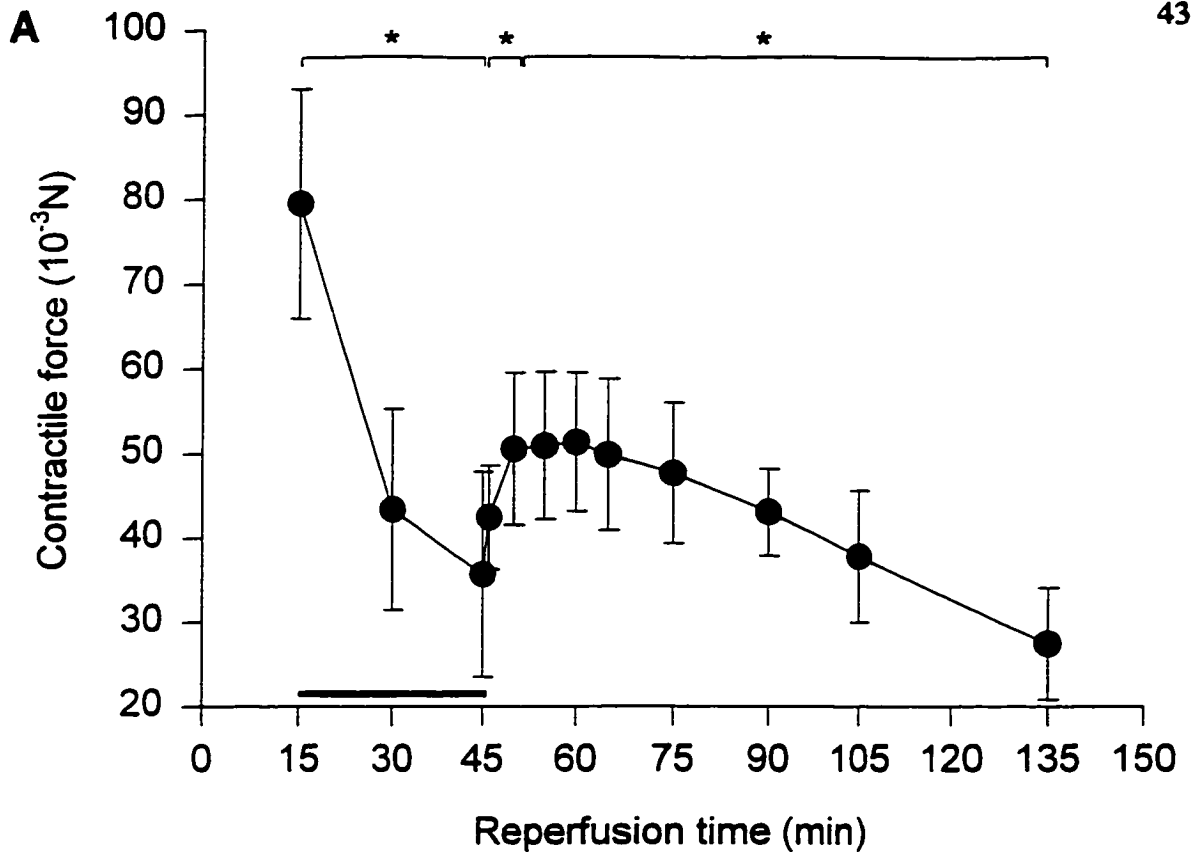
Figure 2.1

Figure 2.2. Accumulation of *Hsp70* mRNA in ischemic hearts. a) *Hsp70* mRNA

accumulates in the ischemic region of the heart after 30 minutes of coronary artery

occlusion during 90 minutes of reperfusion. b) Minimal *Hsp70* mRNA accumulates in

hearts perfused for 135 minutes with no ischemic insult. c) No *Hsp70* mRNA

accumulates in the ischemic region of hearts with 120 minutes of coronary artery

occlusion, with no reperfusion.

Figure 2.2

Top panel:

Figure 2.3. Necrotic area and *Hsp70* mRNA accumulation in ischemic hearts.

Necrotic area (N) was determined by 2,3,5 triphenyl tetrazolium chloride staining (a).

*In situ* hybridization (b) was performed on the same 50 μm sections.

Bottom panel:

Figure 2.4. *Hsp70* mRNA *in situ* hybridization using film and NTB2 emulsion on an

ischemic heart. a) Film autoradiography revealed *Hsp70* mRNA accumulation around

the necrotic area (N). b) NTB2 emulsion autoradiography of the same heart examined

by light microscopy revealed silver grains localized over all cell types including the

cardiomyocytes in the same region as in figure a. NTB2 emulsion autoradiography

revealed only a few silver grains over cells in the non-ischemic area (c) or necrotic

region (d).
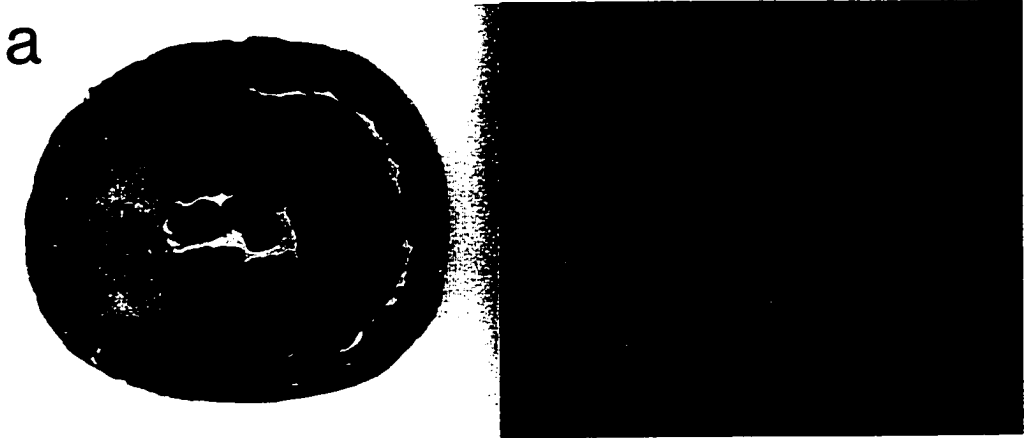
Figure 2.3
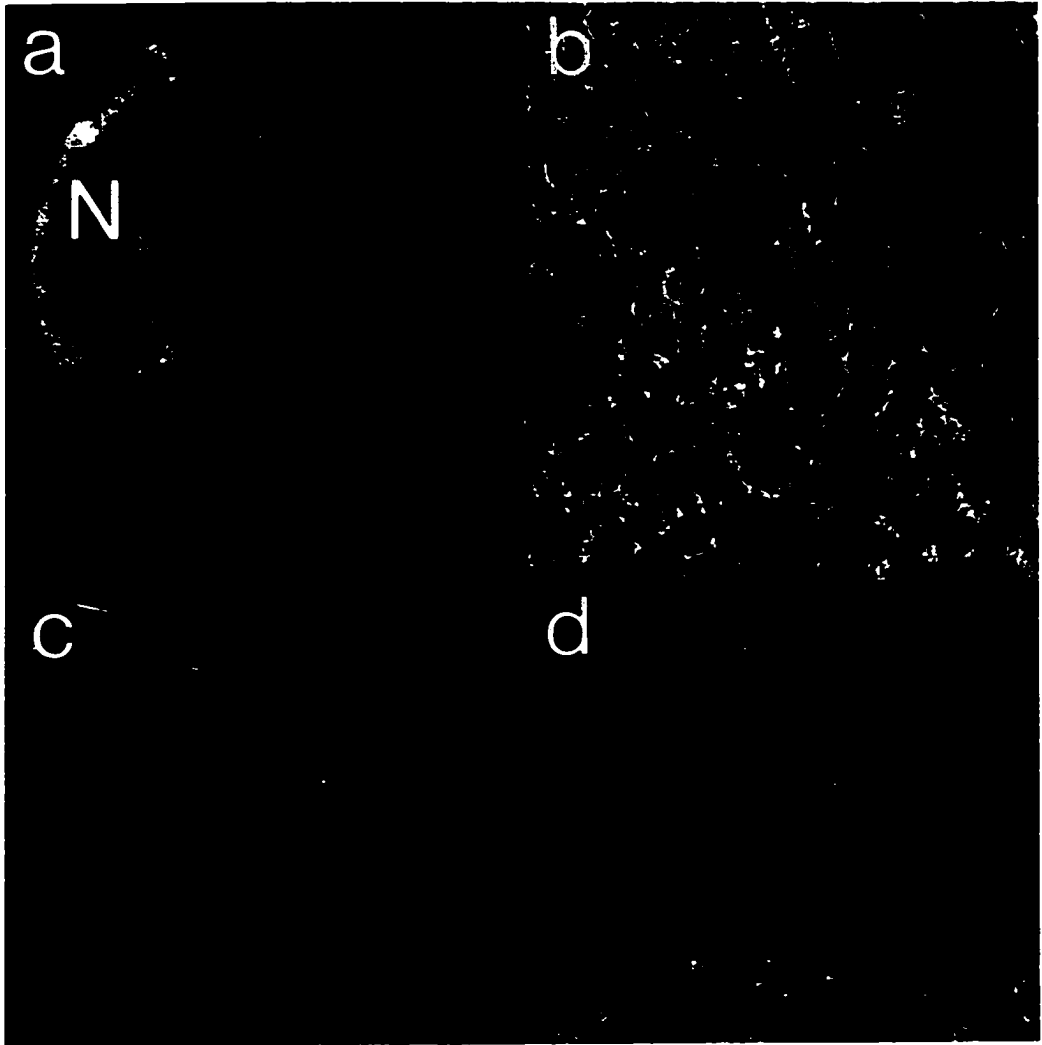


Figure 2.4

Figure 2.5. Localization of *Hsp70* and *β-actin* mRNA in serial heart sections after 30

minutes of coronary artery occlusion and 90 minutes of reperfusion. a, *Hsp70*; b, *β-*

*actin*.
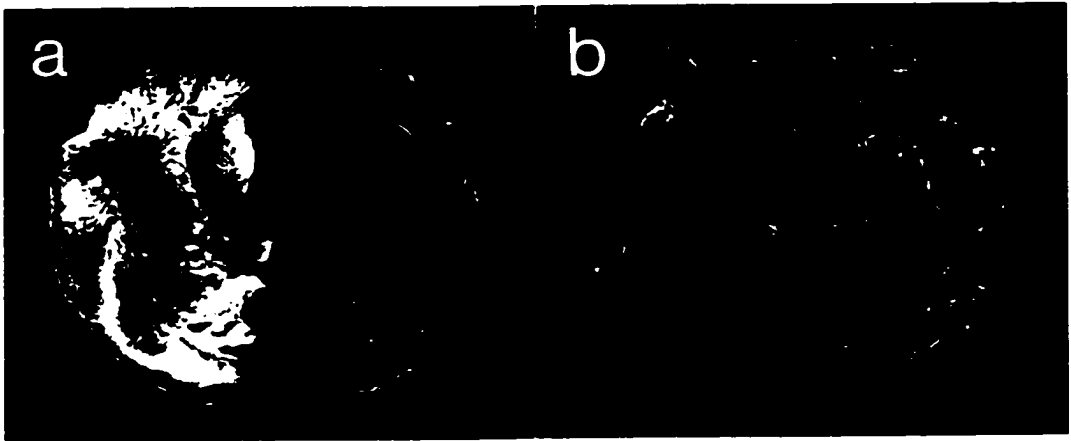
Figure 2.5

Figure 2.6. Localization and accumulation of *c-fos*, *c-jun*, *Hsc70*, and *Hsp70* mRNA

in serial heart sections after 30 minutes of coronary artery occlusion and 0, 30, 60 or

90 minutes of reperfusion.
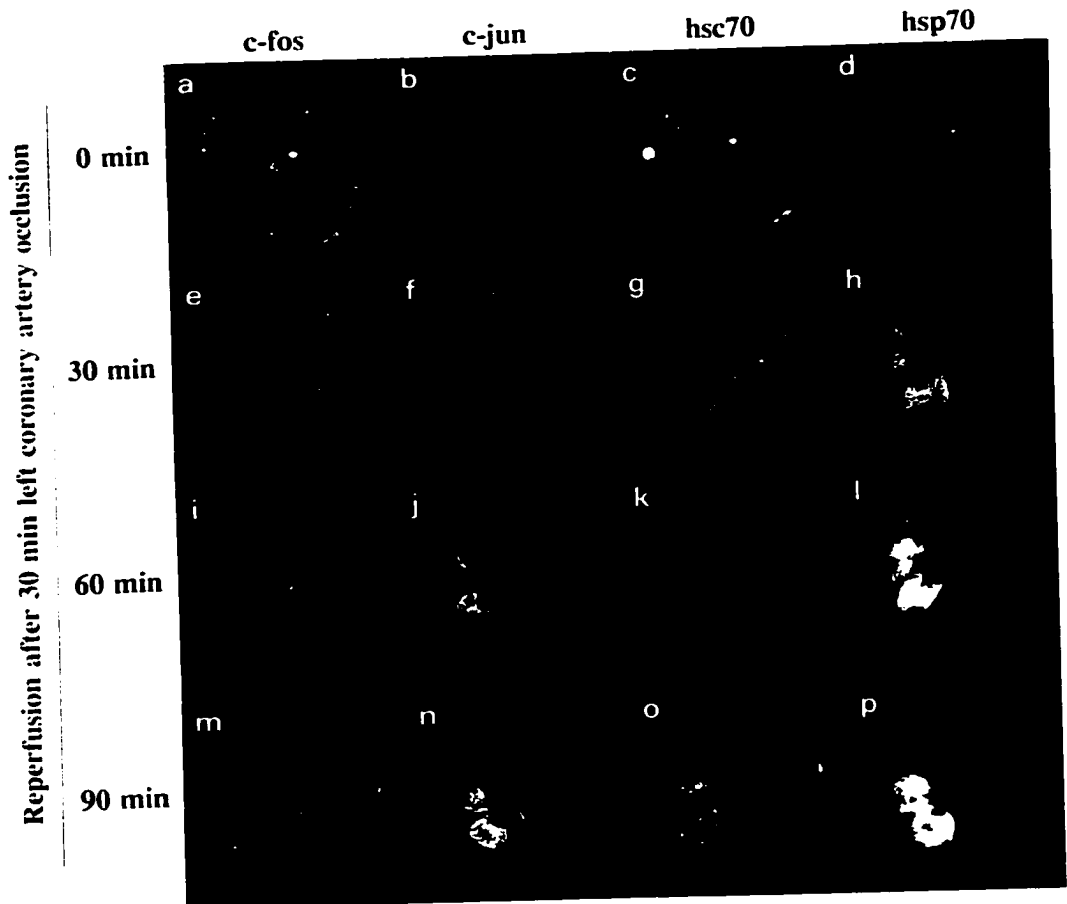
Figure 2.6

Figure 2.7. Localization and accumulation of stress gene and immediate early gene

mRNA in serial heart sections after 30 minutes of coronary artery occlusion and 90

minutes of reperfusion. Probes are *Hsc70*, a; *Hsp70*, b; *erg-1*, c; *jun-B*, d.
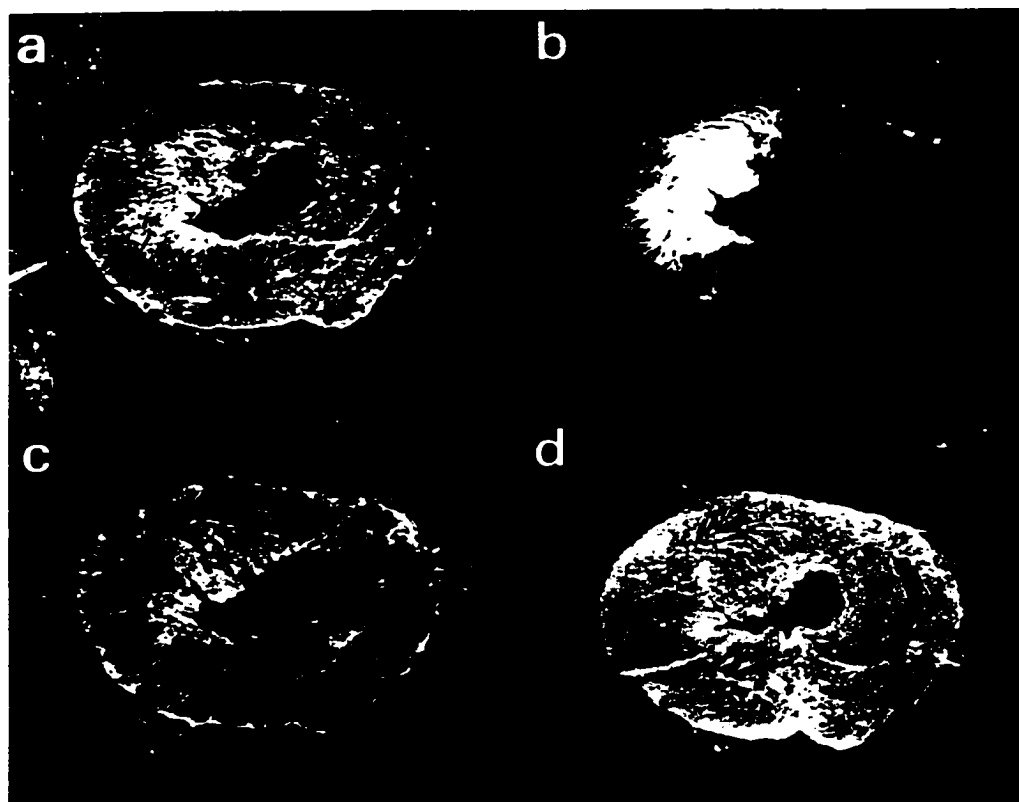
Figure 2.7

## Discussion

Occlusion of a coronary artery followed by reperfusion induces the accumulation of mRNA for heat shock proteins and for immediate early gene products in the ischemic area of the heart. mRNA for *Hsc70*, *Hsp70*, *c-fos*, *c-jun*, *erg-1*, and *jun-B* accumulates in the ischemic area of the hearts during the reperfusion period. In addition, *jun-B* appears to increase in the non-ischemic area of the heart. These results suggested that a rapid synthesis of Hsp70 and other stress genes may play a role in enhancing myocardial survival following ischemic injury.

### Assessment of the ischemic injury

The sharp decrease in contractile force after occlusion of the left anterior descending coronary artery confirmed that part of the heart was subjected to an ischemic insult (Figure 2.1a). Similarly, the detection of the intracellular enzyme, creatine kinase, in the effluent buffer during reperfusion revealed that cellular injury had occurred and was indicative of the ischemic insult to the heart (Figure 2.1b).

### Gene expression after ischemia

Following 30 minute-ischemic injury and 90 minutes of reperfusion, mRNA for *Hsc70*, *Hsp70*, *c-fos*, *c-jun*, *erg-1*, and *jun-B* was localized in the ischemic area of each heart. In addition, there was co-localization of *Hsc70*, *Hsp70*, *c-fos*, *c-jun* and *erg-1* mRNA (Figure 2.6 and Figure 2.7) in the ischemic area and *jun-B* in both the ischemic and non-ischemic areas of the heart (Figure 2.7).

Ischemic injury has been shown to induce the expression of a number of immediate early genes (Brand et al., 1992; Das et al., 1995) and heat shock genes (Currie et al., 1987; Mehta et al., 1988; Mestril and Dillmann, 1995; Knowlton et al., 1991; Knowlton, 1995). *c-jun* was slightly increased while *c-fos*, *erg-1* (also called *ngfi-a*), and *jun-B* genes were all highly induced after ischemia in the pig heart (Brand et al., 1992). Interestingly, in the pig heart, *jun-B* was detectable in both the ischemic and non-ischemic areas as shown by Northern analysis. In the present study, *jun-B* was also clearly expressed in both the ischemic and non-ischemic parts of the heart.

Similar dissociation between the expression of members of FOS-JUN family has also been reported in cultured neonatal cardiac myocytes (Webster et al., 1994). Inhibition of the respiration and lactate production by a combination of cyanide and deoxyglucose induced a four-fold increase of *c-fos* or *c-jun* with only minor changes in *jun-B*. However, *jun-B* mRNA accumulation reached similar levels as *c-fos* and *c-jun* mRNA accumulation following iodoacetic acid treatment which produced a more potent metabolic inhibition of the respiration. Similarly, mRNAs for *jun-B* and *c-fos* accumulated in response to elevation of extracellular ATP (Zheng et al., 1994). It seems that while *c-fos* and *jun-B* share some pathways of induction, there are clearly different and specific mechanisms that regulate these genes. Since immediate early genes are involved in regulation of other genes through AP-1 binding, differential induction allows control of late gene activation (Curran and Franza, 1988). *Jun-B* has been demonstrated to be a negative inhibitor of *c-jun* (Chiu et al., 1988; Deng and

Karin, 1993; Schütte et al., 1989). *jun-B* expression may therefore be important in particular forms of cell death where *c-jun* expression seems to play an important role (Estus et al., 1994; Ham et al., 1995). Our results illustrated different regulation mechanisms between two members of the Jun family. The mechanism of induction of *jun-B* and its role in the non-ischemic area are presently unknown.

This study clearly showed that 30 minutes of coronary artery occlusion followed by reperfusion induced the accumulation of mRNA for heat shock proteins and immediate early gene products during the reperfusion period. During the ischemic period there was no detectable accumulation of these transcripts, but during the reperfusion period the transcripts accumulated in a time-dependent fashion. In pig heart subjected to a 10 minute-coronary artery occlusion, immediate early genes have been reported to accumulate even before any reflow (Brand et al., 1992). This was especially evident with *erg-1* which increased 6 fold in the ischemic area compared to the non-ischemic area. While there is a clear difference in the pig and the rat model (duration of occlusion, degree of collateral flow), it seems likely that during ischemia injury, there is a gradient of transcriptional activity from the non-ischemic area to the ischemic area. In the non-ischemic area transcription continues relatively normally, while in the centre of the ischemic area, there is little or no transcriptional activity. At some point in this gradient of transcriptional activity, it is likely that there is induction of stress-induced genes. After 30 minutes of ischemia, during reperfusion, transcriptional activity was restored to a large part of the ischemic zone and immediate

early and heat shock gene products were transcribed. If transcriptional activity is not restored because of the severity of the ischemic injury in the centre of the ischemic zone one would expect to see little or no accumulation of mRNA for these stress-induced genes. Indeed, when the left carotid artery was occluded for 120 minutes, *Hsp70* mRNA accumulation was not detected by *in situ* hybridization (Figure 2.2a). Similar results have been reported in severe global ischemia. When the coronary flow was reduced to 1 ml/minute or less, *Hsp70* mRNA in ischemic rat hearts was not detected by Northern analysis (Myrmel et al., 1994). As mentioned earlier, examination of the *c-fos*, *c-jun*, *Hsc70* and *Hsp70* labeled areas after 90 minutes of reperfusion (Figure 2.6) revealed a small unlabeled area in the centre of the labeled area. Staining with 2,3,5-triphenyl tetrazolium chloride demonstrated that the unlabeled central area corresponded to the necrotic area (Figure 2.3). Whether the different cell types in the area expressing *Hsp70* mRNA (Figure 2.4) and other stress gene products were reversibly injured or irreversibly injured and targeted for death is still speculative. In the brain, focal ischemia produced concentric zones that have been delineated by detection of *Hsp70* expression: a necrotic area in the center of the ischemic core with no *Hsp70* mRNA and a surrounding region expressing *Hsp70* mRNA in neurons (Kinouchi et al., 1993). This area could further be divided into an internal region where no Hsp70 protein was detected and an external region where Hsp70-immunoreactivity was present. It has been suggested that the region expressing Hsp70 protein will survive the ischemic insult (Kinouchi et al., 1993). It is suggested that a

rapid synthesis of Hsp70 may therefore be sufficient to enhance myocardial survival following ischemic injury.

# CHAPTER 3:

# OVEREXPRESSION OF THE HUMAN Hsp70 IN TRANSGENIC MICE

# INCREASES MYOCARDIAL RECOVERY AFTER GLOBAL ISCHEMIA

**Introduction**

Transgenic mice expressing high levels of specific gene products have increased resistance to cerebral ischemia (MacMillan et al., 1993; Yang et al., 1994) or have enhanced myocardial function (Milano et al., 1994). In fact, heat shock-induced changes in gene expression have been associated with cellular protection and improved function for more than a decade (Mitchell et al., 1979; Li and Werb, 1982; Landry and Chrétien, 1983). More recently, in isolated and perfused heart studies, heat shock treatment and expression of heat shock proteins were associated with improved post-ischemic myocardial contractile recovery (Currie et al., 1988; Karmazyn et al., 1990; Yellon et al, 1992). In *in vivo* experiments, myocardial infarct size was significantly reduced in heat shock-treated animals (Donnelly et al., 1992; Currie et al., 1993; Marber et al., 1993). And indeed, a direct correlation has now been shown between the amount of the highly inducible member of the Hsp70 family of stress-induced proteins and the degree of myocardial protection, as measured by reduction in infarct size (Hutter et al., 1994).

While heat shock treatment is associated with myocardial protection, it is difficult to know whether the protection is due to the overexpression of one protein, several proteins, or some other unrelated adaptive process. For example, heat shock treatment also increased the activity of the antioxidative enzyme, catalase, and blockade of catalase activity reduced heat shock-induced protection against ischemia in rat and rabbit hearts (Karmazyn et al., 1990; Currie et al., 1993). Overexpression of Hsp70

alone was demonstrated to protect cells from thermal injury and increase cell survival

(Angelidis et al., 1991; Li et al., 1991). The use of transgenic mice engineered to

express constitutively high levels of the human inducible Hsp70 might clarify Hsp70

contribution to myocardial protection. The purpose of this study was to determine the

role of Hsp70 in myocardial protection against ischemic injury.


## Materials and methods

### Transgenic mice

Mice were cared for in accordance with the *Guide to the Care and Use of*

*Experimental animals* of the Canadian Council on Animal Care. Transgenic mice and

their littermates were a generous gift from Dr. G.N. Pagoulatos (Laboratory of General

Biology, University of Ioannina Medical School, Ioannina, Greece). Transgenic mice

were produced by a collaborative work between Dr. H. Kazlaris and Dr. G. Kollias

(Department of Molecular Genetics, Hellenic Pasteur Institute, Athens, Greece) and

Dr. C.E. Angelidis and Dr. G.N. Pagoulatos (Laboratory of General Biology,

University of Ioannina Medical School, Ioannina, Greece). Original inbred CBA and

C57B1/6 mice were obtained from IFFA-CREDO (France) and maintained in the

Hellenic Pasteur Institute's facilities. CBA x C57B1/6 transgenic mice contained the

Apr-HS70 expression vector (Angelidis et al., 1991) which consists of the human

inducible *Hsp70* gene under the regulation of the *β-actin* promoter. Southern blot

analysis of tail biopsies confirmed the presence of the transgene. Additional S1

nuclease analysis from animal tissues, including heart and brain, demonstrated the

general distribution of the transgene. In transgenic hearts, the copy number of the

transgene was estimated to be approximately 50.

## Protein analysis

Hearts, livers and kidneys from four transgenic and four non-transgenic mice

were analyzed by one-dimensional and two-dimensional gel electrophoresis.

Hyperthermic treatment (42°C rectal temperature for 15 minutes) was applied to 2

transgenic and 2 non-transgenic mice. The hyperthermia-treated mice were allowed to

recover for 30 minutes before injection of the radiolabel. Hyperthermia-treated and

control mice were given ip an injection of 0.25 mCi of L-[$^{35}$S]-methionine (New

England Nuclear, specific activity > 1,000Ci/millimole) and 2 hours later, overdosed

with sodium pentobarbital and organs excised. Mice receiving hyperthermic treatment

were injected with radioactive label 30 minutes after the end of the heat shock.

## One-dimensional gel electrophoresis

Proteins (40 μg protein/lane) were separated by electrophoresis on sodium

dodecyl sulfate-polyacrylamide (7.5%) gel. Gels were stained with Coomassie brilliant

blue R, destained and photographed. Gels were then processed for fluorography and

exposed to X-OMAT AR Kodak film.

## Two-dimensional gel electrophoresis and Western blot analysis

Protein samples from heart ventricular muscle were analyzed by two-

dimensional sodium dodecyl sulfate-polyacrylamide gel electrophoresis (O'Farrell,

1975) as previously described (Currie, 1986). For Western blotting, proteins were

transferred to Immobilon-P membranes (Millipore, Toronto, Ontario) at 200 mA,

overnight, according to the method of Towbin et al. (1979). Blots were incubated in

PBS containing 5% skim milk powder to block non-specific binding sites on the

membranes (Jonhnson et al., 1984). Blots were immunoreacted, firstly, with a 1:7,500

dilution of a rabbit (#799) anti-human Hsp70 polyclonal antibody graciously provided

by Dr. R.M. Tanguay (Université Laval, Québec). Secondly, blots were incubated in a

1:500 dilution of a peroxidase-conjugated goat anti-mouse IgG. 4-chloro-1-naphthol

was used as the substrate for the visualization of the reaction product. Blots were

counterstained with amido black to show other proteins.

### Langendorff perfusion protocol

Adult mice (25-35 grams) were anesthetized with sodium pentobarbital (50

mg/kg body weight, ip). Hearts were excised rapidly, immersed in ice-cold buffer and

the aorta was cannulated on a Langendorff apparatus. Hearts were retrogradely

perfused with Krebs-Henseleit buffer consisting of (mM) NaCl 120, NaHCO$_3$ 20, KCl

4.63, KH$_2$PO$_4$ 1.17, MgCl$_2$ 1.2, CaCl$_2$ 1.25, and glucose 8 (pH 7.4), at a flow of 3

ml/minute for 30 minutes. The perfusion system was regulated, during the pre-

ischemic, ischemic and reperfusion periods, at 37 °C using a water-jacketed chamber

and coil. Hearts were made ischemic by turning off the buffer flow for 30 minutes and

then reperfused with buffer for 30 minutes at a rate of 3 ml/minute. Hearts were paced

at 390 beats/minute (400 stimulations/minute, 3.3 volts, 3 milliseconds) with a Grass

S44 stimulator (Grass Instruments, Quincy, Massachusetts) (Sakai et al., 1983; Ng et

al., 1991). Mechanical activity was measured throughout each perfusion experiment

according to previously described methods (Currie et al., 1988; Karmazyn et al.,

1990). Briefly, apicobasal displacement was obtained by attaching a Grass FT.03 strain

gauge transducer to the heart apex. The transducer was positioned to yield an initial

resting tension of 0.3 gram. Perfusion pressure was measured using a Gould P23 ID

pressure transducer. Recordings of mechanical activity and pressure were recorded on

a Grass Model 7 polygraph.

### Creatine kinase analysis

Creatine kinase release from hearts was measured in the effluent buffer.

Samples were collected during the last minute of pre-ischemic perfusion, and at 1, 5,

10, 20 and 30 minutes of reperfusion. Creatine kinase content was determined as

described in chapter 2.

### Catalase assay

Catalase activity was determined in hearts using a modification of previously

described methods (Beers and Sizer, 1952; Cohen et al., 1970). Briefly, 100 mg of

heart was homogenized in 0.5 ml ice-cold Tris sucrose buffer containing 0.25 M

sucrose, 10 mM Tris-HCl, 1 mM EDTA, 0.5 mM dithiothreitol, 0.1 mM

phenymethylsulfonyl fluoride at pH 7.5. Samples were centrifuged at 3,000g for 15

minutes and the supernatants recovered. Protein concentration of the supernatants was

determined by the method of Lowry et al. (1951). Samples of heart supernatants (40

μg of protein) were brought to 1 ml volume with an assay buffer of 35 mM phosphate

buffer pH 7.2 and 0.02% triton X-100. The enzymatic reaction was started by adding

30 μl of 1% hydrogen peroxide to the assay mixture. Catalase activity was estimated

by measuring the rate of $H_2O_2$ consumption at 240 nanometers in a Beckman DU 50

spectrophotometer. Optical density was recorded at 15, 25, 35, 45, and 55 seconds and

the velocity of the reaction (slope) was determined.

## Statistical analysis

All values expressed are mean±SEM. Differences were determined by

comparison of the calculated test statistic with the two-tailed significance limits of

Student's distribution.

## Results

### Protein analysis

One-dimensional gels stained with Coomassie brillant blue R and fluorograms of

livers and kidneys of transgenic and non-transgenic mice, and of heat shocked

transgenic and non-transgenic mice are presented in Figure 3.1. Comparison of liver or

kidney from non-transgenic (Figure 3.1A) and transgenic mice (Figure 3.1B) revealed

no apparent difference in the steady state level of proteins separated by one-dimension

gel electrophoresis. Following hyperthermic treatment (lanes 2 and 4), there appears to

be a similar increased accumulation of several protein bands in the liver and kidney of

non-transgenic and transgenic mice (compare Figure 3.1A with Figure 3.1B). *De novo*

protein synthesis was assessed by L-[$^{35}$S]methionine radiolabeling of heat shocked and non-heat shocked transgenic and non-transgenic mice. L-[$^{35}$S]methionine incorporation was similar for livers and for kidneys of transgenic and non-transgenic mice (data not shown). Fluorography revealed no apparent difference in protein synthesis between the non-transgenic (Figure 3.1C) and transgenic mice (Figure 3.1D). Both non-transgenic and transgenic mice appeared to respond in a similar fashion to the hyperthermic treatment (lanes 2 and 4). Several protein bands have increased incorporation of L-[$^{35}$S]methionine in liver and kidney (compare Figure 3.1C with Figure 3.1D).

L-[$^{35}$S]methionine labeled proteins from hearts were separated by two-dimensional gel electrophoresis and processed to reveal the proteins synthesized during the 2 hour-labeling period. Fluorograms of L-[$^{35}$S]-methionine-labeled proteins revealed little or no detectable basal level of synthesis of either the mouse inducible Hsp70 or the human Hsp70 (transgene product) in the non-transgenic or transgenic mouse hearts (Figure 3.2A and Figure 3.2B). Following the hyperthermic treatment, the mouse inducible Hsp70 was easily detectable, in the non-transgenic mouse hearts (Figure 3.2C). In the transgenic mouse hearts there was also an increase in the mouse inducible Hsp70 while there was little or no increase in the human Hsp70 gene product (Figure 3.2D; compare with Figure 3.3D).

Western analysis of two-dimensional gels of normal and hyperthermia treated, non-transgenic and transgenic hearts is presented in Figure 3.3. Two-dimensional gel electrophoresis analysis and Western-blot analysis revealed the presence of one spot in

protein extracts from non-transgenic hearts and two spots in protein extracts from

Hsp70-transgenic hearts (compare Figure 3.3A and 3.3C). One of the two protein

spots showed similar molecular weight and iso-electric point as that from the non-

transgenic mice and correspond to the endogenous mouse Hsp70. The other protein

spot showed a similar molecular weight but a more acidic iso-electric point and

correspond to the transgene human Hsp70 (Figure 3.3C). A small amount of the mouse

inducible Hsp70 was detectable in the non-stressed non-transgenic mouse heart (Figure

3.3A, A'). Following hyperthermic treatment, the accumulation of the mouse inducible

Hsp70 was visibly increased (Figure 3.3B, B') in the non-transgenic mouse hearts.

Interestingly, from the non-stressed transgenic mouse heart, the mouse inducible Hsp70

and the human Hsp70 gene products fractionated into discrete spots (Figure 3.3C, C').

A small accumulation of the mouse inducible Hsp70 was detectable adjacent to a larger

accumulation of the human Hsp70 gene product. Following hyperthermic treatment, in

the transgenic mouse hearts, the accumulation of the mouse inducible Hsp70 was

visibly increased while there was no discernible change in the amount of the human

Hsp70 transgene product (Figure 3.3D, D').

*Contractile force*

Contractile force for isolated hearts from both groups of animals is illustrated in

Figure 3.4. None of the parameters differed during the equilibration period (t = 0 - 30

minutes). The resting tension was adjusted to 0.3 gram during and at the end of the

equilibration period. Ischemia produced a complete reduction in contractile force

within 15 minutes (t = 45 minutes) with a progressive increase in resting tension. The

physiological data during ischemia did not differ significantly between the non-

transgenic and transgenic hearts although the rate of relaxation and the rate of

contraction appeared to decrease more slowly in transgenic hearts (data not shown).

However, substantial differences in contractile recovery were evident following

restoration of the normal flow. After 30 minutes of reperfusion (t = 90 minutes),

hearts of transgenic animals had significantly increased recovery of force ($3.4\pm0.8$

versus $1.6\pm0.5$ $10^{-3}$N) (Figure 3.4), rate of contraction ($891.8\pm97.9$ versus

$461.9\pm137.2$ $10^{-3}$N/second), and rate of relaxation ($923.0\pm101.4$ versus $513.4\pm127.9$

$10^{-3}$N/second) when compared with non-transgenic hearts (data not shown). Relative to

pre-ischemic values, the recovery of force was 70% versus 29%, rate of contraction

was 87% versus 48%, and rate of relaxation was 83% versus 50% for the transgenic

versus control hearts. In addition, the differences tended to increase according to the

reperfusion time. Resting tension changed in a similar fashion for both groups.

### Creatine kinase release

Creatine kinase release during the pre-ischemic perfusion was undetectable in

hearts from transgenic and non-transgenic mice. Upon reperfusion, a high level of

creatine kinase was released from non-transgenic hearts ($67.7\pm23.0$ Units/ml) as

compared to the transgenic hearts ($1.6\pm0.8$ Units/ml) (Figure 3.5). At 5 minutes of

reflow, the level of creatine kinase was considerably reduced in the non-transgenic

hearts and was similar to that of the transgenic hearts (13.7±8.8 versus 19.9±10.1

Units/ml, respectively).

## Catalase activity

Catalase activity was not significantly different in the transgenic and non-

transgenic hearts (1.75 ± 6.46 (4) versus 0.83 ± 4.84 (6) Units/mg protein; (n);

p=not significant; respectively).

## Perfusion pressure

Figure 3.6 illustrates pressure data from transgenic and non-transgenic mouse

hearts. Before ischemia, no significant difference was noted between non-transgenic

(107±12 mmHg) and transgenic hearts (73±14 mmHg) (t=30 minutes). Upon

reperfusion (t=60 minutes), perfusion pressure appeared to be higher for non-

transgenic hearts than transgenic hearts and the two experimental groups (non-

transgenic versus transgenic hearts) differed significantly (109±12 mmHg versus

69±11 mmHg; respectively) after 10 minutes of reflow (t=70 minutes).

Figure 3.1. Sodium dodecyl sulfate -polyacrylamide gels of L-[$^{35}$S]methionine pulse-labeled livers and kidneys. Non-transgenic and transgenic mice with and without heat shock treatment were given an intraperitoneal injection of 0.25 mCi of L-[$^{35}$S]methionine and killed 2 hours later. Mice receiving hyperthermic treatment (lanes 2 and 4) were injected with radioactive label 30 minutes after the end of the 15-minute heat shock. Labeled proteins (40 μg protein/lane) from liver (lanes 1 and 2) and from kidneys (lanes 3 and 4) were separated by sodium dodecyl sulfate-polyacrylamide gel electrophoresis. Coomassie brillant blue R stained gels (A, B) were exposed to autoradiography film (C,D). A, C: Non-transgenic mouse; B, D: transgenic mouse. The top arrow points to the 90-kDa heat shock protein and the bottom arrow to Hsp70.
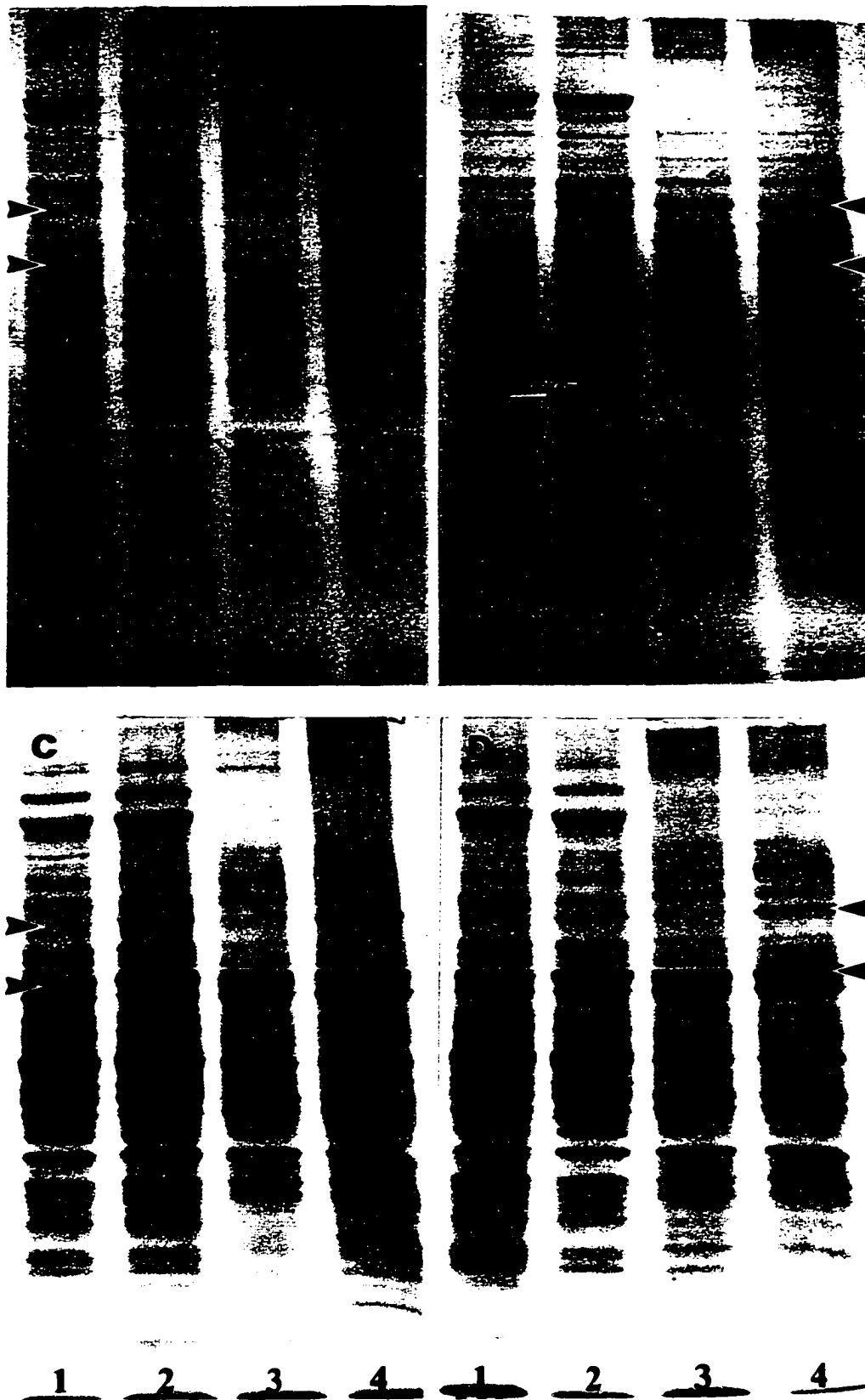
Figure 3.1

Figure 3.2. Sodium dodecyl sulfate -polyacrylamide gels of L-[$^{35}$S]methionine pulse-labeled hearts. Proteins were labeled as described in Figure 3.2. Two-dimensional gel electrophoresis separated radiolabeled proteins (1 mg) extracted from hearts of control non-transgenic mouse (A), control transgenic mouse (B), heat shocked non-transgenic mouse (C), and heat-shocked transgenic mouse (D). The arrow points to the mouse Hsp70.
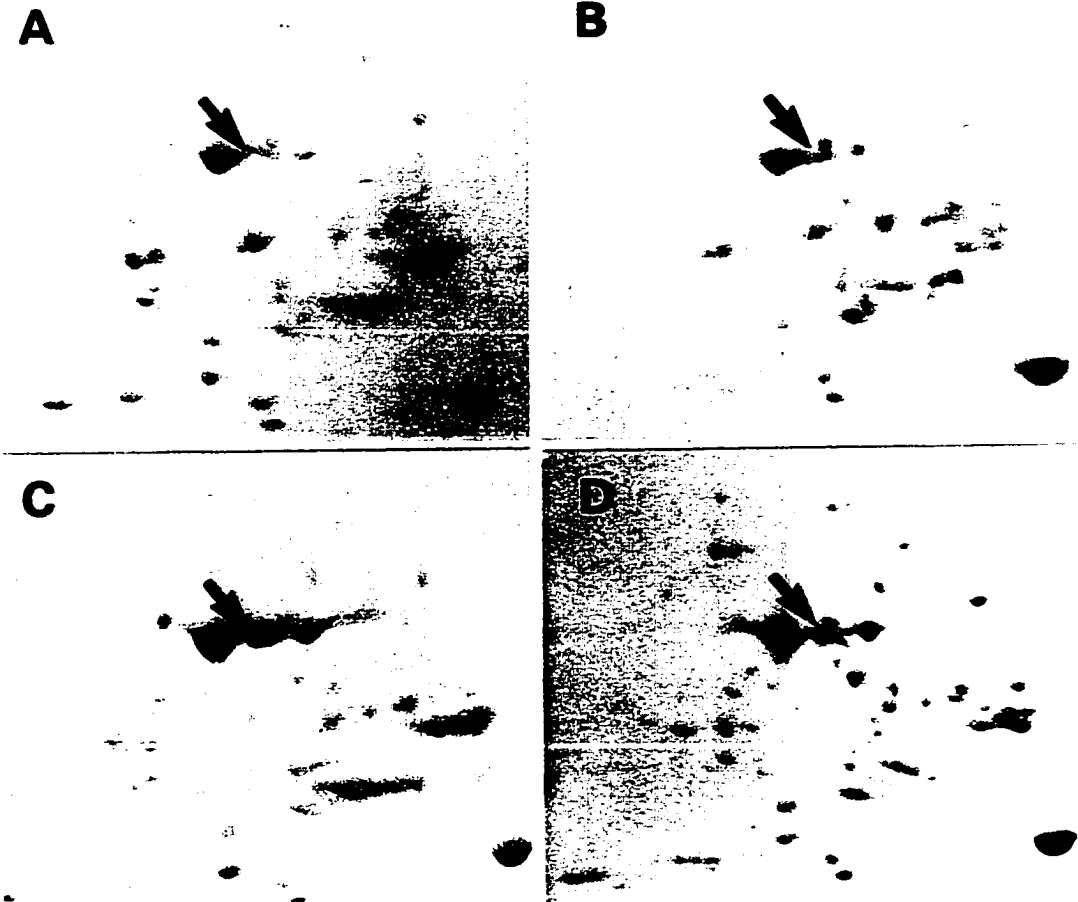
Figure 3.2

Figure 3.3. Western Blot analysis of 70-kDa heat shock proteins in mouse hearts.

Two-dimensional gel electrophoresis separated proteins (1 mg) extracted from hearts of

control non-transgenic mouse (A), heat shocked non-transgenic (B), control transgenic

(C), and heat-shocked (D) mice. After the proteins were transferred to the membrane,

it was immunoreacted with a rabbit polyclonal anti-human Hsp70 antibody. The

secondary antibody was a peroxidase-conjugated goat anti-rabbit IgG. 4-Chloro-1-

naphtol was used as the substrate for the immunoreaction (right). Blots were

counterstained with amido black (left) to show other proteins. The arrows indicate the

mouse Hsp70 (left) and the human Hsp70 (right).
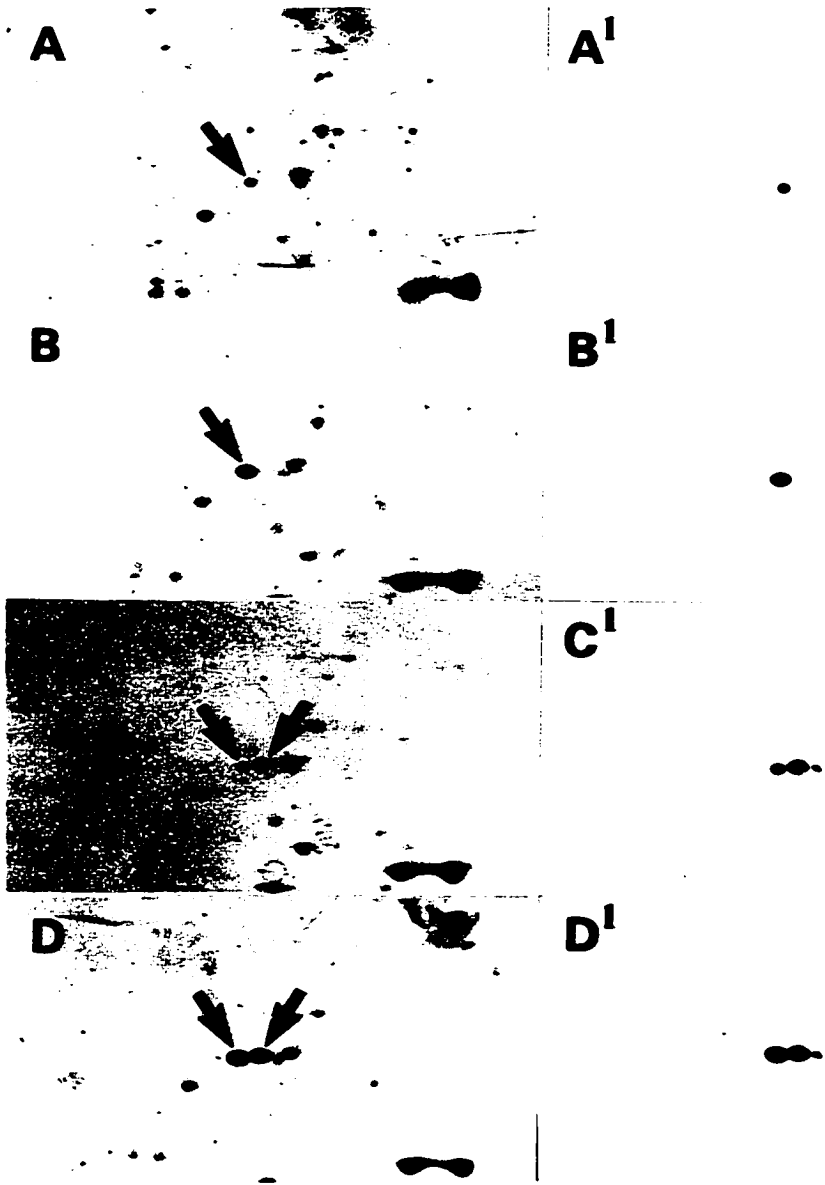
Figure 3.3

Figure 3.4. Contractile force of isolated non-transgenic and transgenic hearts during

perfusion. Hearts from non-transgenic (triangles) and transgenic (squares) were

retrogradely perfused with Krebs-Henseleit buffer at 37°C. Hearts were made ischemic

by turning off the buffer flow for 30 minutes (horizontal bar) and then reperfused for

30 minutes. Apicobasal displacement was measured by force transducer attached to the

heart apex and positioned to yield an initial resting tension of 0.3 gram. Each point

represents the mean±SEM of at least 11 animals. *P<0.05 from non-transgenic values

using Student's t-test for unpaired data.
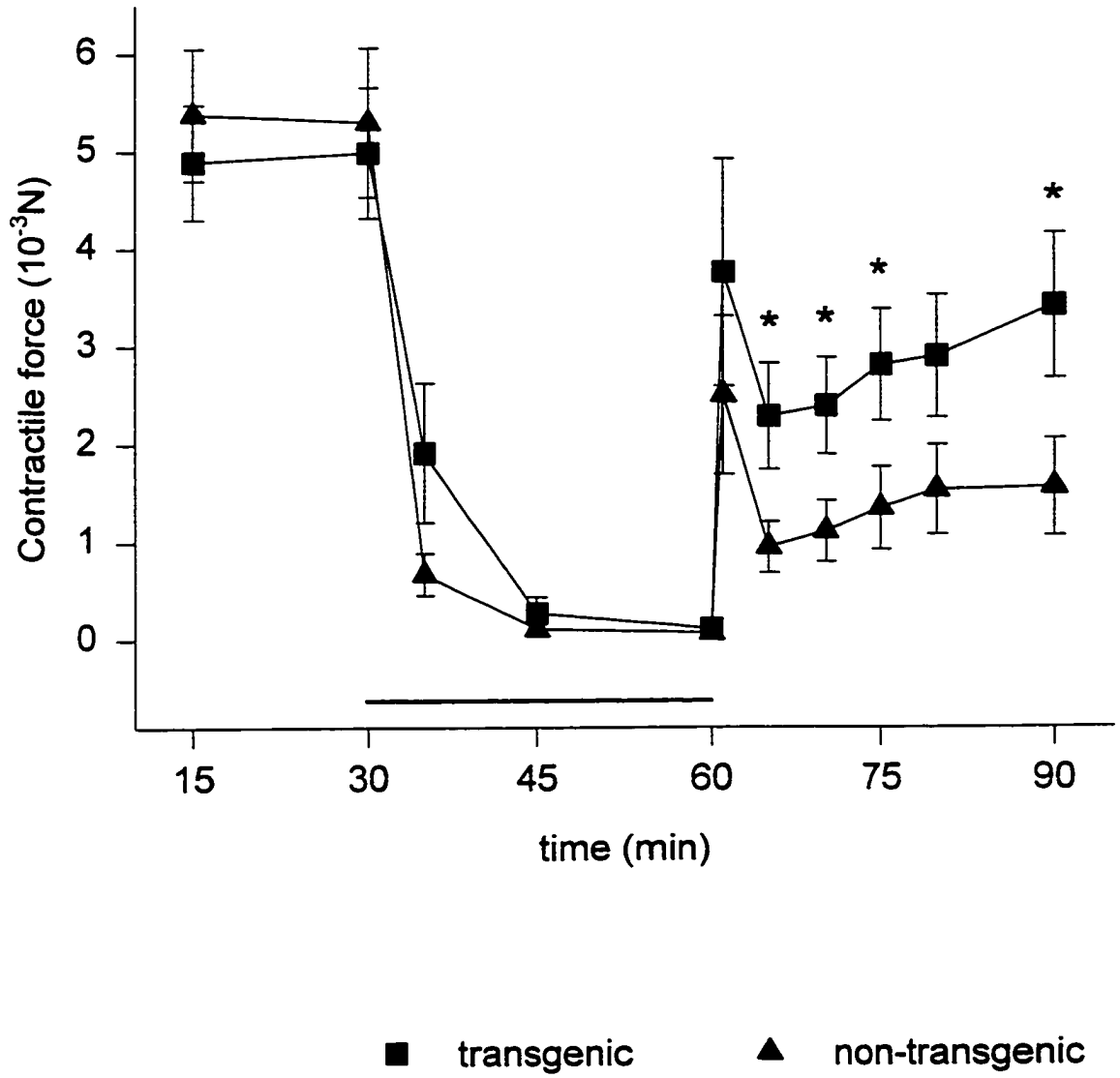
Figure 3.4

Figure 3.5. Creatine kinase release in effluent buffer of isolated hearts during

perfusion. Creatine kinase release was measured at the last minute of the pre-ischemic

period and during the reperfusion hearts from non-transgenic (triangles) and transgenic

mice (squares). Each point represents the mean±SEM of at least 11 animals. *P<0.05

from control values using Student's t-test for unpaired data.
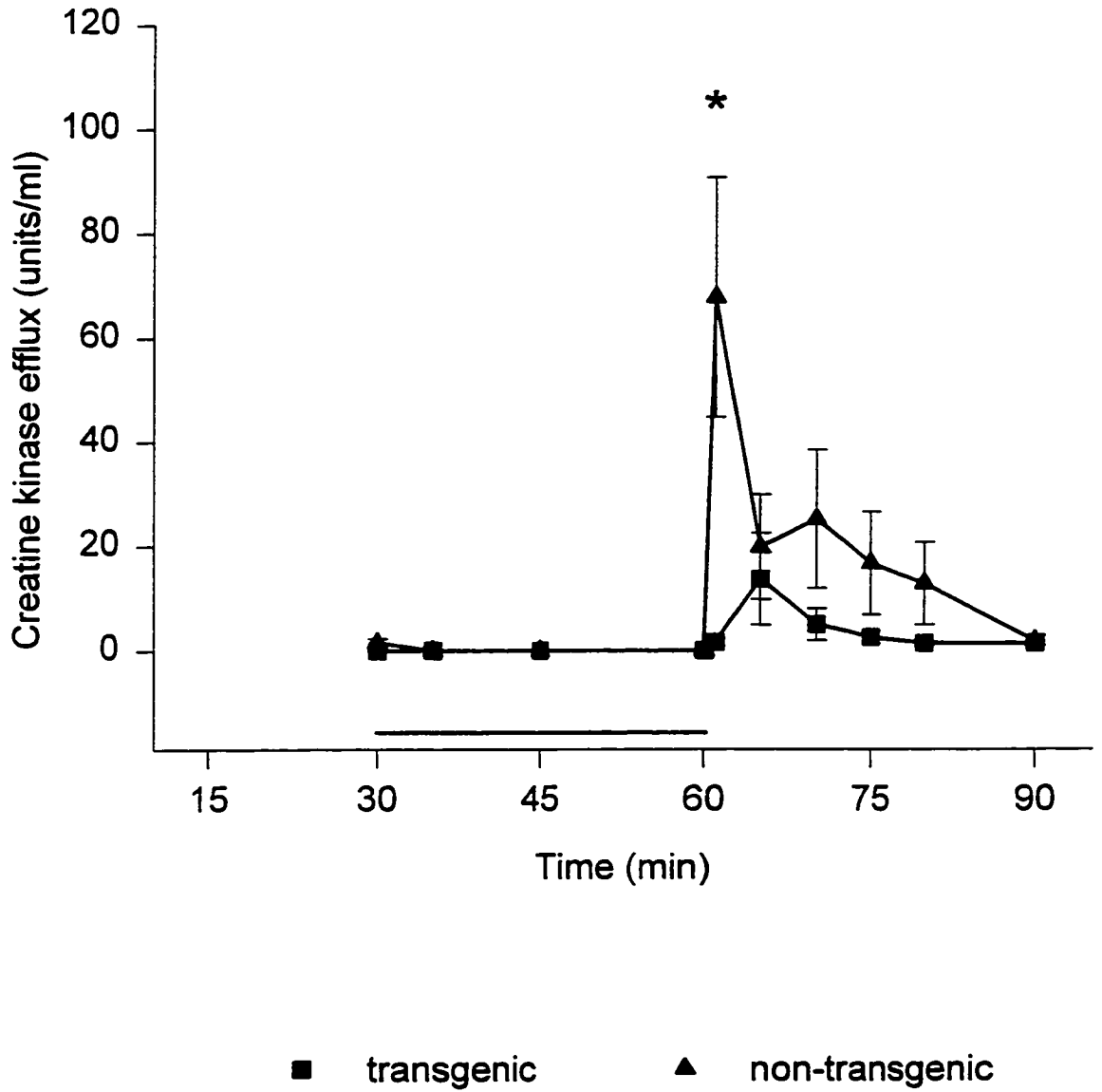
Figure 3.5

Figure 3.6. Perfusion pressure from isolated hearts during perfusion. Hearts from non-

transgenic (triangles) and transgenic (squares) were subjected to ischemia for 30

minutes (horizontal bar). Hearts were perfused at a fixed flow of 3 ml/minute during

pre- and post-ischemic periods. Each point represents the mean±SEM of at least 11

animals. *P<0.05 from control values using Student's t-test for unpaired data.

▲ transgenic     ■ non-transgenic
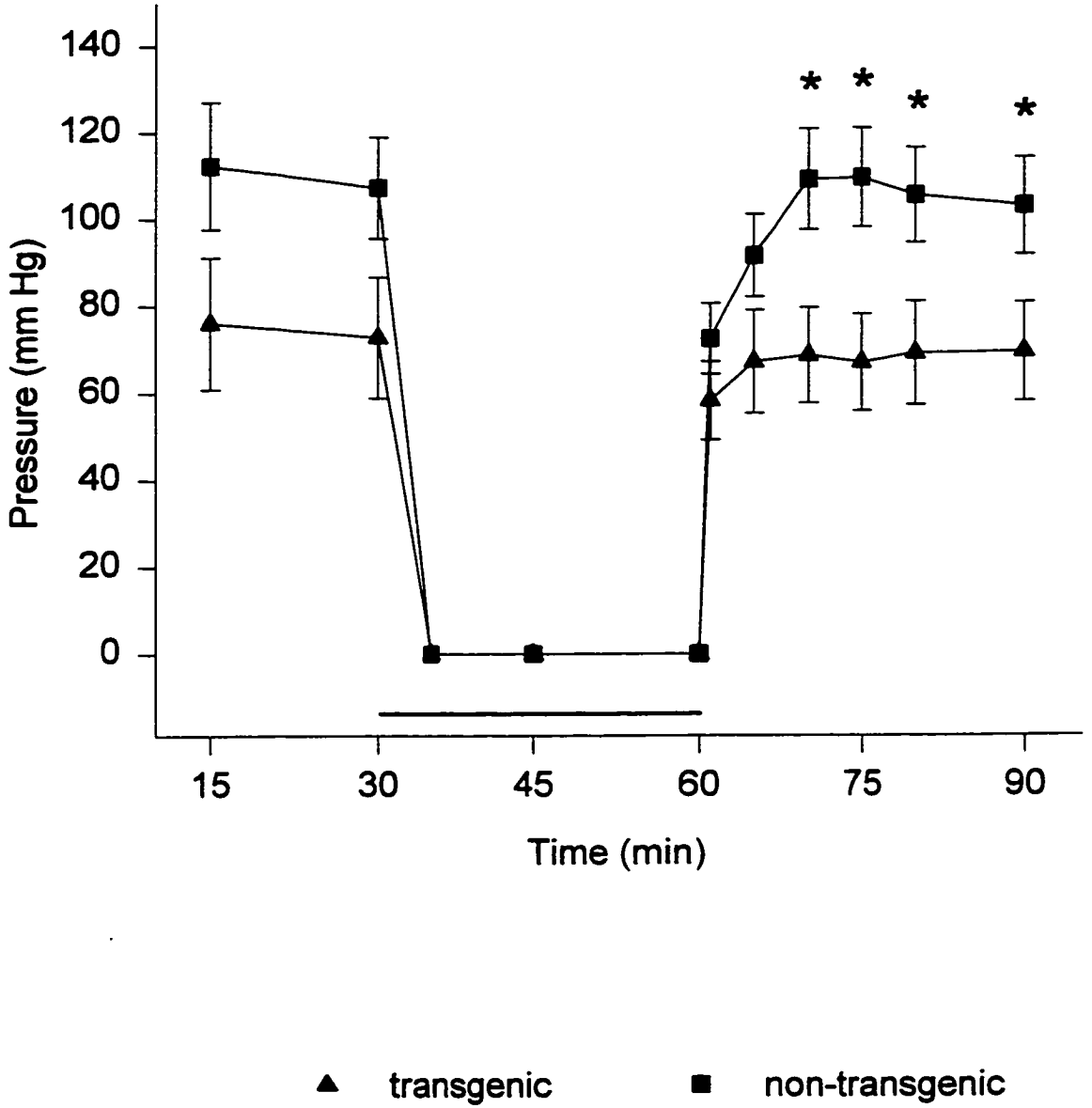
Figure 3.6

**Discussion**

Persistent overexpression of the human Hsp70 gene product in mice does not result in observable changes in basal protein content or synthesis except for the expression of the human Hsp70 protein. Following hyperthermic treatment the transgenic mouse liver, kidney and heart have a similar increase in synthesis of a small number of proteins as the non-transgenic mouse tissues. However, overexpression of the human Hsp70 gene product conveys a significant protection to isolated hearts following ischemic injury, during reperfusion. The transgenic hearts had significantly improved post-ischemic contractile recovery and significantly lower release of creatine kinase.

In previous studies, elevated levels of the highly inducible member of the Hsp70 family of stress induced proteins has been associated with improved post-ischemic recovery (Currie et al., 1988; Karmazyn et al., 1990; Yellon et al., 1992) and with reduction in infarct size in hearts (Donnelly et al., 1992, Currie et al., 1993; Marber et al., 1993). As mentioned earlier, there appears to be a direct correlation between the amount of the inducible Hsp70 and the amount of myocardial protection (Hutter et al., 1994). With transgenic mice overexpressing the inducible human Hsp70, assessment of the contribution of the inducible Hsp70 to cellular protection could be examined.

*Stress response of transgenic mice*

Overexpression of a single protein may induce drastic changes in cell morphology, physiology and cell and animal survival (Discroll, 1992; Gagliardini et

83

al., 1994). However, in the case of the mice studied here, there was no obvious

developmental or morphological differences between the non-transgenic and the

transgenic mice. At the biochemical level, protein analysis revealed no clear

differences in protein profiles of tissues from non-transgenic and transgenic mice.

Even after heat shock treatment, the transgenic tissues respond in a similar fashion as

the non-transgenic tissues with the increased synthesis of several heat shock proteins

(Figures 3.1 and 3.2). Comparison of the two-dimensional gel fluorograms (Figure

3.2) and the Western blots (Figure 3.3) revealed that after heat shock treatment, the

human transgene was not induced while the endogenous mouse gene was induced. It

should also be noted that a small amount of the mouse inducible Hsp70 was present in

the non-heat shocked non-transgenic and transgenic mouse hearts. The primary

antibody used for the Western analysis is extremely sensitive and detects very small

accumulations of the protein. While the mouse inducible Hsp70 was detectable by

Western analysis, its synthesis, as revealed by fluorography, was below a clearly

detectable level in the non-heat shocked hearts. At the protein level it seemed that

transgenic and non-transgenic mice did not differ except for the presence of the human

Hsp70.

Hsp70 has been reported to autoregulate its own expression in a negative

feedback loop (Morimoto, 1993). Hsp70 transcription depends on the availability of

heat shock transcription factor (HSF). Hsp70 binds to the HSF, thereby maintaining

the HSF in an inactive form. In the transgenic model examined here, however, high

levels of human Hsp70 did not alter the mouse Hsp70 constitutive expression in hearts

(Figures 3.2 and 3.3). Moreover, synthesis of the mouse inducible Hsp70 following

heat shock appeared in transgenic and non-transgenic mice. It may be that the human

Hsp70 was not able to bind the mouse HSF and regulate mouse Hsp70 transcription.

Indeed, the mouse Hsp70 and human Hsp70 are not identical. These proteins could be

resolved into discrete spots by two-dimensional gel electrophoresis.

### Transgenic mice and myocardial ischemia

The contractile data revealed no significant difference during the pre-ischemic

perfusion period. While there was no significant difference in contractile force during

the ischemic period, the contractile force of the transgenic hearts appeared to decline

more slowly compared to the non-transgenic hearts. While the temperature of the

perfusion apparatus was regulated at 37°C, the temperature of the hearts may have

decreased slightly during the ischemic period. However, it is unlikely that such a

decrease in temperature would have contributed to the apparent difference in contractile

force during the ischemic period since conditions were similar for the transgenic and

non-transgenic hearts. Significant differences between transgenic and non-transgenic

hearts appeared upon reperfusion. The earliest indication of protection was at 1 minute

of reperfusion. The non-transgenic hearts released a large amount of creatine kinase,

indicating cellular and membrane disruption, while the transgenic hearts released almost

no creatine kinase (Figure 3.5). The contractile force, the rate of contraction and the

rate of relaxation were higher during recovery in mice overexpressing the human

Hsp70 (Figure 3.4). Almost all hearts in both groups recovered contractile force with 1

minute of reperfusion. For both groups, initial contractile force was strong and then

declined at 5 minutes of reperfusion. This decline in contractile force between 1 and 5

minutes of reperfusion may be indicative of free radical injury. The transgenic hearts

clearly had better recovery of contractile force, both initially and over the 30 minute-

reperfusion period.

The perfusion pressure was not significantly different during the pre-ischemic

perfusion period. However, it should be noticed that there was trend of the pre-

ischemic perfusion pressure to be higher in non-transgenic than in transgenic mice

(Figure 3.6). During the reperfusion period, when flow rate was regulated at 3.0

ml/minute, the transgenic hearts had a significantly lower perfusion pressure. At

present it is unclear whether the lower perfusion pressure was a result of the transgene

product in the cells of the microvessels. However, it was previously reported that prior

heat shock treatment did tend to lower the perfusion pressure in isolated rat hearts

(Karmazyn et al., 1990). A low perfusion pressure might indicate vasodilatation

leading to an improved myocardial perfusion.

The presence of human Hsp70 in the transgenic hearts seemed to play a role in

the improved post-ischemic contractile recovery. With reperfusion and the introduction

of oxygen, oxygen free radicals are generated, and membranes are disrupted by lipid

peroxidation. The release of creatine kinase appears to be the result of such injury.

While the human Hsp70 seemed to be involved in reducing this injury, it is unclear

whether the human Hsp70 was involved directly or indirectly. Studies of human Hsp70 transfected myocytes have shown increased resistance to hypoxic or metabolic stresses mimicking ischemia (Williams et al., 1993; Mestril et al., 1994). One possibility is that human Hsp70, by its abilities to renature protein, modifies the activity of enzymes such as antioxidants, that can protect cells from free radical injury. While there is no direct evidence that Hsp70 can change the enzymatic activity of antioxidants, catalase activity (Karmazyn et al., 1990) and reduced glutathione (Yellon et al., 1992) have been reported to be increased after heat shock treatment. In the present experiments, catalase activity did not appear to be increased in the transgenic compared to non-transgenic hearts. However, conclusions about this low catalase activity should be made cautiously, since these measurements were determined in transgenic and non-transgenic hearts that were stored at -80°C for several weeks.

Insights into the role of human Hsp70 can be suggested by analyzing the myocardial contractility during reperfusion. Firstly, the apparent stronger contractile force recovery at 1 minute of reperfusion suggests that there were more myocytes surviving after the 30 minute-ischemic interval. Secondly, contraction rate and relaxation rate of transgenic hearts progressively increased during reperfusion while the non-transgenic hearts progressively decreased (data not shown). This suggests that reperfusion injury was less in the transgenic hearts. One might argue that human Hsp70 protected myocytes against anoxia-induced cell death and increased the resistance of myocytes to oxidative injury. Hsp70 may bind to proteins denatured

during ischemia and promote refolding or renaturation to normal configurations upon reperfusion.

These experiments with transgenic mice strongly suggest that an elevated level of the inducible Hsp70 plays a role in cell survival and recovery following ischemic injury.

# CHAPTER 4:

## OVEREXPRESSION OF THE HUMAN Hsp70 IN TRANSGENIC MICE

## INCREASES RESISTANCE TO CEREBRAL ISCHEMIA

The results presented in this chapter have been submitted for publication in Cell Stress and Chaperones.

**Introduction**

Whole body hyperthermia (41.5 ± 0.2°C) for 15 minutes significantly reduced

ischemic cerebral damage in male rats (Chopp et al., 1989). In that study, occlusion of

both common carotid arteries in combination with hypotension (blood pressure

decreased to about 50mmHg) for 7.5 minutes produced cell death in several regions of

the forebrain such as in the subiculum, hippocampus (CA1 and CA2), cerebral cortex

and dorso-lateral striatum (Chopp et al., 1989). However, when the ischemic insult

occurred 24 hours after heat shock treatment, fewer necrotic neurons were detected in

the CA1 and CA2 hippocampal layer, in the inferior frontal cortex and in the dorso-

lateral striatum. Similarly, heat shock treatment reduced CA1 damage induced by 5

minute-global ischemia in gerbils (Kitagawa et al., 1991b).

A similar tolerance to ischemic injury has been observed following pre-

treatment with a brief ischemic episode (Kitagawa et al., 1990, 1991a; Simon et al.,

1993; Glazier et al., 1994). A brief transient global ischemic insult reduced the extent

of hippocampal cell loss induced by a subsequent severe global ischemia (Kitagawa et

al., 1990, 1991a) and the infarct volume after permanent middle cerebral artery

occlusion (Simon et al., 1993). Similarly, a brief focal ischemic episode could protect

against subsequent damage produced by a global ischemic injury (Glazier et al., 1994).

This 'ischemic tolerance' phenomenon has been associated with the synthesis of the

inducible Hsp70 (Kirino et al., 1991; Nishi et al., 1993; Simon et al., 1993; Glazier et

al., 1994). Recently, the acquisition of 'ischemic tolerance' was inhibited by

intraventricular injection of specific antibodies against Hsp70 and by blocking Hsp70 synthesis with quercetin (Nakata et al., 1993). However, a direct role for Hsp70 in cerebral tolerance to ischemic injury has still to be established.

As reported in Chapter 3, in the heart, overexpression of the human Hsp70 in transgenic mice protected against ischemic injury. Myocardial resistance against ischemia was also observed in two other strains of transgenic mice overexpressing the rat Hsp70 (Marber et al., 1995) or the human Hsp70 (Radford et al., 1996), confirming the results showed in Chapter 3. In this Chapter, the same strain of transgenic mice (as in Chapter 3) overexpressing the human Hsp70 was used to examine *in vivo* the role of Hsp70 in cellular protection against cerebral ischemia.

## Material and methods

### Animals

Mice were cared for in accordance with the *Guide to the Care and Use of Experimental animals* of the Canadian Council on Animal Care. Adult Hsp70-transgenic mice and their non-transgenic littermates were shipped from the Hellenic Pasteur Institute, Athens, Greece (see chapter 3). Transgenic mice were generated by a collaborative work between Dr. Kollias and Dr. Pagoulatos.

### Protein analysis

Two-dimensional SDS-PAGE analysis was performed as described previously (see chapter 3). Brains from transgenic and non-transgenic mice were removed, and

placed in lysis buffer and stored at -20°C. Approximately 1 mg of protein was loaded

on each gel. After migration, proteins were transferred onto a immobilon membrane.

Western blot analysis of the membrane was performed using the polyclonal antibody

specific to the inducible Hsp70 (gift from Dr. Tanguay, Université Laval) that detected

both the mouse and the human Hsp70 (see chapter 3). After immunostaining,

membranes were counterstained with amido black to reveal other proteins.

*Middle cerebral artery occlusion*

The procedure for middle cerebral artery occlusion in mice in the present study

was similar to that described in rats by Zea Longa et al. (1989). Adult mice were

anesthetized under halothane. The body temperature was measured via rectal

thermometer and kept between 37-37.5°C throughout the surgery and recovery from

anaesthesia. The internal and external right carotid arteries were exposed via a midline

incision. The external carotid artery was ligated distally and clamped proximally. A 6-

0 monofilament nylon suture with a blunted end was inserted in the external carotid

artery and pushed in to reach the clamp. At that time, a silk thread was put around the

external carotid tightening the nylon suture in the external carotid artery. The clamp

was removed and the nylon suture was slid through the internal carotid artery until

resistance was felt (about 11 mm) (Figure 4.1). At that point, occlusion of the middle

cerebral artery was obtained. The right internal carotid artery was ligated with the

nylon suture left in place. Skin incision was sutured and the animal was returned to its

cage. Twenty four hours after surgery, mice were killed and perfused intracardially

with 5 ml of 100 mM PBS followed by 10 ml of 4% paraformaldehyde made in 100

mM phosphate buffer. Dissection confirmed the presence of the monofilament in the

anterior cerebral artery. The brain was extracted and post-fixed overnight in 2%

paraformaldehyde in phosphate buffer.

*Histology*

Paraformaldehyde-fixed brains were cut on a vibratome at 50 μm thickness.

The extent of the ischemic damage was assessed by computer image analysis of cresyl

violet (0.1%) stained sections. Stained sections were digitalized using a JVC TKF-F7

300U video camera attached to a dissecting scope or a Leitz orthoplan microscope.

Images were captured on a Macintosh computer using Adobe Photoshop 3.0.5 software.

Digitalized images were analyzed using NIH Image 1.60 software. Prints were made

using a 300 dpi continuous tone dye-sublimation 8600 XLS Kodak printer.

*Statistical analysis*

The size of the area of infarction was measured as a percent of the area of the

coronal section at the level of the anterior commissure. Data were examined for

significant differences using the two-tailed significance limits of Student's t-

distribution.

Figure 4.1. Diagram of the cerebrovascular anatomy in the mouse. Middle cerebral

artery occlusion is obtained by insertion of a 6-0 monofilament nylon suture in the

internal carotid artery. The insertion site of the suture is indicated by the arrow.

Vessel size is disproportionately enlarged for clarity. The territory of middle cerebral

artery irrigation is indicated by the shading on the left side of the diagram (modified

from Zea Longa et al., 1989).

anterior cerebral artery

MIDDLE CEREBRAL ARTERY

posterior communicating artery

posterior cerebral artery

superior cerebellar artery

internal carotid artery

mastoid bulba

basilar artery

pterygopalatine artery

lingual artery

NYLON FILAMENT

external maxillary artery

superior thyroid artery

occipital artery

external carotid artery

common carotid artery

Figure 4.1

## Results

### Protein analysis

Proteins from control brains were separated by two-dimensional gel electrophoresis and transferred onto immobilon membranes (Figure 4.2). Two-dimensional gel patterns were similar for non-transgenic and transgenic mice, except for the presence of a 70-kDa protein in transgenic mice (Figure 4.2.A and Figure 4.2.C). Western blot analysis of the brain of non-transgenic mice revealed one immunoreactive spot for Hsp70 (Figure 4.2.B). Western blot analysis of brain extracts of transgenic mice revealed two immunoreactive spots for Hsp70 (Figure 4.2.D). One of these spots was located in the identical position as the single spot seen in the non-transgenic mouse brain. The second spot had a similar molecular weight but slightly more acidic iso-electric point, corresponding to the human Hsp70 (Figure 4.2).

### Ischemic injury in Hsp70-transgenic mice and non-transgenic littermates

Middle cerebral artery occlusion induced a large infarct throughout the ipsilateral hemisphere in non-transgenic (Figure 4.3.A) and in transgenic (Figure 4.3.B) mice. While no pyknotic nuclei were observed in the contralateral hemisphere (Figure 4.3.C), many pyknotic nuclei were observed in the ipsilateral striatum and cortex of non-transgenic (Figure 4.3.D) and transgenic (Figure 4.3.E) mice. Analysis of the infarct area revealed that the percentage of infarct area was not significantly different between transgenic and non-transgenic mice ($29.2\pm4.0\%$ vs. $21.6\pm8.6\%$, respectively; $n=5$ in each group) (Table 3).

However, all five non-transgenic mice showed injured neurons in the ipsilateral hippocampal pyramidal cell layers as detected by cresyl violet staining (Table 3). CA1 pyramidal neurons in all five non-transgenic mice showed abnormal morphology characterized by pyknotic nuclei in the ipsilateral side but not in the contralateral side (Figure 4.3.C).

While all Hsp70-transgenic mice showed a large infarct area, the morphology of hippocampal neurons (Table 3), including CA1 hippocampal neurons, was similar to that of non-injured hippocampal neurons (as observed in contralateral hemispheres or in non-ischemic mice). None of the five Hsp70-transgenic mice showed pyknotic nuclei in the hippocampal pyramidal layers (Figure 4.3.D; Table 3).

Figure 4.2. Western Blot analysis of 70-kDa heat shock proteins in mouse brain.

Two-dimensional gel electrophoresis separated proteins (1 mg) extracted from control

brains of non-transgenic mouse (A, B) and Hsp70-transgenic mice (C, D). After the

proteins were transferred to the membrane, it was immunoreacted with a rabbit

polyclonal anti-human Hsp70 antibody followed by a peroxidase-conjugated goat anti-

rabbit IgG. 4-chloro-1-naphtol was used as the substrate for the immunoreaction (B,

D). Blots were counterstained with amido black (A, C) to show other proteins. The

arrow indicates the human Hsp70 (hHSP). The acidic (+) and basic (-) sides of the

gels are indicated. High molecular weight proteins are at the top of the gels.

A

−

B

+

C

−

D

+

hHSP
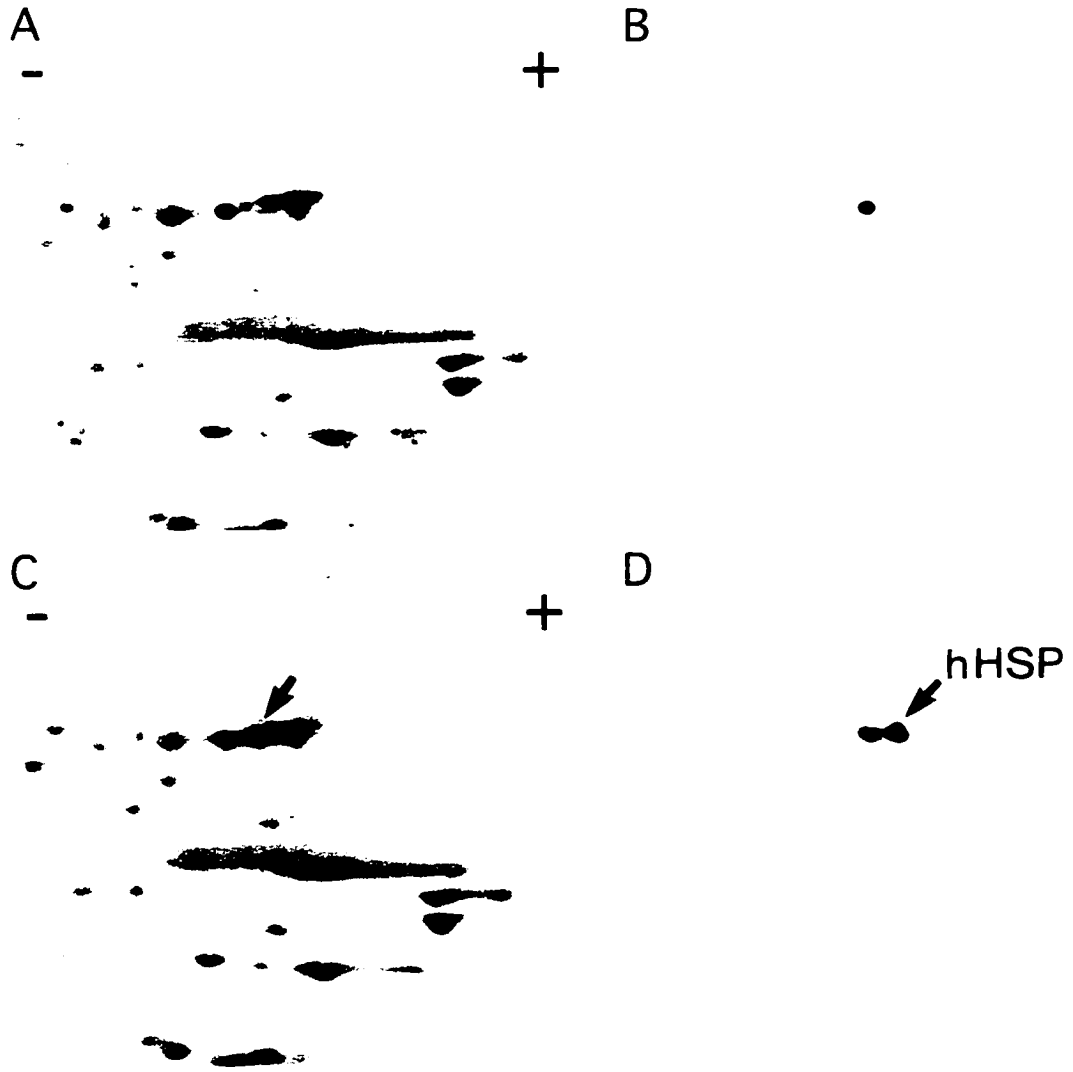
Figure 4.2

Figure 4.3. Cellular damage induced by middle cerebral artery occlusion in Hsp70-transgenic mice and non-transgenic littermates. Twenty four hours after permanent occlusion of the middle cerebral artery brain were stained with cresyl violet. Infarct area was observed in the ipsilateral hemisphere (right side of the brain) in non-transgenic (A) and transgenic (B) mice. While no pyknotic neurons were observed in the contralateral hemisphere of both non-transgenic (C, left boxed area in A) and transgenic mice, many pyknotic neurons were observed in the ipsilateral striatum and cortex of both non-transgenic (D, right boxed area in A) and transgenic (E, boxed area in B) mice. In non-transgenic mice, sections through the hippocampus showed many pyknotic CA1 neurons (F; section from the same animal as in A) while no pyknotic CA1 neurons in transgenic mice (G; section from the same animal as B). Scale bars equal C-E, 200 μm; F and G, 100 μm.
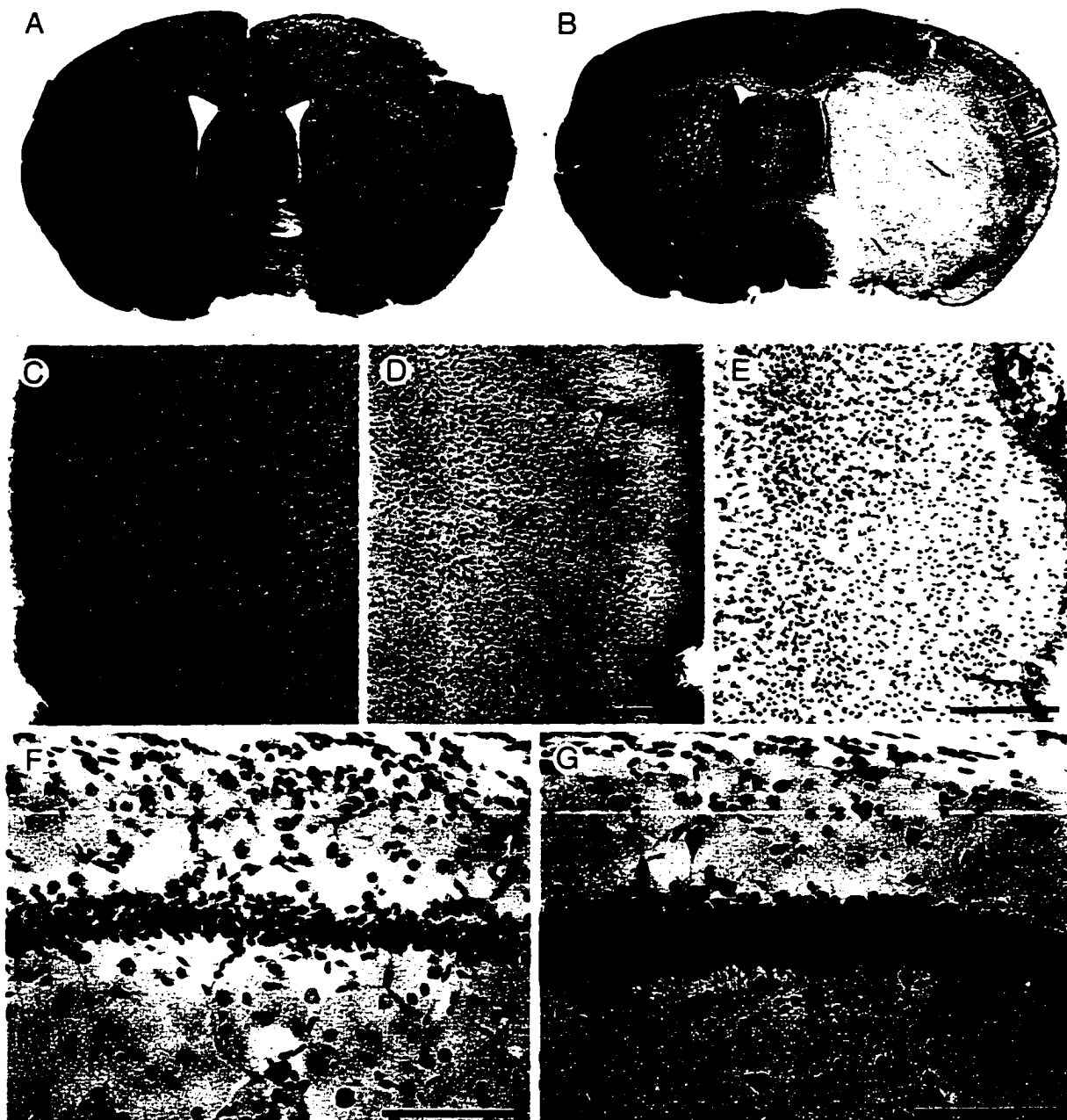
Figure 4.3

Table 3. Comparison of ischemic damage between Hsp70-transgenic mice and their non-transgenic littermates.

| Mice strain | % infarct size | Proportion of mice with pyknotic nuclei in | | |
| --- | --- | --- | --- | --- |
| | | CA1 | CA3 | DG |
| Hsp70-transgenic | 29.2±4.0 | 0/5 | 0/5 | 0/5 |
| non-transgenic | 21.6±8.6 | 5/5 | 2/5 | 3/5 |

The size of the area of infarction was measured as a percent of the area of the coronal section at the level of the anterior commissure. Measures of the infarct area were examined for significant differences using the two-tailed significance limits of Student's distribution. DG, dentate granule cell layer.

## Discussion

Western blot analysis revealed that the human Hsp70 was constitutively expressed in the brain of transgenic mice. After 24 hours of permanent occlusion of the middle cerebral artery, infarct areas were not significantly different between transgenic and non-transgenic mice. However, pyknotic neurons were observed in the CA1 hippocampal layer of non-transgenic mice but not in Hsp70-transgenic mice. These results suggest that Hsp70 expression might not protect neurons against severe ischemic injury but might protect neurons against excitotoxicity-induced delayed cell death.

### Protein analysis

Western blot analysis of two-dimensional gels revealed that the endogenous mouse Hsp70 was present in the brain of non-transgenic mice and that the human Hsp70 was constitutively expressed in addition to the endogenous mouse Hsp70 in brains of transgenic mice. Since the transgene was under the regulation of a β-actin promoter, it seemed likely that the human Hsp70 was expressed in most cell types of the brain, including neurons that have been shown to express constitutively β-actin (Ulloa and Avila, 1996).

### Hsp70-induced protection

Following middle cerebral artery occlusion, there was no significant difference in infarct areas between Hsp70-transgenic and non-transgenic mice. This result differs with those reported in the heart. Hearts of mice overexpressing the human Hsp70 (the same strain of mice as that used in this study) have been reported to be more resistant to

global ischemia and had a greater recovery of contractility than the non-transgenic

littermates (Chapter 3). Similar results have also been reported using other strains of

transgenic mice overexpressing the rat Hsp70 (Marber et al., 1995) or the human

Hsp70 (Radford et al., 1996). These results suggested that the exogenous Hsp70

expressed in transgenic mouse hearts was functional and could participate in the

mechanisms of ischemic protection and functional recovery of the myocardium. Studies

on ischemic protection in the heart have also reported that although heat shock

treatment, and the concomitant expression of Hsp70, improved myocardial recovery

after 30 minutes of ischemia, no improvement was detected in heat shock-treated

animals after 45 minutes of ischemia (Currie et al., 1993). It was suggested that the

injury induced by 45 minutes of ischemia was too severe to be reduced by heat shock

treatment and the concomitant expression of Hsp70. By comparison, in the present

study, one can argue that 24 hour-permanent occlusion of the middle cerebral artery

induced an ischemic injury too severe to be reduced by Hsp70 expression.

Interestingly, middle cerebral artery occlusion also induced hippocampal injury

in 100% of the non-transgenic mice. All non-transgenic mice (n=5) showed neuronal

pyknosis in the hippoccampal pyramidal cell layers, especially in CA1 hippocampal

layer. In contrast, no Hsp70 transgenic mice (n=5) showed pyknotic nuclei in the

hippocampal layers, including in the CA1. This result strongly suggests that expression

of the human Hsp70 might play a role against neuronal injury in the hippocampus.

Hippocampal injury following middle cerebral artery occlusion has also been detected by Hsp70 mRNA accumulation in hippocampal neurons in the mouse (Kamii et al., 1994) and in the rat (Welsh et al., 1992; Kinouchi et al., 1994). Two types of injuries can be responsible for pyknosis in the hippocampus. Firstly, a reduction of the blood supply to the hippocampus can occur. Since blood supply to the hippocampus partially originates from the internal carotid artery via posterior communicating artery in rats (Coyle, 1976), dogs, cats and other mammals (Nilges, 1944), and mice (Barone et al., 1993), it is possible that permanent occlusion of the internal carotid artery reduced the overall blood supply to the hippocampus. In fact, in at least one strain of mice, the Circle of Willis is incomplete and occlusion of the carotid arteries causes extensive cerebral ischemia (Barone et al., 1993). In that case, Hsp70 overexpression in transgenic mice induced resistance of hippocampal neurons against ischemic injury. Secondly, injury of hippocampal neurons might also be related to excitotoxicity caused by ischemic injury of afferent cortical projections such as the piriform cortex and the entorhinal cortex (Kinouchi et al., 1994). Interestingly, heat shock treatment and the concomitant Hsp70 expression have been shown to increase neuronal resistance to excitotoxic injury *in vitro* (Lowenstein et al., 1991; Rordorf et al., 1991). In the present study, although the causes for hippocampal injury after permanent occlusion of the middle cerebral artery are still to be determined, it remains that 100% of Hsp70-transgenic mice showed resistance of hippocampal neurons against injury. This result

suggests that overexpression of Hsp70 might protect neurons against ischemic and/or

excitotoxic injury.

# CHAPTER 5:

## DISTRIBUTION OF Hsp27 IMMUNOREACTIVITY

## IN THE ADULT RAT NERVOUS SYSTEM

## Introduction

In the rat brain, while heat shock proteins were originally reported to be induced

following injury such as heat shock, trauma or ischemia (White, 1980; Currie and

White, 1981; Freedman et al., 1981; Brown, 1983; Nowak, 1985), constitutive

expression of heat shock proteins has also been demonstrated in neuronal and non-

neuronal cells of the nervous system under normal conditions and during development.

For example, in mammals, the constitutive 70-kDa heat shock protein (Hsc70), also

known as clathrin-uncoating ATPase (Chappell et al., 1986), has been observed in

several types of neurons, including motoneurons and interneurons of the spinal cord

(Manzerra and Brown, 1992a), Purkinje cells in the cerebellum (Manzerra and Brown,

1992b) and pyramidal cells of the hippocampus (Abe et al., 1991).

Another heat shock protein, Hsp27 (referred to as Hsp25 in the mouse), has also

been identified in the mammalian nervous system during development (Gernold et al.,

1993). Hsp27 is expressed in large neurons of the spinal cord and in cerebellar

Purkinje neurons in rat embryos (Gernold et al., 1993). However, in adult mouse

brain, Hsp27 was not detected by Western blot analysis even though it was detected in

other organs such as the bladder and the stomach (Tanguay et al., 1993; Klemenz et

al.,1993). In keeping with the apparent absence of Hsp27 in the adult mouse brain,

Hsp27 immunoreactivity was not detected in the cerebral cortex or in the cerebellum of

adult rats (Wilkinson and Pollard, 1993). These results suggested that in the normal

brain, Hsp27 was only expressed during development. However, using a different

antibody and studying serial sections of the entire forebrain, we observed some Hsp27-immunoreactive cells in the adult rat brain (Plumier et al., 1996). These latter observations suggested that some glial cells, and possibly neurons, might constitutively express Hsp27 and that Hsp27 expression in the nervous system may not have been detected by Western blot analysis because of the small number of Hsp27-immunopositive cells. Constitutive expression of Hsp27 is particularly interesting because Hsp27 has been shown to provide some non-neuronal cell lines with tolerance to heat-induced cell death (Landry et al., 1989; Lavoie et al., 1993a), as well as resistance to oxidative stress (Huot et al., 1995; Mehlen et al., 1995; Huot et al., 1996) and apoptosis (Mehlen et al., 1996b). These observations suggest that the constitutively expressed Hsp27 might also have a neuroprotective role.

In this study, we have examined the constitutive expression of Hsp27 in the adult rat central nervous system by immunohistochemistry in order to determine its distribution and whether it is associated with specific classes of neurons. Two-dimensional gel electrophoresis and Western blot analysis were used to confirm the specificity of the polyclonal antibody used for immunohistochemistry and to determine the phosphorylation state of Hsp27.

## Material and methods

Twelve adult male Sprague-Dawley rats (225-300 grams; Charles River Inc., Québec) cared for in accordance with the *Guide to the Care and Use of Experimental*

*animals* of the Canadian Council on Animal Care were killed under halothane and

perfused with 100 mM phosphate-buffered saline (PBS) followed by 4%

paraformaldehyde in 100 mM phosphate buffer. Brain, spinal cord and trigeminal and

dorsal root ganglia were removed and post-fixed overnight in 2% paraformaldehyde in

phosphate buffer at 4°C. Tissues were then either immersed in 20% sucrose made up

in 100 mM phosphate buffer and sectioned at 50 μm on a freezing microtome, or

processed for paraffin embedding and cut at 10 μm on a rotary microtome.

### Hsp27 antibody

Western blot analyses and immunohistochemical studies (Head et al., 1994;

Plumier et al., 1996) have demonstrated that the rabbit polyclonal antibody raised

against the murine Hsp25 (StressGen Biotechnologies Corp., Victoria, British

Columbia, Canada) that was used in this study, specifically recognizes the rat homolog

protein, Hsp27.

### Two-dimensional gel electrophoresis and Western blot analysis

Cortical and spinal cord samples (n=2; each) were analyzed by two-dimensional

gel electrophoresis according to previously described methods (chapter 3) with only one

modification. A 12% SDS-polyacrylamide gel electrophoresis was used to improve the

resolution in low molecular range. For Western blot analysis, membranes were

incubated in PBS containing 5% skim milk powder and reacted overnight at 4°C with

the primary rabbit polyclonal antibody raised against the mouse Hsp25 (1:1,000;

StressGen Biotechnologies Corp.). After three PBS washes, membranes were

incubated one hour in PBS containing a peroxidase-conjugated goat antibody raised

against rabbit IgG (1:500; Vector Laboratories Inc., Burlingame, California, U.S.A.).

After three PBS washes, membranes were reacted in PBS containing 4-chloro-1-

naphthol (0.05% W/V). Membranes were photographed, counterstained with amido

black and photographed again.

### Hsp27 immunohistochemistry

Coronal, sagittal or horizontal 50 μm sections were rinsed three times, 10

minutes each, in PBS containing 0.2% Triton X-100. Sections were then incubated 30

minutes in 1% hydrogen peroxide in PBS, rinsed three times in PBS and incubated

overnight in primary rabbit polyclonal antibody raised against mouse Hsp25 (1:5,000;

StressGen Biotechnologies Corp.) made up in PBS containing 2% goat serum. The

following day, after three PBS washes, sections were incubated for one hour in

biotinylated secondary goat antibody raised against rabbit IgG (1:400; Vector

Laboratories Inc.). After three PBS washes, sections were incubated for one hour in

avidin-biotin-horseradish peroxidase complex (1:1000; Vector Laboratories Inc.) and

then washed three times in PBS. Sections were then incubated in PBS containing 0.3

mg/100 ml glucose oxidase, 40 mg/ml ammonium chloride and 200 mg/100ml β-D(+)

glucose (Sigma Chemical Co., St. Louis, Missouri, U.S.A.) and 0.05%

diaminobenzidine-tetrahydrochloride (Sigma Chemical Co.). After rinses, sections

were mounted on slides and dried overnight at room temperature. Then, sections were

processed through series of alcohol, cleared in xylene and coverslipped. Some sections

were counterstained with cresyl violet (0.1%) in order to visualize non-immunoreactive cells. No immunoreactivity was detected when the primary antibody was omitted in the overnight incubation.

Percentage of Hsp27-immunoreactive neurons in a given nucleus and estimation of the dimensions of Hsp27-positive neurons are means ± SEM calculated on measurements made in 3 rats (3 sections per measurement in each rat).

*Microscopy and image processing*

Sections were studied and photographed using bright-field, dark-field and differential interference contrast microscopy on a Zeiss Axoplan microscope. Some stained sections were digitalized as described in chapter 4.

**Results**

*Western blot analysis*

Two-dimensional gel electrophoresis and Western blot analysis demonstrated the absence of proteins immunoreactive to the polyclonal antibody raised against the mouse Hsp25 in the rat cortex (Figure 5.1A). In the spinal cord, three spots of a similar molecular weight but different iso-electric points were immunoreactive (Figure 5.1C). These three spots probably correspond to phosphorylated isoforms of Hsp27 because alkaline phosphatase treatment partially reduced the number of spots (data not shown). This antibody has been previously shown to cross-react specifically with the rat Hsp27 (Head et al., 1994; Plumier et al., 1996). The membranes shown in figures 5.1A and

C were counterstained to reveal the presence of non-immunoreactive proteins in cortex and in spinal cord extracts, respectively (Figures 5.1B and D).

*Immunohistochemistry for Hsp27*

Hsp27 immunoreactivity was observed in a subset of neurons and their processes in the rat brain stem (Figure 5.2), including the diencephalon, mesencephalon, pontine tegmentum and medulla oblongata. Neuronal staining was absent in the telecephalon. Hsp27 immunoreactivity was most intense in general somatic and special visceral efferent motoneurons while staining was sporadic in nuclei containing general visceral efferent neurons. The intensity of staining varied from cell to cell but was typically uniform throughout the cytoplasm of the cell and its processes. In some nuclei there was a wide range of intensities of staining whereas a more uniform staining was present in others. The extensive staining of dendrites of motoneurons was particularly striking, often extending beyond the boundaries of the motor nuclei. Certain sensory cranial nerve nuclei and their peripheral ganglia were also positive for Hsp27 immunoreactivity. Positively stained processes were differentially distributed in the laminae of the medullary and spinal dorsal horns, and subpopulations of sensory neurons in peripheral ganglia showed Hsp27 immunoreactivity. In the spinal cord, motoneurons and their processes were intensely stained.

In addition to neuronal staining, Hsp27 immunoreactivity was observed in non-neuronal cells (Figure 5.2A) such as occasional astrocytes, ependymal cells, cells and processes in the pia/arachnoid layer, and cells of the choroid plexus.

## Diencephalon

Neurons with Hsp27 immunoreactivity were identified in and around the arcuate nucleus (Figure 5.3). A few stained neurons were observed outside the lateral borders of the arcuate nucleus and in the median eminence (Figure 5.3A). Hsp27-positive neurons were typically multipolar, often exhibiting three or four primary dendrites with a few secondary branches, but there were also occasional fusiform neurons with two major dendrites (Figure 5.3B). The cells measured $14.1 \pm 0.8 \times 20.8 \pm 0.8$ $\mu$m in the transverse plane and $15.4 \pm 2.5 \times 24.2 \pm 2.7$ $\mu$m in the sagittal plane with dendrites extending up to 500 $\mu$m from the cell body. The neurons were distributed over a rostrocaudal distance of approximately 2.25 mm (Figure 5.3B) and were found primarily within the boundaries of the arcuate nucleus. Axons of a few of these neurons were identified but could only be followed a short distance.

## Mesencephalon

*Oculomotor and trochlear nuclei.* Motoneurons of the oculomotor and trochlear nuclei and their nerve fascicles showed Hsp27 immunoreactivity (Figure 5.4). Strong staining was observed in many but not all motoneurons in the motor nuclei of the oculomotor (Figures 5.4A and B) and trochlear (Figures 5.4C and D) nuclei. The intensity of staining of motoneurons ranged from very light to intense, with many not

showing detectable Hsp27 immunoreactivity (Figure 5.4D). Neuronal counts with the aid of dark-field, bright-field and differential interference contrast microscopy revealed that $39\pm3$ % of oculomotor and $51\pm5$ % of trochlear motoneurons were positive for Hsp27 immunoreactivity. Dendrites of the motoneurons of the oculomotor nucleus extended beyond the boundaries of the nucleus in a fan-like fashion for up to 700 $\mu$m, primarily in a ventrolateral direction, but also dorsally (Figure 5.4B) and laterally for 350-400 $\mu$m. Dendritic ramifications of trochlear motoneurons also extended beyond the boundaries of the nucleus and although less extensive than those of the oculomotor nucleus, medial and lateral branches extended over 450 $\mu$m beyond the boundaries of the nucleus. The proximal branches of the dendrites of both nuclei were smooth and gradually tapering whereas many of their distal branches were characterized by varicosities.

In keeping with the fact that many oculomotor and trochlear motoneurons did not have immunocytochemically detectable levels of Hsp27 immunoreactivity, numerous axons in the intracranial fascicles of the two nerves were not immunopositive.

*Mesencephalic nucleus of the trigeminal nerve.* A subset of large pseudo-unipolar neurons of the mesencephalic nucleus of the trigeminal nerve located at the lateral margin of the periaqueductal gray and in the rostral pontine tegmentum stained positively for Hsp27 (Figure 5.5). Staining was uniform throughout the cytoplasm and the proximal part of the axon was clearly stained in many of the cells (Figure 5.5B, C).

The intensity of staining however varied considerably and many of the mesencephalic neurons were not stained. Overall, 46±4 % of the sensory neurons showed Hsp27 immunoreactivity. Stained and unstained neurons were often in close proximity (Figures 5.5B and C).

## Pontine tegmentum

*Trigeminal motor nucleus.* Many motoneurons of the trigeminal motor nucleus (76±2%) and its accessory nucleus were intensely positive for Hsp27 (Figures 5.2A, 5.6, and 5.15A). The dendrites and axons of the motoneurons formed a rich plexus in the motor nucleus proper. Dendrites of the motoneurons radiated in all directions from the nucleus, including dorsally where they stopped abruptly at the border of the vestibular complex (Figure 5.5A). Some distal branches extended up to 650 $\mu$m from the motor nucleus and, laterally, they encroached upon the territory of the principal sensory nucleus of the trigeminal nerve (Figure 5.6B). The distal ends of trigeminal motoneuron dendrites frequently had a striking beaded appearance or tortuous endings.

*Abducens nucleus.* Many but not all motoneurons of the abducens nucleus were strongly stained for Hsp27 immunoreactivity (Figure 5.7), with positive staining being present in long dendrites, some with varicosities in their distal parts. These dendrites extended up to 400 $\mu$m ventrolaterally. An estimated 39±6% of abducens motoneurons were Hsp27-positive. Stained axons could be followed in the intracranial fascicles of the abducens nerve. Only some of the axons in the nerve fascicles showed Hsp27 immunoreactivity, again in reflection of the fact that not all motoneurons were stained.

*Facial nucleus.* Many (70±2%) motoneurons of the facial nucleus and their processes were strongly stained for Hsp27 (Figures 5.2, 5.8A, 5.8B, and 5.10A). Facial motoneuron dendrites extended in all directions beyond the boundaries of the nucleus. In figure 5.8A, dendritic ramifications were extensive medially and laterally, in the latter instance occasionally extending into the territory of the spinal trigeminal nucleus pars oralis (Figure 5.6C). Facial motoneuron dendrites also extended rostrally and caudally in the pontine reticular formation (Figure 5.8C) for up to 800 $\mu$m. Distal dendrites of facial motoneurons were frequently beaded or followed a twisted or tortuous course at their distal endings (Figures 5.6C and 5.8D). Neurons of the accessory facial nucleus also showed Hsp27 immunoreactivity (Figure 5.2A).

*Pontine reticular formation.* Hsp27 immunoreactivity was present in large neurons of the caudal pontine reticular nucleus and gigantocellular reticular nucleus at levels between the trigeminal and facial motor nuclei (Figure 5.8C). The neurons were large, measuring 34.9±5.3 x 49.8±1.5 $\mu$m, and were multipolar with smooth, tapering dendrites radiating in all directions in both the transverse and sagittal planes. Some multipolar reticular formation neurons were distributed among the ascending axons of facial motoneurons. The location of some Hsp27-positive neurons in the reticular formation between the facial nucleus and the trigeminal motor nucleus suggested that they correspond to the suprafacial nucleus (Semba and Egger, 1986).

*Other neurons.* Small positive neurons were observed adjacent to the abducens nucleus and the genu of the facial nerve (Figures 5.8A and B). These were located in a

position that suggested that they correspond to the inferior salivatory nucleus which contains parasympathetic preganglionic neurons.

*Principal sensory and spinal trigeminal nuclei.* Hsp27 immunoreactivity was widespread in the sensory nuclei of the trigeminal nerve (Figures 5.2B, 5.2C, 5.6A, 5.8A, and 5.9). This immunoreactivity appeared to correspond to central terminations of peripheral afferent fiber systems. In keeping with this, most neurons in the trigeminal ganglion stained positively for Hsp27 and heavy staining was present in the trigeminal nerve, its central rootlets and in the spinal trigeminal tract. In the trigeminal nerve and spinal trigeminal tract, stained axons were coarse relative to the fine ramifications in the principal sensory nucleus and subnuclei of the spinal trigeminal complex. In the principal sensory nucleus (Figure 5.6A), staining consisted primarily of fine processes and was light and relatively uniform with occasional denser patches. As well, Hsp27 immunoreactivity was present in the spinal trigeminal nucleus, partes oralis, interpolaris and caudalis. In the pars oralis (Figure 5.8A), there was widespread light staining of thick and thin fibers throughout the region with occasional denser patches. Staining in the pars interpolaris was similar to that in the pars oralis with, in addition, patches of strongly stained axon preterminal arborizations dorsomedially. In the pars caudalis, the pattern of staining was distinctly layered (Figure 5.9) with staining being relatively light adjacent to the spinal trigeminal tract, including lamina I. Hsp27 immunoreactivity in the substantia gelatinosa or lamina II of the medullary dorsal horn was heavy in the outer part of lamina IIo, very light in the inner part of

lamina IIo, and heavy in lamina IIi (Figures 5.9B and C). There was moderate staining in the outer part of lamina III while lamina IV had light neuropil staining as well as many thick heavily stained axons in its depths adjacent to the medullary reticular formation.

## Medulla oblongata

*Nucleus Ambiguus.* Hsp27 immunoreactivity was intense in motoneurons and processes in three major subdivisions of the principal column of the nucleus ambiguus, namely the compact, semicompact and loose formations (Figures 5.2A, 5.2B, and 5.10). There was little or no staining of neurons in the external formation of the nucleus ambiguus. The axons of nucleus ambiguus motoneurons were strongly stained, coursing dorsomedially and then ventrolaterally in intramedullary fascicles to exit the brain stem.

Strongly stained dendrites of compact formation motoneurons were oriented longitudinally and were largely restricted to the boundaries of the subnucleus. Dendrites of the semicompact formation radiated extensively ventrally and ventrolaterally in a fan-like fashion for over 700 $\mu$m throughout the lateral tegmental field of the medullary reticular formation (Figures 5.10B and 5.15C). The distal processes of these dendrites sometimes had numerous bead-like swellings along their course (Figure 5.15C). As well, the strong staining of longitudinally-oriented dendritic bundles (Figures 5.10B and C) was evident in the semicompact formation. The rostral and lateral part of the semicompact formation, the location of cricothyroid

motoneurons, also contained Hsp27-positive motoneurons. Dendrites of the loose formation formed longitudinal bundles between motoneuronal cell groups and also radiated in all directions into the surrounding medullary reticular formation, extending up to 600 $\mu$m from the motoneuronal cell column, often with striking beading distally.

*Hypoglossal nucleus.* Motoneurons in the hypoglossal nucleus, including the small group of genioglossus motoneurons (Figure 5.11B) outside the main nucleus (Aldes, 1995), were strongly positive for Hsp27 immunoreactivity and their efferent axons were strongly stained as they passed ventrally in the intramedullary fascicles of the hypoglossal nerve. Dendrites and axons in the neuropil of the nucleus were heavily stained and stained dendrites radiated widely for up to 900 $\mu$m beyond the boundaries of the nucleus (Figures 5.11 and 5.12). Distal dendrites frequently exhibited extensive beading, sometimes forming loose bundles (Figures 5.12A-C).

*The dorsal motor nucleus of the vagus nerve.* The dorsal motor nucleus of the vagus nerve contained scattered, lightly- to intensely-stained neurons with dendritic arbours ramifying throughout the motor nucleus (Figure 5.11) as well as occasionally into the overlying nucleus of the tractus solitarius. These Hsp27-positive neurons tended to be fusiform measuring $13.3 \pm 1.1 \times 24.0 \pm 2.8$ $\mu$m in the transverse plane and $12.4 \pm 0.6 \times 29.1 \pm 0.9$ $\mu$m in the sagittal plane. Counts of motoneuronal profiles by means of bright- and dark-field microscopy indicated that $26 \pm 3\%$ of the neurons were positive for Hsp27. Rostrally, there were some smaller Hsp27-positive cells that were

typical of preganglionic neurons projecting to structures innervated by the glossopharyngeal nerve.

*Medullary reticular formation.* There were a very few large, lightly-stained multipolar neurons in the medial reticular formation. In middle regions of the medial longitudinal fasciculus, Hsp27 immunoreactivity was present in a small population of thick axons. Staining of axons in the fasciculus could be followed from the level of the pontine reticular formation to the spinomedullary junction.

*The nucleus of the tractus solitarius.* The nucleus of the tractus solitarius had numerous fine and medium-sized axonal processes in several of its subnuclei (Figure 5.11). This staining was consistent with intense Hsp27-positive axonal staining in the tractus solitarius. In the rostral nucleus of the tractus solitarius, Hsp27 immunoreactivity was medium to heavy consisting of sharply defined axonal processes. At middle levels of the nucleus, Hsp27 immunoreactivity was present in the form of fine granular and preterminal axonal staining in the interstitial and central subnuclei (Figure.5.11A). Caudally, Hsp27 immunoreactivity was very strong in the dorsolateral and commissural subnuclei (Figure 5.11B) as well as in the subnucleus gelatinosus. Little or no staining was present in the ventral and ventrolateral subnuclei.

*Area postrema.* The area postrema had moderate Hsp27 immunoreactivity consisting of fine and coarse granular staining as well as smooth and varicose processes (Figure 5 11B).

*Dorsal column nuclei.* The gracile and cuneate nuclei were heavily stained for Hsp27 immunoreactivity (Figure 5.11B), the gracile being substantially more heavily stained than the cuneate. The fiber tracts of the dorsal columns were also very heavily stained with the gracile fasciculus being most heavily stained.

## Spinal cord

*Motoneurons.* General somatic motoneurons of the ventral horn were heavily stained at all levels of the spinal cord (Figures 5.13 and 5.14). Their dendritic arbors ramified extensively, the majority being smooth and tapering but beaded distal dendrites were also apparent. Many motoneurons in the ventral horn ($72\pm3\%$) showed Hsp27 immunoreactivity. Smaller cells within the motoneuronal cell groups were also unstained (Figure 5.15B). In the thoracic and upper lumbar segments, sympathetic preganglionic neurons in the intermediolateral cell column were stained but not all of them exhibited Hsp27 immunoreactivity (Figure 5.14D). Other cells such as the intermediomedial nucleus and central autonomic cells around the central canal were rarely and only faintly Hsp27-positive. All motoneuronal cell groups in the sacral spinal cord, including Onuf's nucleus, were strongly stained for Hsp27 immunoreactivity.

*Dorsal root ganglia, dorsal horn and dorsal columns.* Hsp27 immunoreactivity was present in the somata of dorsal root ganglion neurons (Figure 5.15D) and in the dorsal roots. In the spinal cord, the dorsal columns were Hsp27 positive with the gracile fasciculus being more heavily stained, especially with thick, intensely stained

axons. The laminae of the dorsal horn of the spinal cord were differentially stained but in patterns that differed somewhat from those observed in the medullary dorsal horn.

In middle levels of cervical spinal cord (Figure 5.13), Hsp27 immunoreactivity was present in lamina I mainly in the form of granular labeling. Lamina II was largely devoid of Hsp27 immunoreactivity except for staining of thick passing fibers that entered and ramified in lamina III (Figure 5.13B). Laminae IV and V did not exhibit Hsp27 immunoreactivity. The upper cervical spinal cord also had strong Hsp27 immunoreactivity in relatively thick commissural fibers passing dorsal to the central canal (Figure 5.13A). These crossing fibers originated from the medial division of the entering dorsal roots.

At a lower level of the cervical spinal cord as well as in the thoracic, lumbar and sacral spinal cord (Figure 5.14), Hsp27 immunoreactivity was present primarily in laminae I and III. In the sacral spinal cord, commissural fibers were also evident and afferent axons could be seen entering laminae V and approaching the dendritic fields of motoneurons in lamina VII, with their respective territories overlapping.

Figure 5.1. Western blot protein analysis of cerebral cortex and spinal cord of the adult rat. Proteins from the cerebral cortex (A and B) and from the spinal cord (C and D) were separated by two-dimensional gel electrophoresis and transferred onto immobilon membranes. The membranes were then reacted with a polyclonal rabbit antibody raised against the murine 25-kDa heat shock protein which recognized the rat homolog protein, Hsp27 (A and C). The same membranes were further reacted with amido black to reveal the presence of other proteins (B and D). The acidic (+) and basic (-) sides of the gels are indicated. High molecular weight proteins are at the top of the gels.
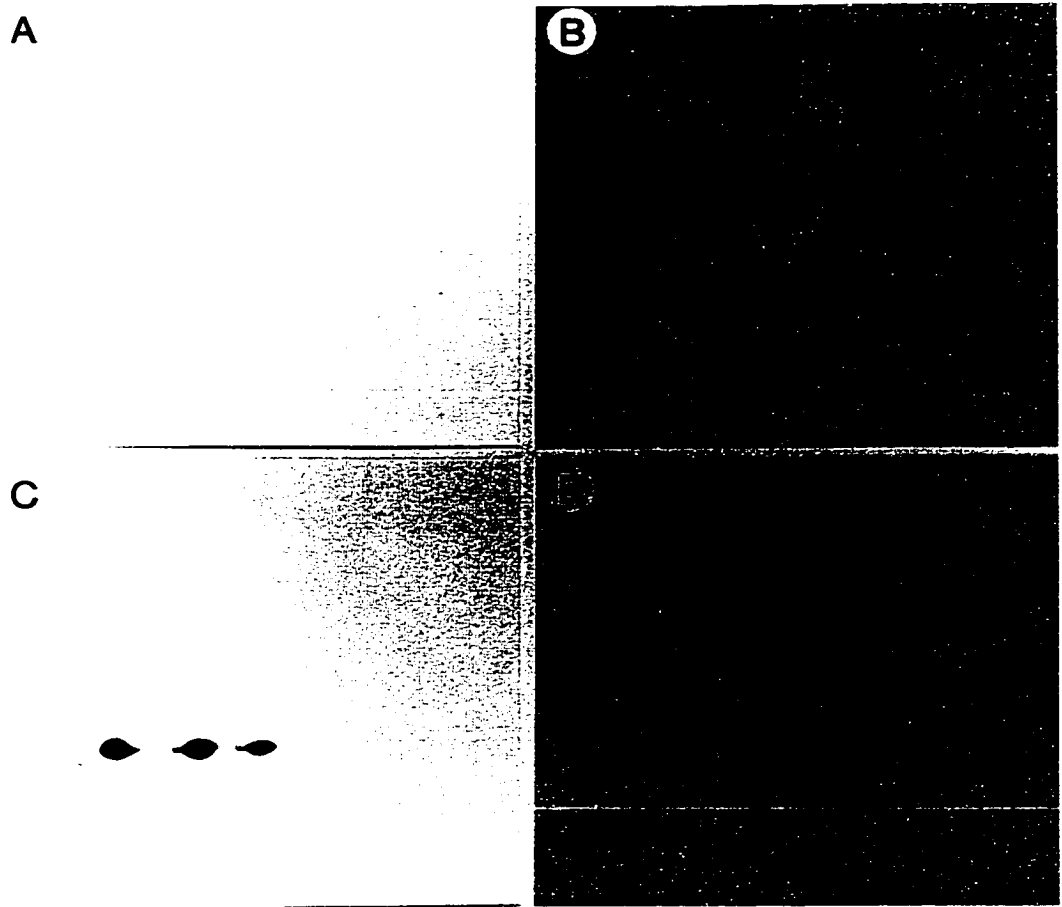
Figure 5.1

Figure 5.2. Overview of Hsp27 immunoreactivity in the adult rat brain. **A.** Sagittal

section of the brain showing strong immunoreactivity in the brain stem and absence of

immunoreactivity in the forebrain and cerebellum. **B.** Transverse section through the

pons and cerebellum showing immunoreactivity in cranial nerve nuclei and intracranial

sensory and motor axons. **C.** Transverse section of the medulla oblongata showing

immunoreactivy in sensory and motor nuclei. Note Hsp27 immunoreactivity in

pia/arachnoid and fornix. Abbreviations: Amb, nucleus ambiguus; f, fornix/fimbria;

gVII, genu of the facial nerve; MeV, mesencephalic nucleus of the trigeminal nerve;

MoV, trigeminal motor nucleus; SpV, spinal trigeminal nucleus; spV, spinal trigeminal

tract; VI, abducens nucleus; VII, facial nucleus; VIIn, facial nerve root; XII,

hypoglossal nucleus; XIIn, hypoglossal nerve root. Scale bars: A-C, 1 mm.
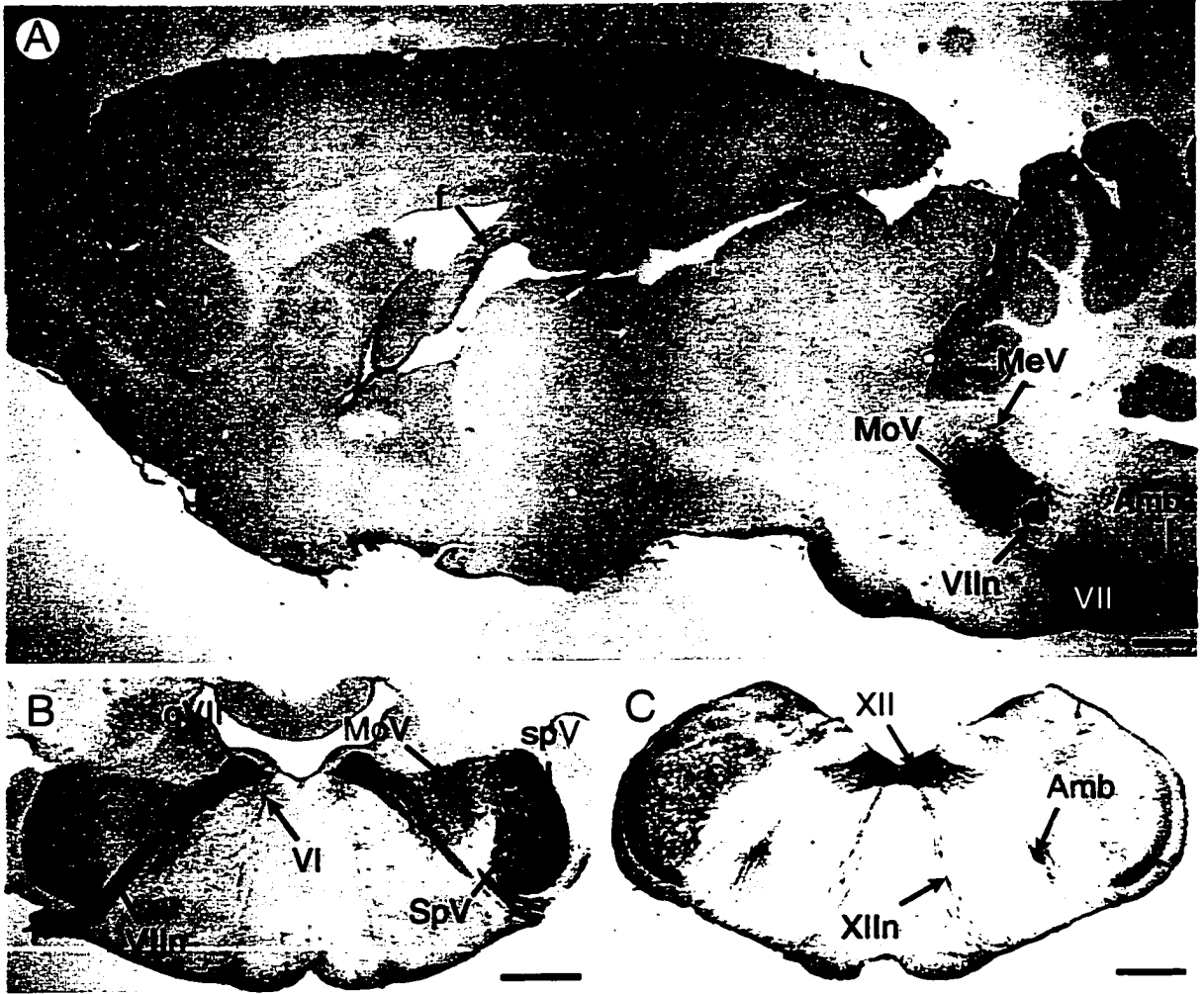
Figure 5.2

Figure 5.3. Photomicrographs of Hsp27 immunoreactivity in the arcuate nucleus and

median eminence. A. Transverse section through the third ventricle (III). B. Sagittal

section through the arcuate nucleus. Note long dendrite (arrowheads) of a fusiform

neuron. Scale bars: A, B, 200 $\mu$m.

Figure 5.3

Figure 5.4. Hsp27 immunoreactivity in the oculomotor and trochlear nuclei. **A.**

Transverse section of motoneurons, dendrites (arrowheads) and axons (double

arrowheads) of the oculomotor nucleus. **B.** Sagittal section of the oculomotor nucleus

showing radiating dendrites (arrowheads). mlf, medial longitudinal fasciculus. **C.**

Dark-field photomicrograph of a transverse section through the trochlear nucleus. **D.**

Boxed area in C showing stained and unstained (arrows) neurons; differential

interference contrast microscopy. Scale bars: A, 100 $\mu$m; B, C, 200 $\mu$m; D, 50 $\mu$m.
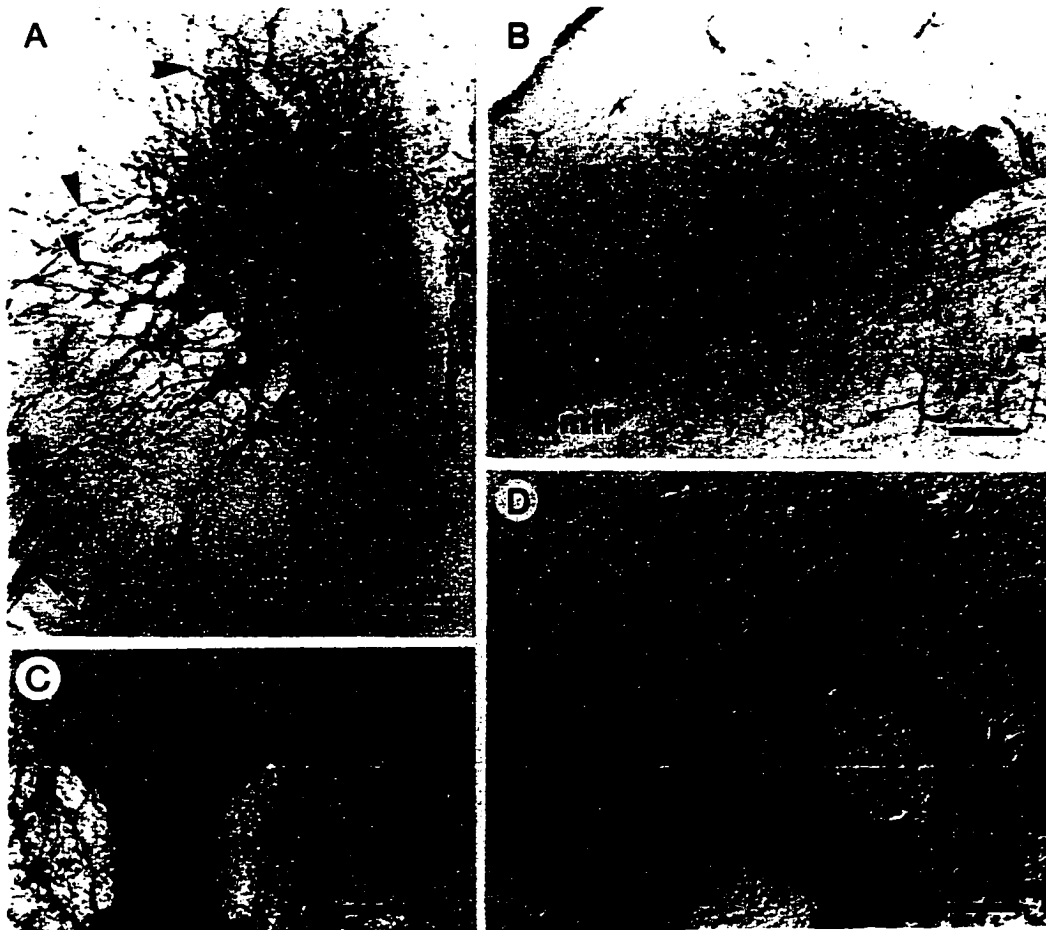
Figure 5.4

Figure 5.5. Hsp27 immunoreactivity in the mesencephalic and motor nuclei of the

trigeminal nerve. **A.** Sagittal section through the mesencephalic trigeminal nucleus

(box) and the motor trigeminal nucleus. **B.** Hsp27-positive and Hsp27-negative

neurons (arrows) in the mesencephalic nucleus at the level of the periaqueductal gray.

Sagittal section, differential interference contrast. **C.** Boxed area in A showing stained

and unstained (arrows) neurons. Scale bars: A, 100 $\mu$m; B, C, 50 $\mu$m.
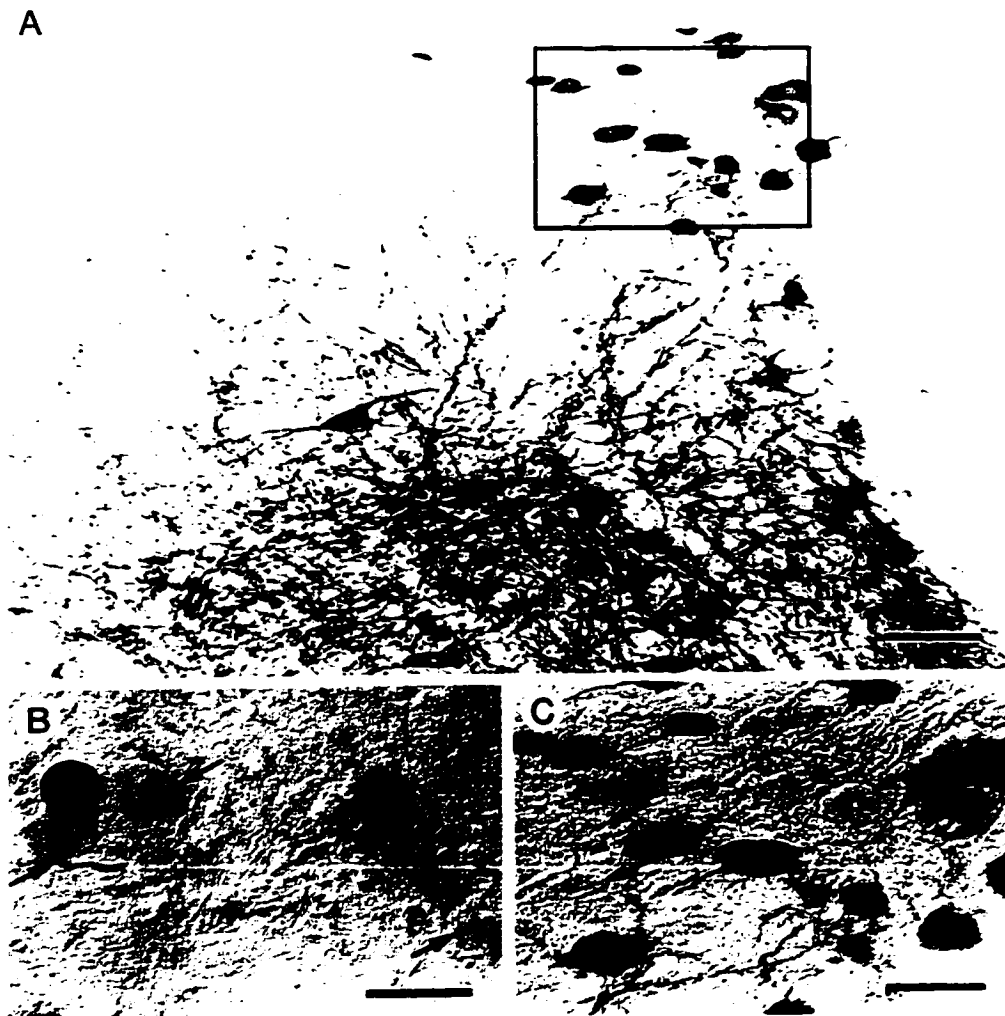
Figure 5.5

Top panel:

Figure 5.6. Hsp27 immunoreactivity in the motor nucleus and sensory nuclei of the

trigeminal nerve. A. Trigeminal motor nucleus and dendrites bordering on and

invading the principal sensory nucleus. Note heavy labeling in the spinal trigeminal

tract (spV). B. Dendrites from boxed area in A. C. Dendrites from facial

motoneurons extending into the spinal trigeminal nucleus, pars oralis. Scale bars: A,

500 $\mu$m; B, C, 100 $\mu$m.

Bottom panel:

Figure 5.7. Hsp27 immunoreactivity in the facial nerve and motoneurons of the

abducens nucleus. A. Hsp27 immunoreactivity in the genu (g) of the facial nerve and

motoneurons of the abducens nucleus in a transverse section. Double arrowheads point

to axons of the abducens motoneurons. B. Hsp27-positive and negative (arrows)

neurons in the abducens nucleus. Scale bars: A, 200 $\mu$m; B, 50 $\mu$m.
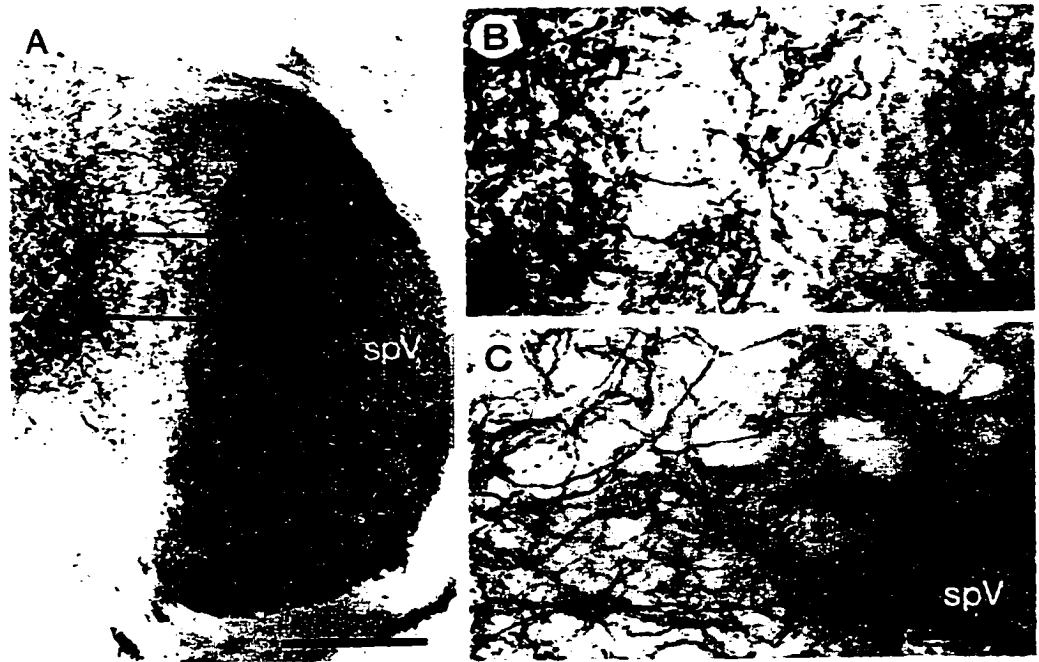
Figure 5.6
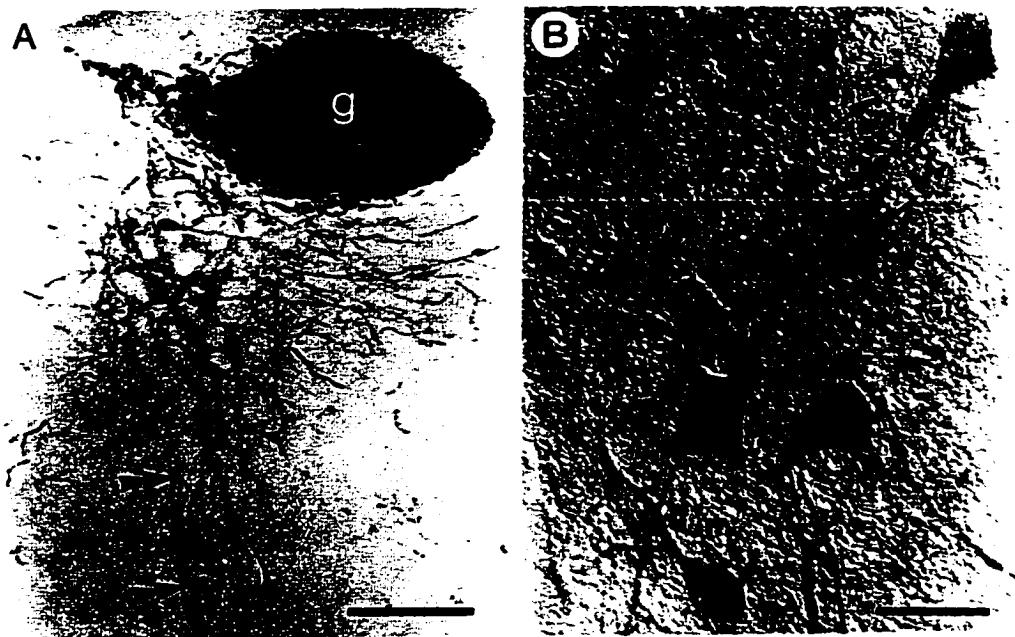


Figure 5.7

Figure 5.8. Hsp27 immunoreactivity in the lower pontine tegmentum. A. Transverse

section through the facial nucleus and spinal trigeminal nucleus pars oralis (SpVo). B.

Inferior salivatory nucleus and dendrites from boxed area in A. C. Sagittal section

showing the facial nucleus and neurons in the pontine reticular formation. D. Sagittal

section showing longitudinally-oriented, beaded dendrites of facial motoneurons from

boxed area in C. Scale bars: A, 1 mm; B, D, 50 $\mu$m; C, 500 $\mu$m.
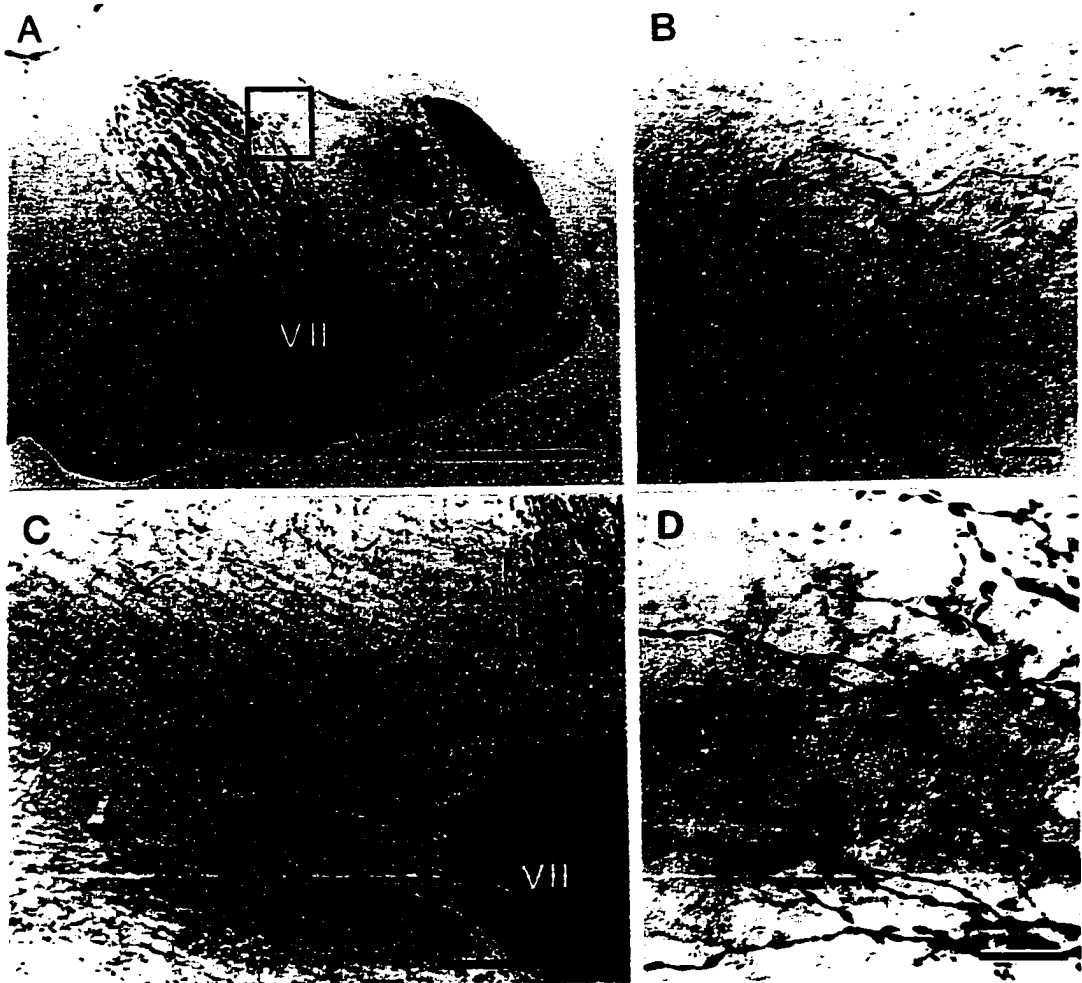
Figure 5.8

Figure 5.9. Hsp27 immunoreactivity in the medulla oblongata. **A.** Hsp27

immunoreactivity in a transverse section of the medulla oblongata. **B.** Differential

staining of laminae in the medullary dorsal horn from boxed area in A. **C.** Dark-field

photomicrograph of B to show lamination in the substantia gelatinosa (SG) of the

medullary dorsal horn. Asterisks mark blood vessels for reference. Scale bars: A, 200

$\mu$m; B,C, 100 $\mu$m.
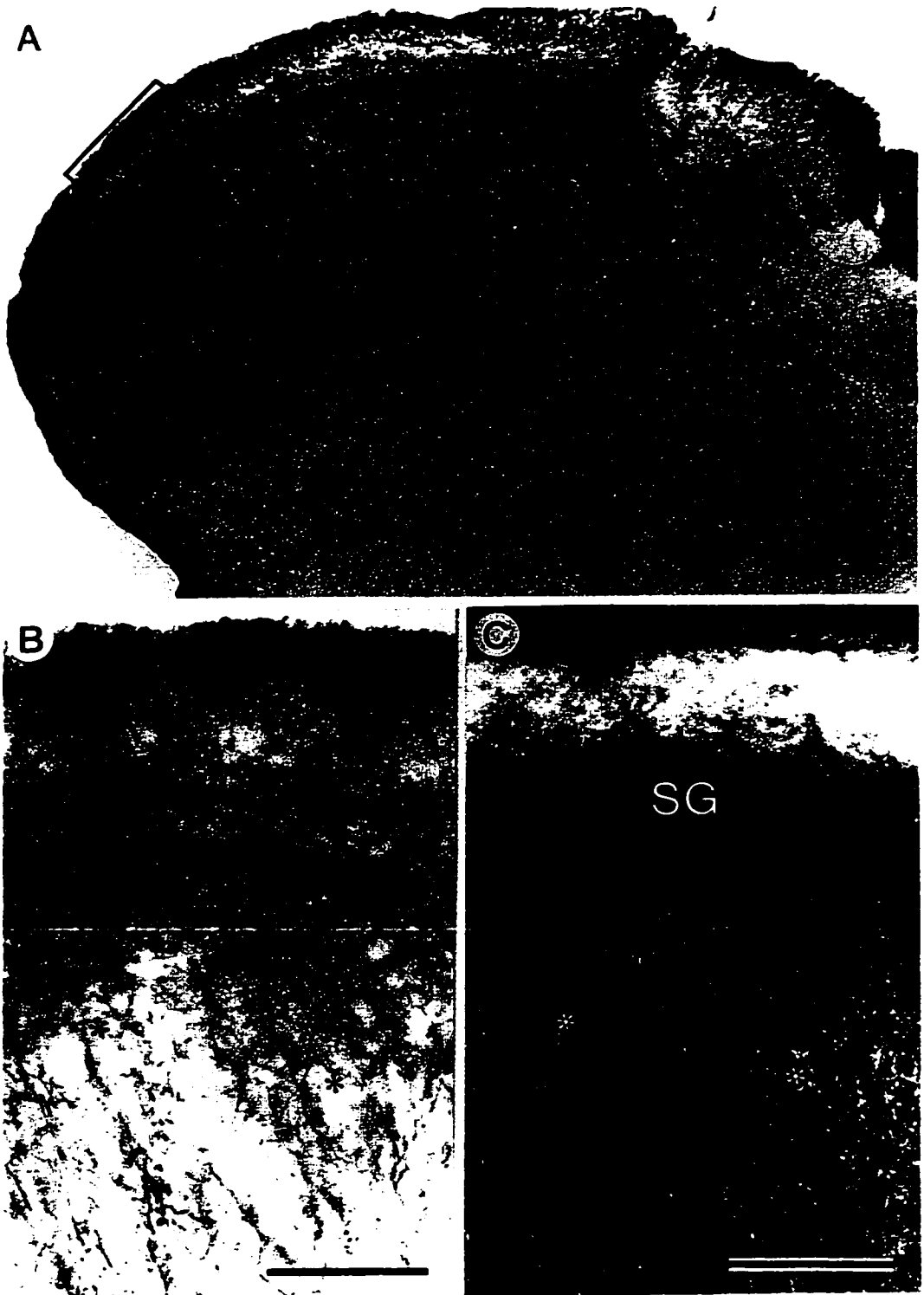
Figure 5.9

Figure 5.10. Hsp27 immunoreactivity in a sagittal section through the facial nucleus

and the nucleus ambiguus. **A.** Facial nucleus (VII) and the compact (c), semicompact

(sc) and loose (l) formations of the nucleus ambiguus. **B.** Semicompact and loose

formations showing extensive dendritic ramifications ventrally. **C.** Somata and

longitudinally oriented dendritic bundles in the semicompact formation from boxed area

in B. Scale bars: A, B, 500 $\mu$m; C, 50 $\mu$m.
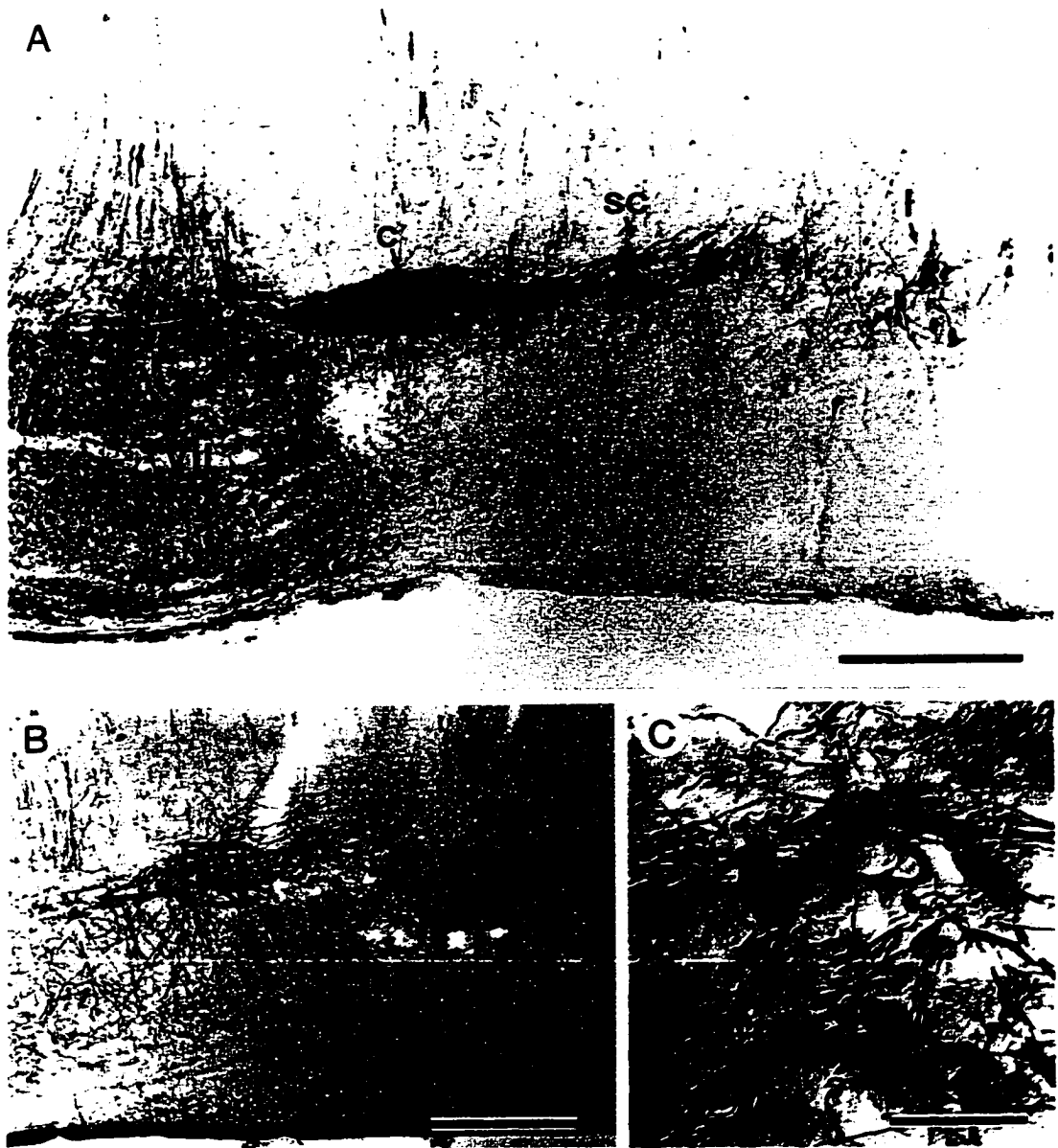
Figure 5.10

Figure 5.11. Hsp27 immunoreactivity in transverse sections of the middle (A) and

caudal (B) dorsomedial medulla oblongata. Abbreviations: AP, area postrema; cen,

central subnucleus of the nucleus of the tractus solitarius; com, commissural

subnucleus; CU, cuneate nucleus; DMV, dorsal motor nucleus of the vagus nerve; GR,

gracile nucleus; is, interstitial subnucleus; ts, tractus solitarius; XII, hypoglossal

nucleus. Open arrow in B points to genioglossus motoneurons. Scale bars: A, B, 200

$\mu$m.
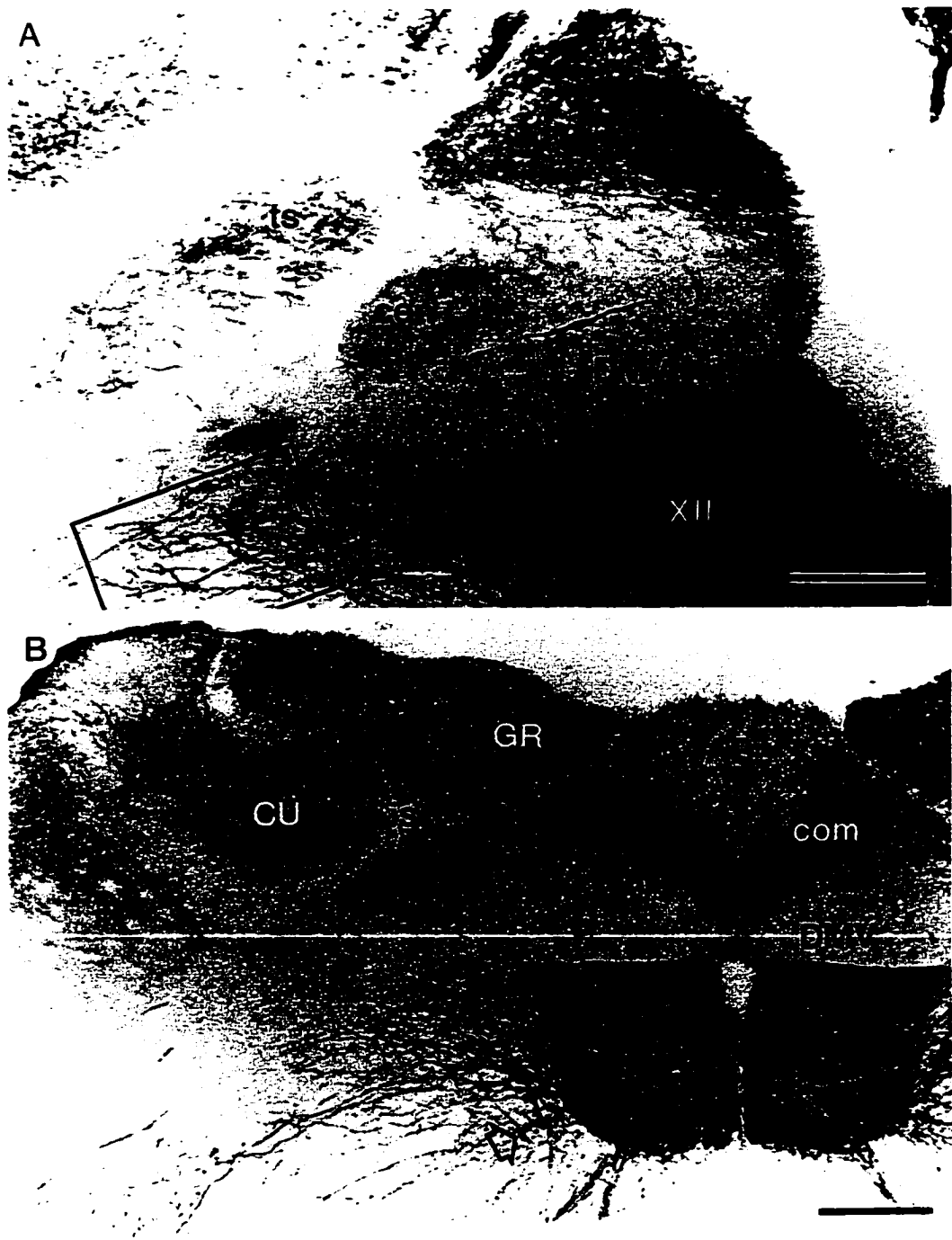
Figure 5.11

Figure 5.12. Hsp27 immunoreactivity in dendrites of motoneurons from the

hypoglossal nucleus. **A.** Beaded dendrites and bundles extending ventrolaterally from

the hypoglossal nucleus. **B.** Boxed area in A. **C.** Beaded dendrites extending laterally

from the hypoglossal nucleus and axon (arrowheads) from the dorsal motor nucleus of

the vagus nerve from boxed area in figure 5.11A. Scale bars: A, 100 $\mu$m; B, C, 50

$\mu$m.
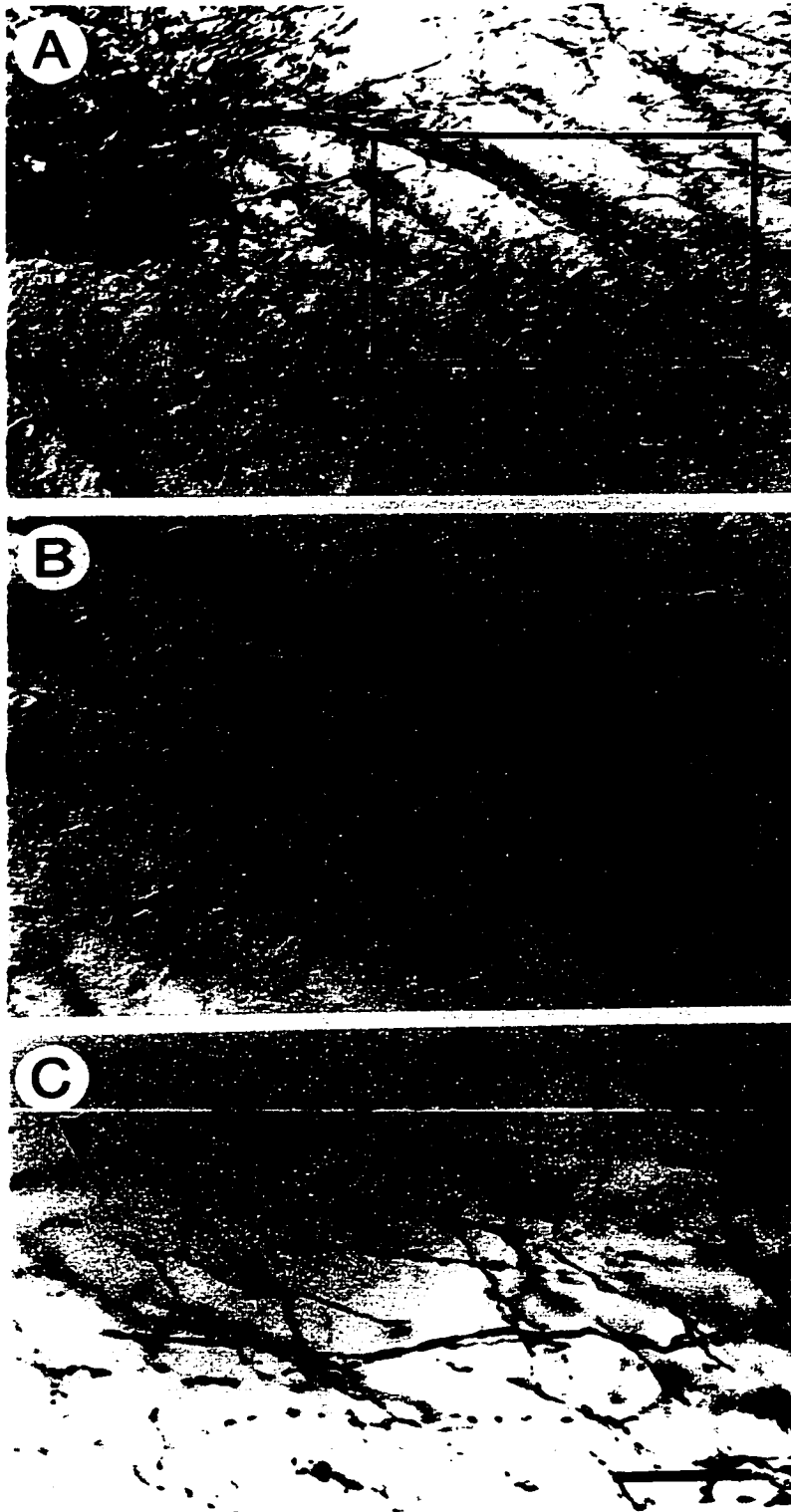
Figure 5.12

Top panel:

Figure 5.13. Hsp27 immunoreactivity in transverse sections of the upper cervical spinal cord. **A.** Upper cervical spinal cord showing commissural axons (arrowheads). **B.** Dorsal horn of upper cervical cord from boxed area in A showing staining in lamina III and absence of Hsp27 immunoreactivity in the substantia gelatinosa. Scale bars: A, 1mm; B, 50 μm.

Bottom panel:

Figure 5.14. Hsp27 immunoreactivity in transverse sections of the spinal cord. **A.** Cervical enlargement. **B.** Upper lumbar (L1) segment. **C.** Sacral segment (S4). **D.** Intermediolateral nucleus in the thoracic spinal cord. Note unlabeled neurons (arrows) adjacent to Hsp27-positive neurons. Scale bars: A-C, 500 μm; D, 50 μm.
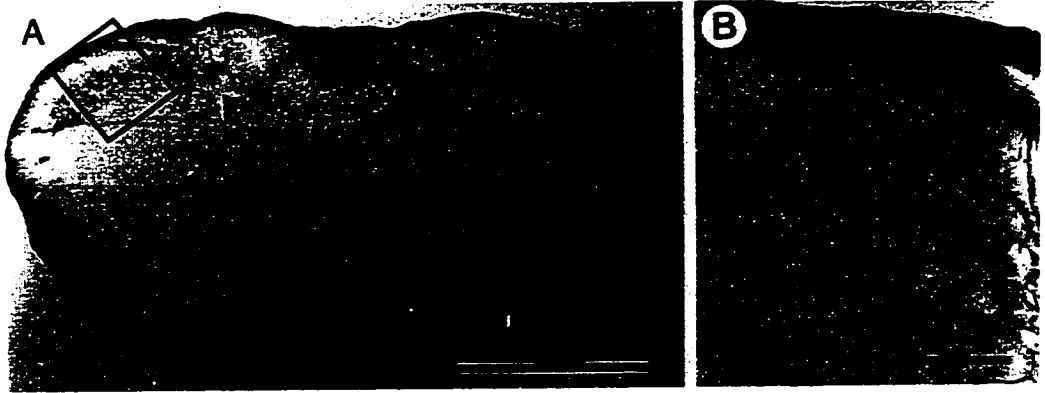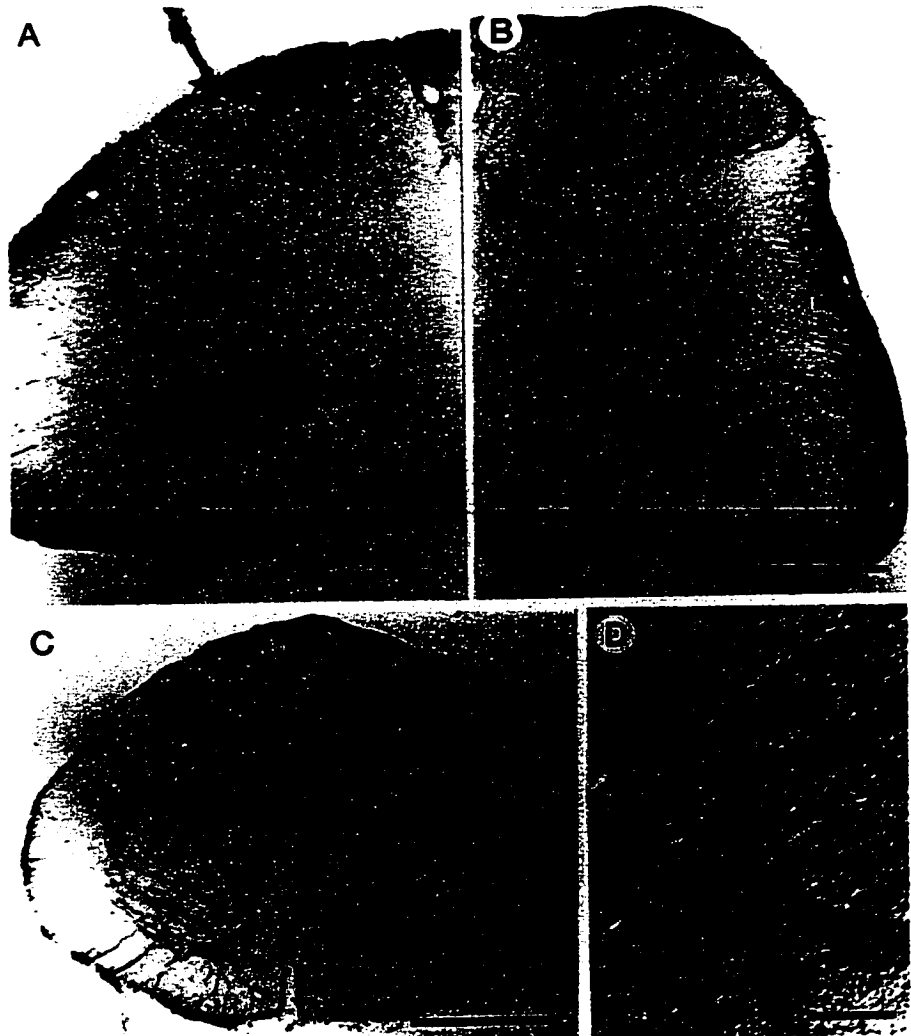
Figure 5.13



Figure 5.14

Figure 5.15. Hsp27 immunoreactivity in motoneurons and a dorsal root ganglion. **A.**

Trigeminal motor nucleus. **B.** Ventral horn of spinal cord. **C.** Beading in distal

dendritic ramifications of nucleus ambiguus motoneuron in the semicompact formation.

Note that the proximal dendrite (arrowhead) has a smooth morphology while its distal

branches are beaded. **D.** Dorsal root ganglion neurons. Note neurons in A, B and D

(arrows) that are not Hsp27-positive; cresyl violet counterstain. Scale bars: A, B, 50

$\mu$m; C, 100 $\mu$m; D, 20$\mu$m.
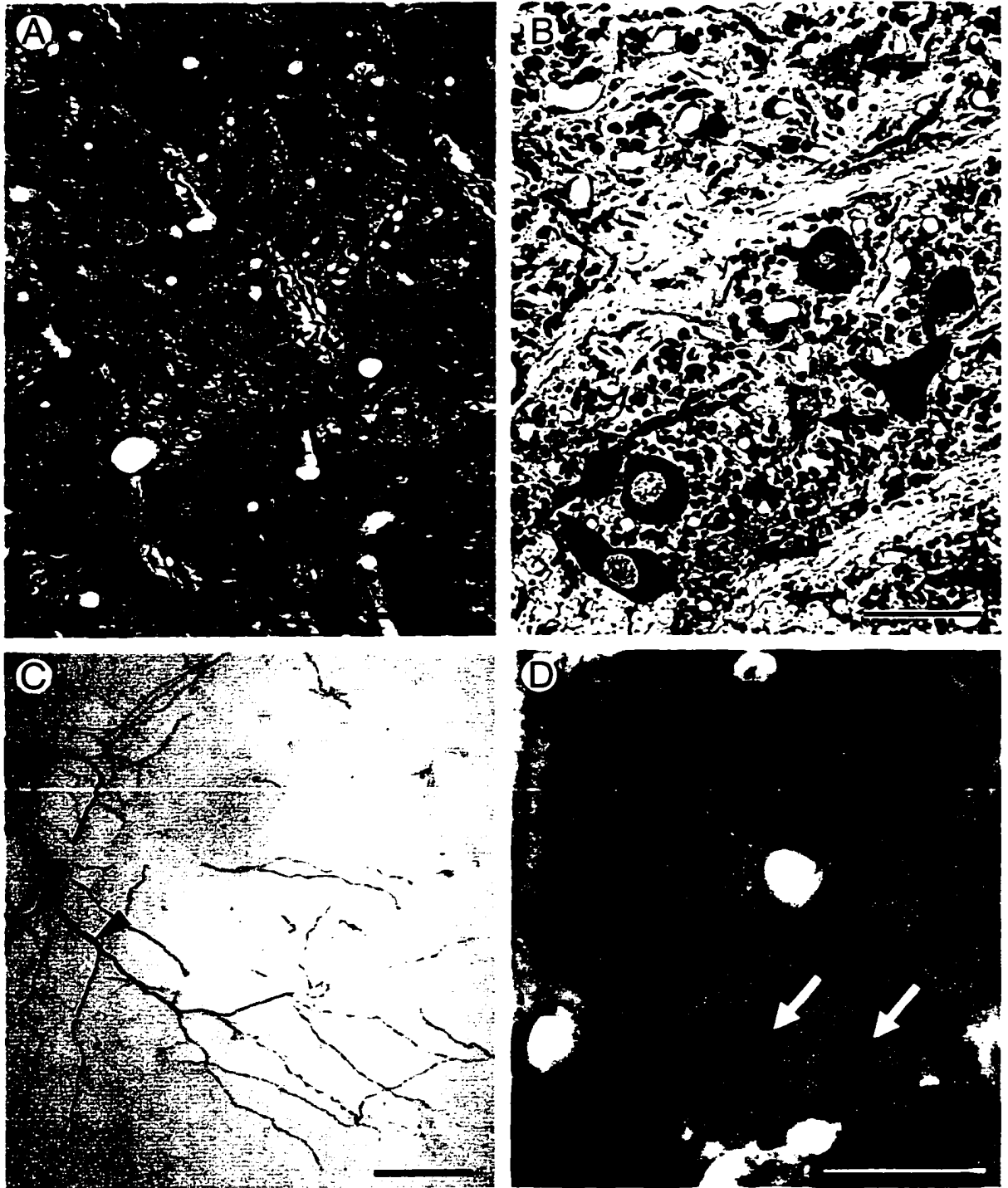
Figure 5.15

**Discussion**

Western blot analysis confirmed that Hsp27 was absent in the rat cerebral cortex and present in high levels in the spinal cord of the adult rat. Strong Hsp27 immunoreactivity was observed in the cytoplasm and neurites of select populations of brain stem and spinal cord motoneurons, often resulting in a Golgi-like pattern of staining. Motor nuclei could be classified into four groups on the basis of their patterns of staining. Most special visceral efferent motoneurons of the cranial nerve nuclei were Hsp27-positive as were the general somatic efferent motoneurons of the hypoglossal nucleus and spinal motor columns. In contrast, smaller subpopulations of the general somatic efferent motoneurons for eye muscles were stained. As well, only a few general visceral efferent neurons, i.e., parasympathetic and sympathetic preganglionic neurons were stained for Hsp27. Many pseudo-unipolar sensory neurons were stained and the patterns of staining in central sensory nuclei suggested that specific subpopulations of sensory neurons contained Hsp27.

*Specificity of rat Hsp27 immunoreactivity*

Immunoreactivity was observed in the rat nervous system using a polyclonal antibody raised against the recombinant murine Hsp25. This antibody has been shown to detect exclusively the murine Hsp25 and its homolog in the rat, Hsp27 (Head et al., 1994; Plumier et al., 1996) but not the human homolog Hsp27. In fact, two-dimensional gel Western blot analysis revealed that this antibody detected three

isoforms of the rat Hsp27 (Plumier et al., 1996) and did not detect other proteins in the rat nervous system.

Western blot analysis and immunohistochemistry revealed that Hsp27 was undetectable in the cerebral cortex of the adult rat. These results confirmed previous works reporting that Hsp27 was not detected in the brain or the cerebellum of untreated adult rodents (Tanguay et al., 1993; Klemenz et al.,1993; Wilkinson and Pollard, 1993). Although Hsp27 was not detected in the cerebral cortex by Western blot analysis, immunohistochemistry revealed the presence of sparse Hsp27-immunopositive neurons in the basal hypothalamus. In contrast, the brain stem and the spinal cord showed high levels of Hsp27 by Western blot analysis and immunohistochemistry.

In the rat spinal cord, Hsp27 was localized in processes within the dorsal horn and in motoneurons of the ventral horn. A similar immunoreactivity distribution was observed in the mouse nervous system (data not shown). Western blot analysis of human spinal cord also revealed the constitutive presence of Hsp27 (Iwaki et al., 1993; Brosnan et al., 1996). However, so far, immunohistochemical studies of Hsp27 in the human spinal cord have failed to detect Hsp27 immunoreactivity in normal subjects (Renhawek et al., 1994; Iwaki et al., 1993; Brosnan et al., 1996). Similarly, no Hsp27 immunostaining was observed in human spinal cord tissues using a polyclonal antibody raised against a peptide sequence of the human Hsp27 nor using a monoclonal antibody against the human Hsp27 (data not shown). On the other hand, Hsp27 has been reported in a small number of neurons under pathological conditions such as

Alzheimer's disease (Renhawek et al., 1994) and Creutzfeldt-Jakob disease (Kato et al., 1992b) as well as in astrocytes of patients with multiple sclerosis (Brosnan et al., 1996) and Alzheimer's disease (Renhawek et al., 1994). Similarly, cerebral ischemia (Kato et al., 1994, 1995) or status epilepticus (Plumier et al., 1996) induced Hsp27 immunoreactivity in reactive astrocytes in the adult rat.

This discrepancy between detection of Hsp27 by Western blot analysis and absence of Hsp27-positive staining with immunohistochemistry of human spinal cord was also observed in the rat nervous system using a polyclonal antibody raised against a short amino acid sequence of the mouse Hsp25 (Plumier et al., 1996; data not shown). These discrepancies between results from Western blot analyses and immunohistochemistry could be accounted for in part by the unavailability of epitopes on the native Hsp27 to the antibodies. During SDS gel electrophoresis and subsequent Western blot analysis, proteins are denatured and linearized, exposing internal epitopes for antibody recognition. In contrast, denaturation and linearizarion of proteins do not occur in immunohistochemistry. In addition, Hsp27 immunohistochemistry in human spinal cord was performed using the antibody raised against a single epitope or against a short amino acid sequence of Hsp27. This contrasts with the present study where a polyclonal antibody raised against the entire recombinant protein was used. Finally, observations of immunoreactivity in astrocytes or in neurons under pathological conditions might also reflect changes in substrates for Hsp27 or alterations in Hsp27 conformation, revealing protein-bound or internal epitopes otherwise unavailable for

detection. This suggests that a polyclonal antibody raised against the entire human Hsp27 might reveal a constitutive expression of Hsp27 in the human nervous system and that Hsp27 distribution in the nervous system might be similar in humans and rodents.

### Hsp27 staining of central and peripheral neurons

The arcuate nucleus and, to a lesser extent, the median eminence contained numerous intensely stained Hsp27 neurons. In spite of the relatively uniform histological appearance of this region of the brain in Nissl stains, neurons in the region have a rich complement of different enzymes and neuropeptides (Everitt et al., 1986). Although notably present in the arcuate nucleus, many neurons with these markers are not confined to the boundaries of the nucleus, being found in neurons adjacent to the region or in other parts of the nervous system (Everitt et al., 1986). However, a few markers and neuropeptides such as glutamic acid decarboxylase, growth hormone releasing factor and corticotropin-like intermediate peptide have restricted distributions in the arcuate nucleus (Everitt et al., 1986) that overlap the pattern seen for Hsp27-positive neurons. This correspondence raises the possibility that the subset of Hsp27 neurons identified in the present study could also contain one or more of the markers found in this region.

All cranial nerve motor nuclei and spinal cord motoneuronal cell columns had many neurons that expressed Hsp27. The intensity of motoneuronal staining ranged from no detectable staining in some neurons to very intense staining in the majority of

neurons within a given nucleus, and also varied considerably among the different motor

nuclei. As the proportion of stained motoneurons was consistent from animal to

animal, this variation in staining cannot be attributed to technical factors such as

penetration of the antibody. In particular, the oculomotor nuclei as a group had a

smaller proportion of stained neurons than did the hypoglossal nucleus and the motor

nuclei containing special visceral efferent motoneurons, i.e., trigeminal, facial and

ambiguus nuclei. In marked contrast, only about one quarter of the neurons of the

dorsal motor nucleus of the vagus nerve were stained. These Hsp27-positive neurons

had dendrites ramifying within the nucleus and, less frequently, in the nucleus of the

tractus solitarius dorsally. The size and morphology of these immunoreactive neurons

in the dorsal motor nucleus suggest that they are all preganglionic motoneurons (Fox

and Powley, 1992). Relatively few general visceral efferent motoneurons in other

regions, including the external formation of the nucleus ambiguus and the

intermediomedial cell column, were Hsp27-positive. The significance of these

differences is unknown but they do suggest that there may be correlations between the

expression and regulation of Hsp27 and different functional classes of motoneurons.

One of the striking characteristics of the Hsp27 staining of motoneurons was the

extensive Golgi-like staining of their dendritic trees. Hsp27 staining demonstrated that

many motoneuronal dendrites extended for long distances beyond the borders of the

cranial nerve motor nuclei. These extranuclear dendrites indicate that most cranial

nerve motor nuclei are "open" nuclei as conceptualized by Mannen (1960). The

dendrites often extended into the reticular formation of the brain stem which would

provide these motoneurons with a morphological substrate to receive and integrate a

wide range of inputs in common with neurons of the reticular formation. In addition,

dendrites of neurons of the oculomotor nucleus extended into the periaqueductal gray

and those of the facial nucleus extended into the spinal trigeminal nucleus as has been

reported by Mannen (1960). In fact, it appears that Hsp27 staining gives an even more

complete picture of the dendritic arbours of motoneurons than Golgi staining as

Mannen reported less extensive dendritic fields for the trigeminal and facial nuclei.

Many distal dendrites of Hsp27-positive motoneurons showed extensive beading

or varicosities, especially distally. Beading of proximal dendrites has been reported to

be associated with neuronal degeneration (Grant, 1965) but as the present material is

from normal animals, it is unlikely to be an abnormal feature. In addition, smooth and

beaded dendrites were found adjacent to each other and the same dendritic tree may

have both smooth and beaded dendrites (Figure 15C) as has been noted previously for

distal dendrites of spinal motoneurons (Romanes, 1964, see his figure 18). In fact,

there are abundant examples in the literature which suggest that beaded or varicose

dendrites are relatively common. For example, beading, varicosities and specialized

endings of distal dendrites have been reported or illustrated in Golgi preparations,

intracellular fills or retrograde tracing studies of trigeminal (Lingenhöhl and Friauf,

1991), hypoglossal (Odutola, 1976; Wan et al., 1982; Altschuler et al., 1994) and

nucleus ambiguus motoneurons (Bieger and Hopkins, 1987; Bras et al., 1987;

Altschuler et al., 1991). Dendritic beading has also been studied at the ultrastructural level where it has been shown that distal dendritic varicosities of laryngeal motoneurons consist of "racket-shaped dilatations" connected by very narrow profiles with prominent microtubules (Bras et al., 1987). Both the varicosities and the interconnecting isthmus region had synapses.

In the pontine and medullary reticular formation, a number of large, multipolar neurons were Hsp27-positive. Their distribution and morphology are comparable to that of reticulospinal neurons (Newman, 1985a, b) and, in keeping with this, stained axons were present in the central parts of the medial longitudinal fasciculus that carries descending reticulospinal axons.

Populations of pseudo-unipolar sensory neurons were also Hsp27-positive. In the mesencephalic nucleus of the trigeminal nerve, approximately 45% of the neurons were stained while most sensory neurons in the trigeminal ganglion were stained. The possibility that stained and unstained neurons represent different functional classes is suggested by the striking laminar distributions in the medullary and spinal dorsal horns. Also, in the nucleus of the tractus solitarius, differences in distribution of Hsp27 immunoreactivity corresponded to known patterns of afferent input (Altschuler et al., 1989).

Differences in staining of primary afferents within the substantia gelatinosa have been correlated with differences in sensory modality and neuropeptide complement (Hunt and Rossi, 1985; Ribeiro-da-Silva, 1995). In the spinal trigeminal nucleus pars

caudalis, Hsp27 immunoreactivity was strongest in lamina IIo and inner part of lamina

IIi, extrapolating from the spinal cord substantia gelatinosa terminology. In the spinal

cord, lamina IIo and the inner part of IIi (lamina IIBv, Ribeiro-da-Silva, 1995) contain

neurons that are primarily responsive to noxious and innocuous stimuli, respectively.

Fluoride-resistant acid phosphatase histochemistry, a marker for nociceptive fibers

(Knyihár and Csillik, 1977), is localized rather precisely to the outer part of lamina IIi,

i.e., lamina IIBd. This relationship matches the patterns observed in the superficial

laminae of the pars caudalis of the spinal trigeminal nucleus, including the localization

of fluoride-resistant acid phosphatase staining (D.A. Hopkins, personal observations) to

a thin band lying between lamina IIo and the inner part of lamina IIi that contains little

Hsp27. Thus, Hsp27-positive trigeminal afferent fibers have a distinct laminar

distribution in the medullary dorsal horn that is likely to be related to specific subsets of

cutaneous afferent fibers, presumably Aδ fibers (Nagy and Hunt, 1983; Hunt and

Rossi, 1985). Interestingly, the distribution of Hsp27 immunoreactivity in the spinal

dorsal horn differs from that in the medullary dorsal horn. In the spinal cord, there is

staining in laminae I and III but lamina II is virtually devoid of staining except for

fibers that penetrate to deeper layers. This suggests that Hsp27 is associated with

different functional sets of afferent fibers in the brain stem and spinal cord. In the

spinal cord, strong staining was also present in the dorsal column system which implies

that many mechanoreceptive afferents are Hsp27-positive. Finally, a population of

commissural afferents (Jacquin et al., 1982; Pfaller and Arvidsson, 1988) was also

Hsp27-positive.

### Heat shock proteins in the nervous system

Hsp27 is not the only heat shock protein reported to be constitutively expressed

in the rat nervous system. For example, immunoreactivity for Hsp32, also known as

heme oxygenase-1, was observed in numerous neurons throughout the rat brain and

brain stem (Ewing et al., 1992). Hsp32-immunoreactive neurons were detected in a

number of nuclei where no Hsp27 immunoreactivity was observed, including the

hippocampal formation (CA1, CA3, hilus), the paraventricular nucleus, the inferior

colliculus, the red nucleus, the dorsal raphe nucleus, the cochlear nucleus and

vestibular nucleus neurons. However, several brain stem nuclei, such as the trigeminal

motor nucleus or the abducens nucleus, that showed Hsp27-immunopositive neurons in

the present study were not reported to be Hsp32-immunopositive (Ewing et al., 1992).

Despite these differences, there also are some similarities between Hsp27 and Hsp32

immunostaining. For example, both Hsp32 immunoreactivity and Hsp27

immunoreactivity were observed in the oculomotor nucleus, the mesencephalic

trigeminal nucleus, and the ventromedial hypothalamic nuclei adjacent to the median

eminence. In addition, variation in Hsp27 immunoreactivity intensity within a given

nucleus was also observed in Hsp32 immunostaining. It remains unknown to what

extent Hsp27-immunoreactive neurons were also Hsp32-positive in these nuclei.

Another heat shock protein, Hsc70 (the clathrin-uncoating ATPase), has also been reported to be constitutively expressed in several types of neurons, such as Purkinje cells in the cerebellum (Manzerra and Brown, 1992b) and the pyramidal cells of the hippocampus (Abe et al., 1991). In the spinal cord, Manzerra and Brown (1992a) showed that Hsc70 was expressed in the gray matter. However, Hsc70 expression was not restricted to motoneurons of the spinal cord but was also detected in neurons of the dorsal horn.

These differences between Hsp27, Hsp32 and Hsc70 distributions reflect the complex mechanisms of regulation of heat shock proteins in the normal nervous system. Although all heat shock proteins could be regulated by a common pathway such as that reported after heat shock, there apparently are also specific mechanisms that differentially regulate the expression of each heat shock protein under normal and stressful conditions. For example, Hsp27 but not Hsp32 is detected in trigeminal motor nucleus, and while Hsc70 is detected in Purkinje neurons or in dorsal horn neurons, Hsp27 is not. In addition, several different mechanisms might be involved in the constitutive expression of a given heat shock protein. For example, Hsp27 might be regulated through activation of hormone-responsive pathway in neurons of the arcuate nucleus and through different transcription factors in spinal cord motoneurons.

### Hsp27 functions in the nervous system

At least three functions have been suggested for Hsp27: 1) antioxidative enzyme regulation, 2) regulation of actin dynamics and 3) molecular chaperoning. Firstly,

constitutive expression of Hsp27 in Hsp27-transfected cells has been shown to reduce

intracellular levels of reactive oxygen species and increase total levels of glutathione.

(Mehlen et al., 1996a). However, glutathione level regulation might not be a relevant

function for constitutive Hsp27 in neurons since glutathione was not detectable in

neurons *in vitro* (Slivka et al., 1987) or *in vivo* (Raps et al., 1989). Secondly, it has

been suggested that Hsp27 plays a role in the regulation of actin filament dynamics by

inhibition of actin polymerization and enhancement of actin filament depolymerization

*in vitro* (Miron et al., 1988, 1991; see reviews by Arrigo and Landry, 1994; Landry

and Huot, 1996). Overexpression of Hsp27 in transfected cells induced modification of

cellular actin distribution, with an increase in cortical F-actin and a decrease in

cytoplasmic stress fibers (Lavoie et al., 1993b). In peripheral neurons, actin and actin-

binding protein have been suggested to have an essential role in the architecture of the

inner axonal cytoskeleton (Fath and Lasek, 1988), to participate in axonal transport

(Kuznetsov et al., 1992) and contribute to the growth in diameter of axons (Cleveland,

1996). Therefore, it is possible that Hsp27, as actin-binding protein, could contribute

in the regulation of some of these mechanisms via a modulation of actin dynamics.

Some growth factors and cytokines have been shown in cell cultures to regulate Hsp27

expression and phosphorylation (Löw-Friedrich et al., 1992; Satoh and Kim, 1995). It

is tempting to speculate that Schwann cells which are known to regulate axonal

cytoskeleton or axonal transport (de Waegh and Brady, 1990) also regulate both Hsp27

expression and Hsp27 phosphorylation in peripheral neurons. Finally, it has been

shown that Hsp27 can function as a molecular chaperone *in vitro* in preventing protein

aggregation and in promoting the refolding of denatured proteins (Jakob et al., 1993).

In the present study, Western blot analysis of rat spinal cord samples revealed

the presence of three isoforms of Hsp27 corresponding to various levels of

phosphorylation (Arrigo and Landry, 1994). Therefore, it would seem that a portion of

the total amount of Hsp27 was in a functionally active state in the rat spinal cord. In

cell cultures, phosphorylation of Hsp27 has been related to Hsp27 protective functions

(Landry et al., 1991; Lavoie et al., 1993a; Benndorf et al., 1994; Mehlen et al., 1995).

Phosphorylation of Hsp27 was required for Hsp27 regulation of actin dynamics,

enhancing resistance of actin filaments against depolymerization induced by

cytochalasin D treatment (Lavoie et al., 1995) or by oxidative stress (Huot et al., 1996)

and by consequence, phosphorylation of Hsp27 increased cellular survival. It remains

to be established whether neurons expressing Hsp27 are more resistant to injury such as

oxidative stress, axotomy-induced cell death or apoptosis. In keeping with this

protection against apoptosis, it is worth noting that some neurons have been reported to

express Hsp27 during development (Gernold et al., 1993; see review by Arrigo and

Mehlen, 1994), raising the possibility that Hsp27 might play a role in neuronal

selection during development.

Finally, it is interesting to note that Hsp27 has been found in neurofibrillary

tangles (Renhawek et al., 1994), suggesting that Hsp27 expression might be of

relevance in neurodegenerative diseases. Aggregation of proteins, including

neurofilaments, in the perykaryon and proximal axon is also the hallmark of

motoneuron neurodegeneration occurring in amyotrophic lateral sclerosis (Lee et al.,

1994; Collard et al., 1995; see review by Cleveland, 1996). In addition, several

different mutations in the antioxidative enzyme SOD-1 gene have been linked to

familial amyotrophic lateral sclerosis (Xu et al., 1994; Brown, 1995; Wong and

Borchelt, 1995), raising the possibility that misfolding due to oxidative stress or

mutations might progressively deplete constitutive levels of molecular chaperones from

their usual cellular targets. A lack of or deficiency in molecular chaperones for normal

folding of their target-proteins such as cytoskeleton proteins, might in turn lead to an

accumulation of nascent polypeptides that eventually aggregate, leading to a progressive

neuronal dysfunction and eventually neuronal death. This appealing hypothesis would

suggest that many examples of different types of neurodegeneration could be related to

a common mechanism involving protein folding in which heat shock proteins play a

role (Taubes, 1996).

## Conclusions

Select populations of neurons in the brain stem, spinal cord and peripheral

sensory ganglia constitutively express Hsp 27 in the perikarya, dendrites and axons.

Hsp27 is widely distributed in general somatic and special visceral efferent

motoneurons, a subpopulation of autonomic preganglionic neurons and in many sensory

neurons. Except for the Hsp27 neurons in the arcuate nucleus and median eminence

and reticular formation, all Hsp27 neurons were either sensory or motor with an axon

in the periphery. The differential staining of motoneurons and subsets of sensory neurons (e.g., mesencephalic nucleus of the trigeminal nerve, cranial nerve ganglia and dorsal root ganglia) suggests that functional differences related to Hsp27 may be present in these different populations. The important physiological functions of Hsp27 and its differential distribution and specific localization in the brain stem and spinal cord support an important role for this stress-related protein in normal and pathological physiology.

# CHAPTER 6:

## INDUCTION OF Hsp27

## FOLLOWING FOCAL CEREBRAL ISCHEMIA

# Introduction

Brain injury, such as ischemia, has been reported to induce the expression of several genes (Herrera and Robertson, 1989; Gonzalez et al., 1991). Following brain injury, *c-fos* mRNA and protein accumulate in a rapid and transient manner in the entire cerebral cortex of the lesioned side (Dragunow and Robertson, 1988; Herrera and Robertson, 1989, 1990; Comelli et al., 1993; Jacobs et al., 1994). In addition to the induction of *c-fos* and other immediate early genes, brain injury also induces expression of heat shock proteins. Following cortical wounding, Hsp70 has been reported in the region surrounding the lesion site (Brown et al., 1989). Hsp27 has been reported to be expressed in astrocytes following cerebral ischemia (Kato et al., 1994, 1995) and following kainic acid-induced status epilepticus in the rat (Plumier et al., 1996). In addition, Hsp27-immunoreactive astrocytes have been reported in brains of persons with chronic cerebral infarction (Iwaki et al., 1993).

This stress response is believed to be related to cell repair and survival and, furthermore, failure to produce a rapid and complete stress response may be one cause for cell death and degeneration (Kogure and Kato, 1993). Immediate early genes by acting as transcription factors can modify the expression of genes that play a role the recovery from the ischemic injury. Similarly, heat shock proteins have been shown to protect against cellular damage (Landry et al., 1989) and improve physiological recovery after injury (Marber et al., 1995; Radford et al., 1996; see chapter 3). Constitutive expression of the inducible 70-kDa heat shock protein in transfected cells

or in transgenic animals provided resistance to metabolic stresses (Williams et al., 1993; Mestril et al., 1994; Marber et al., 1995; Radford et al., 1996; see chapter 3).

In the present study, the temporal and spatial induction of three stress-induced genes (*c-fos*, *Hsp70* and *Hsp27*) in rat brain following photothrombotic infarction was examined.

## Material and methods

### Rat photothrombotic infarction

All the surgery was done by Nigel I. Wood at SmithKline Beecham Pharma Inc. (Harlow, UK) according to the method described by Watson et al. (1984). Rats were cared for in accordance with the United Kingdom Animals (Scientific Procedures) Act (1986), and the experimental procedures were approved by an Animal Ethics Committee of SmithKline Beecham Pharma Inc. (Harlow, UK). Eighteen male Lister hooded rats (Charles River, UK), weighing 387-467 grams, were used. Animals were anaesthetized with halothane in oxygen and rectal temperature was maintained at 37 ± 1°C by a heated blanket with feedback control. The rats were placed in a stereotaxic frame and a single fibre optic light guide (diameter 3.0 mm) connected to a 300 Watt xenon arc lamp (Oriel Scientific Ltd) was positioned on the skull at the level of bregma, with the head of the light guide centered 2.5 mm to the right side of the midline. An in-line water filter located between the arc lamp and light guide removed the infrared component. Control studies revealed no increase in skull temperature below the fibre

optic light guide (N.I. Wood, unpublished findings). Rose Bengal dye (Aldrich),

20mg/kg, was infused over a period of 60 seconds into a lateral tail vein, and the right

side of the skull illuminated for 5 minutes. Upon illumination, the dye produces free

radical species that trigger platelet aggregation and the formation of a blood clot,

resulting in permanent occlusion of blood vessels. The scalp was then sutured and the

animals were returned to their home cages to recover. At intervals of 1, 3, 6, 12, 24

hours and 7 days post-surgery, animals were given an overdose of sodium

pentobarbitone and were perfused, via the left ventricle, briefly with PBS and then with

100 mM phosphate buffer containing 2% paraformaldehyde and 0.2% gluteraldehyde.

After perfusion, each brain was placed in a vial containing ice cold 2%

paraformaldehyde in 100 mM phosphate buffer and shipped by courier to Dr.

Robertson's laboratory.

### In situ hybridization

*In situ* hybridization was performed as described in the material and methods

section of chapter 2. Oligonucleotide probe sequences for *Hsp70* mRNA and for *c-fos*

mRNA are shown in table 2.

### Fos and Hsp27 immunohistochemistry

Each brain was sectioned (50 $\mu$m) on a vibratome in ice-cold PBS.

Immunohistochemistry was performed on free floating sections. For Fos

immunohistochemistry, sections were incubated in 0.3 % hydrogen peroxide/PBS,

rinsed three times in PBS and incubated one hour in 10% rabbit serum made in PBS.

After 3 PBS washes, sections were incubated 2 days at 4°C in PBS containing a sheep

polyclonal antiserum that recognizes c-Fos (1:20,000; Genosys Biotechnologies, The

Woodlands, Texas, U.S.A.). After three PBS rinses, sections were incubated in PBS

containing a biotinylated rabbit polyclonal antibody raised against sheep IgG (1:500;

Vector Laboratories Inc., Burlingame, California, U.S.A.). Sections were then

immersed one hour in avidin-biotin-horseradish peroxidase complex (1:1,000; Vector

Laboratories Inc.). After PBS washes, sections were immersed in diaminobenzidine-

tetrahydrochloride (0.05%; Sigma Chemical Co., St. Louis, Missouri, U.S.A.) made

up in PBS containing 0.3 mg/100 ml glucose oxidase, 40 mg/ml ammonium chloride

and 200 mg/100 ml β-D(+)glucose (Sigma Chemical Co.).

Hsp27 immunohistochemistry was performed as described chapter 5.

*Image processing and analysis*

*In situ* hybridization images on autoradiography film and immunohisto-

chemically- or cresyl violet-stained sections were digitalized as described in chapter 4.

Digitalized images of *Hsp70* mRNA expression were analyzed using NIH Image

1.60 software. For each time point, 2 sections through the lesion from each of three

rats were analyzed for the area of brain section, the area of *Hsp70* mRNA expression,

and the area of necrosis. The area of *Hsp70* mRNA expression and the area of necrosis

were determined as a percentage of the brain section area. One-way analysis of

variance and Student-Newman-Keuls multiple comparison tests were used to compare

areas between groups.

## Results

### c-fos expression

Photothrombotic injury activated *c-fos* expression in the ipsilateral cortex

(Figure 6.1). *c-fos* mRNA was detected by *in situ* hybridization in the ipsilateral

hemisphere 1 hour after photothrombotic injury (Figures 6.1A). No expression of c-fos

was observed in control rats (n=3; data not shown). c-Fos immunoreactivity was

detected in the ipsilateral hemisphere 3 hours after photothrombotic injury (Figure

6.1B). *c-fos* mRNA and Fos immunoreactivity were observed in the cingulate cortex,

in the fronto-parietal cortex and in the piriform cortex. In the ipsilateral cortex, Fos

immunoreactivity was detected 1, 3, 6 and 12 hours but not 24 hours after the

photothrombotic injury. Within the lesion, minimal or no *c-fos* mRNA or Fos

immunoreactivity was detected. Minimal Fos immunoreactivity was observed in the

fronto-parietal cortex of the contralateral side (Figure 6.1C). In the ipsilateral cortex,

Fos immunoreactivity was detected in the nuclei of cells in all the cortical layers

(Figure 6.1D).

### Hsp70 expression

*In situ* hybridization revealed *Hsp70* mRNA exclusively around the site of the

lesion 1 to 24 hours after photothrombotic injury (Figure 6.2). One hour after

photothrombotic injury, *Hsp70* mRNA was located in a zone (Figure 6.2A) adjacent

and peripheral to the photothrombotic lesion (Figure 6.2B). At 3 and 12 hours after the

photothrombotic injury, the *Hsp70*-positive zone appeared to become narrower (Figure

6.2C and Figure 6.2D, respectively). Twenty-four hours after the photothrombotic

injury, *Hsp70* mRNA was localized to a narrow zone (Figure 6.2E) at the periphery of

the lesion area (Figure 6.2F). Seven days following photothrombotic injury, *Hsp70*

mRNA was undetectable (data not shown).

Table 4 shows the semi-quantitative analysis of the area of *Hsp70* mRNA

expression, area of necrosis and the area of injury (the combined areas of *Hsp70*

expression and of necrosis) after photothrombotic injury. Overall, the area of *Hsp70*

expression decreased ($p < 0.05$) and conversely the area of necrosis increased ($p < 0.05$)

from 1 to 24 hours after photothrombotic injury. The areas of injury were not

significantly different at 1, 3, 12 or 24 hours after photothrombotic injury.

### Hsp27 expression

Immunohistochemistry revealed that Hsp27 was expressed in the ipsilateral

cortex following the photothrombotic injury (Figure 6.3). Hsp27 immunoreactivity was

not observed in the ipsilateral cortex of rats that had been allowed to recover one hour

after injury (Figure 6.3A) but was first detected 12 hours after injury and was still

observed 7 days after injury. Hsp27 immunoreactivity was observed in the fronto-

parietal cortex and piriform cortex 24 hours and seven days after injury, including

cingulate and retrosplenial cortices (Figure 6.3B and Figure 6.3C, respectively).

However, at 1, 12, 24 hours and at 7 days after the photothrombotic injury, Hsp27

immunoreactivity was not detected in the entire cingulate cortex. The morphology of

the Hsp27-immunoreactive cells in the parietal cortex appeared similar to that of

astrocytes (Figure 6.3D).

Figure 6.1. *C-fos* expression in the rat brain following photothrombotic injury. At 1

hour after injury, *in situ* hybridization revealed *c-fos* mRNA throughout the ipsilateral

cortex but not around the site of injury (A). At 3 hours after injury,

immunohistochemistry revealed c-Fos immunoreactivity in the ipsilateral cortex (B).

Note that *c-fos* mRNA and protein were observed in the cingulate cortex, fronto-

parietal cortex and piriform cortex. Fos immunoreactivity was minimal in the

contralateral non-injured parietal cortex (C) while Fos immunoreactivity was observed

in all layers of the ipsilateral injured parietal cortex (D). Scale bar equals 500 μm.
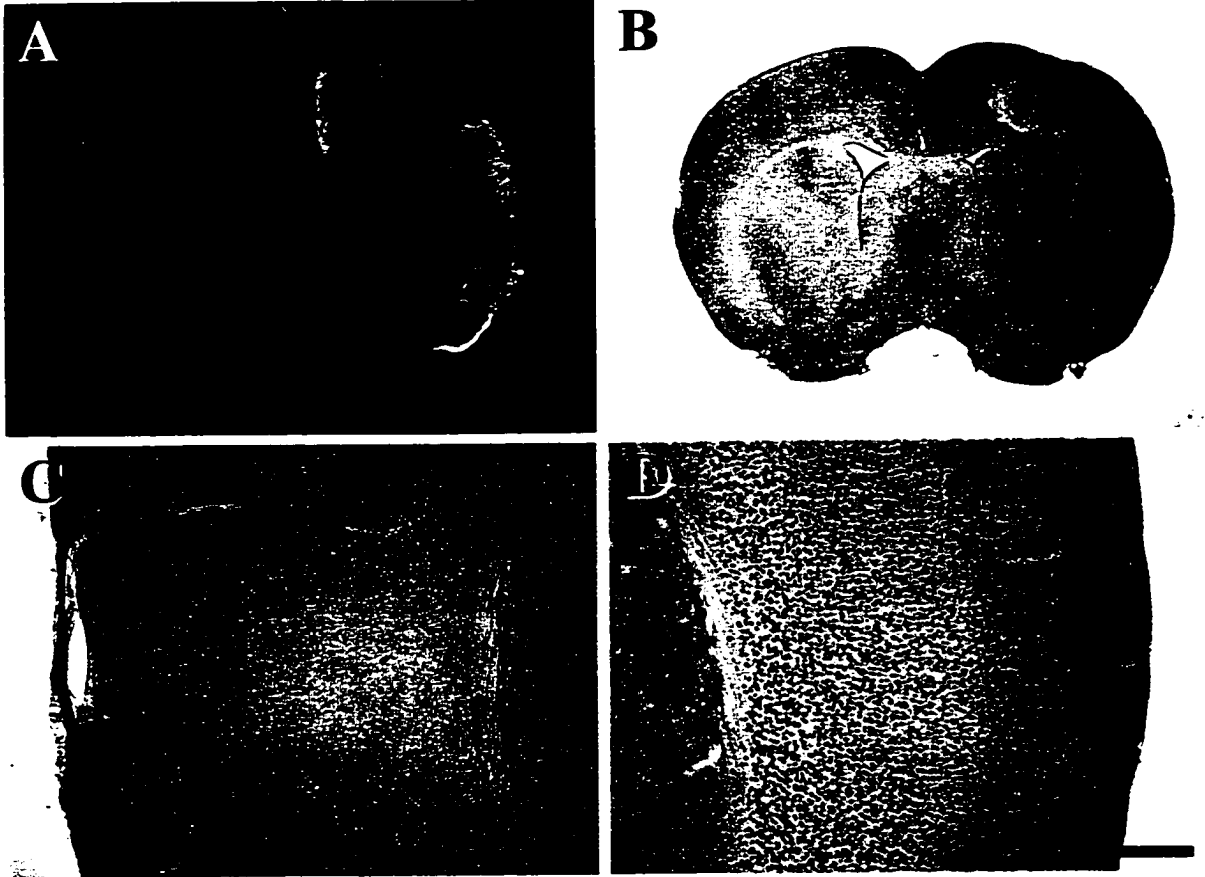
Figure 6.1

Figure 6.2. *In situ* hybridization for *Hsp70* mRNA in the rat brain following

photothrombotic injury. At 1 hour after the photothrombotic injury, *Hsp70* mRNA was

detected in a zone adjacent and peripheral to the necrotic zone (A). At 1 hour after

injury, the necrotic area was visualized by cresyl violet staining of an adjacent section

(B; arrows indicate the edge of the lesion). At 3 and 12 hours after injury, *Hsp70*

mRNA was detected in a progessively narrower zone of tissue surrounding the lesion

site and necrotic area (C, and D, respectively). At 24 hours after injury, *Hsp70* mRNA

was detected in a narrow zone of tissue adjacent and peripheral to the necrotic area (E).

At 24 hours after injury, the necrotic area was visualized by cresyl violet staining of an

adjacent section (F).
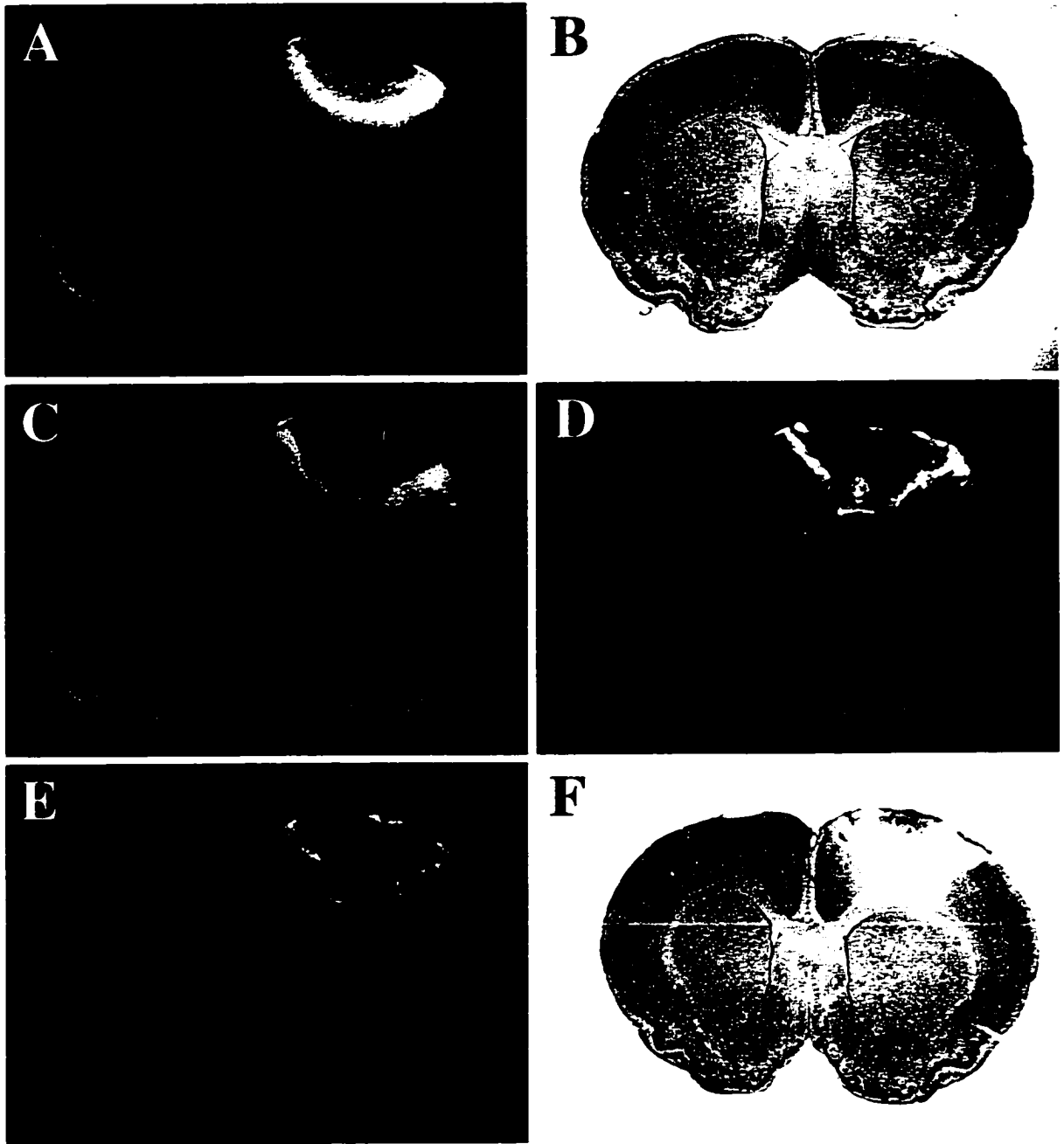
Figure G.2

Table 4. Semi-quantitative analysis of the areas of *Hsp70* expression, necrosis and

injury.

| Recovery | % Area of *Hsp70* | % Area of necrosis | % Area of injury |
|---|---|---|---|
| 1 hour | 6.0 ± 0.7 | 3.6 ± 0.3 | 9.6 ± 0.5 |
| 3 hours | 3.8 ± 0.2 | 3.8 ± 0.7 | 7.6 ± 0.7 |
| 12 hours | 3.5 ± 0.3 | 5.9 ± 0.9 | 9.4 ± 1.0 |
| 24 hours | 3.1 ± 0.3 | 7.2 ± 0.2 | 10.3 ± 0.2 |

The total area of the section, the area of *Hsp70* expression and the area of necrosis

were outlined and measured using NIH Image 1.60 software. The area of *Hsp70*

expression, area of necrosis, and area of injury (combined areas of *Hsp70* expression

and necrosis) are expressed as a percentage of the total area of the brain section.

Values are Mean ± SEM from 2 sections of each of 3 animals. Statistical comparisons

were done using one-way analysis of variance and Student-Newman-Keuls multiple

comparison tests. Statistical differences ($p < 0.05$) for % area of *Hsp70* expression

were observed between 1 and 3 hours, 1 and 12 hours, and 1 and 24 hours. For %

area of necrosis, statistical differences ($p < 0.05$) were observed between 1 and 12

hours, 1 and 24 hours, 3 and 12 hours, and 3 and 24 hours. There was no statistical

difference in the % area of injury at 1, 3, 12 or 24 hours after photothrombotic injury.

Figure 6.3. Hsp27 immunoreactivity in the rat brain following photothrombotic injury.

No Hsp27 immunoreactivity was observed in rats that had recovered for one hour

following injury (A). Hsp27 immunoreactivity was detected in the fronto-parietal and

piriform cortex 24 hours (B) and seven days (C) after injury. Note that Hsp27

immunoreactivity was observed in only the superficial layers of the cingulate cortex.

Hsp27-immunoreactive cells in the parietal cortex of a rat that had recovered seven

days after the photothrombotic injury showed a morphology similar to astrocytes (D;

Scale bar equals 50 µm).
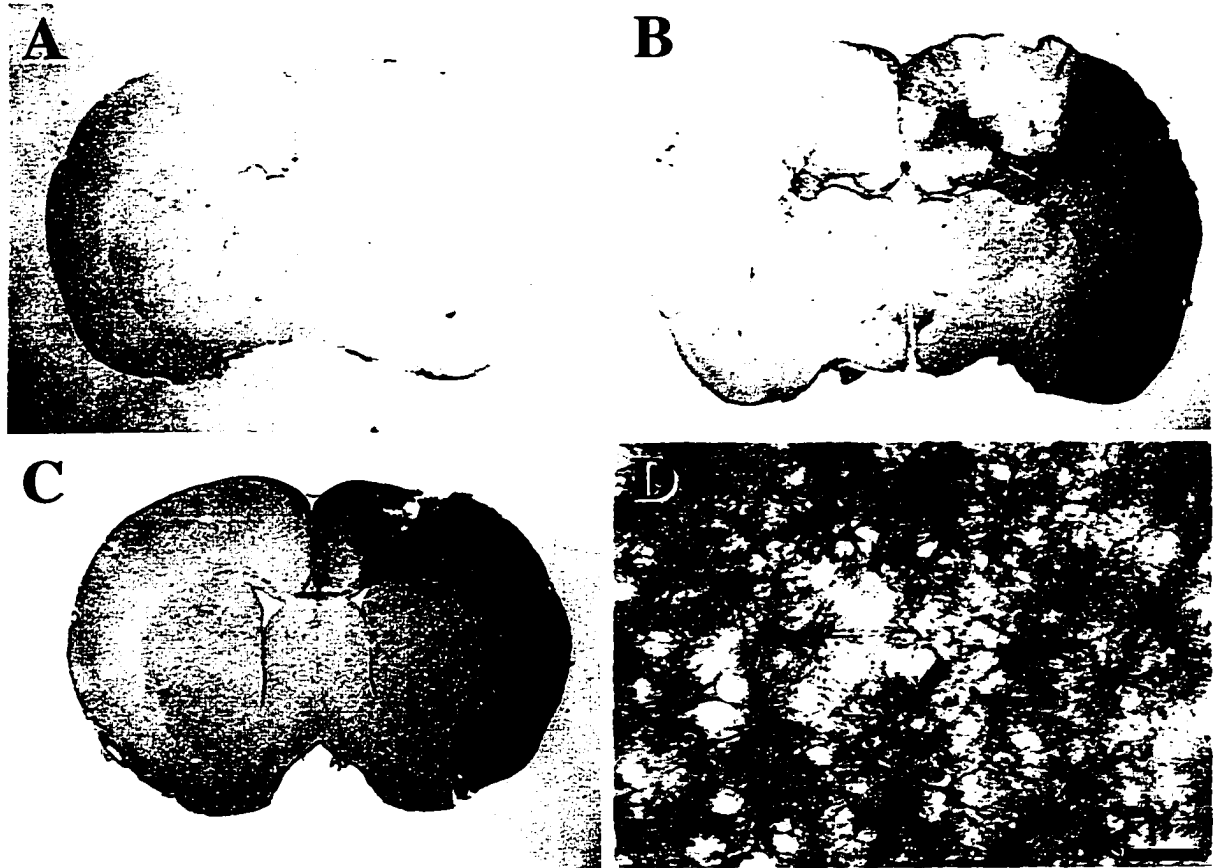
Figure 6.3

## Discussion

In this study, the distribution of *c-fos*, *Hsp70* and Hsp27 expression in the rat brain following photothrombotic injury was examined. Each gene showed a specific pattern of expression: *c-fos* induction was detected throughout the ipsilateral cerebral cortex; *Hsp70* expression was restricted to the zone adjacent and peripheral to the lesion; and Hsp27 expression was observed throughout the ipsilateral cerebral cortex but not in the entire cingulate cortex. In addition, Hsp27 expression was observed in astrocytes. These results suggest that the stress response induced by photothrombotic injury was dependent on cell types and brain regions.

### *c-fos expression*

Photothrombotic injury induced *c-fos* expression in a similar manner as that reported following mechanical or chemical unilateral cortical injury (Dragunow and Robertson, 1988; Herrera and Robertson, 1989, 1990; Comelli et al., 1993; Jacobs et al., 1994). *c-fos* expression occurred throughout the entire cerebral cortex in all cerebral layers and in both neurons and glial cells (Dragunow and Robertson, 1988). This pattern of expression following unilateral cortical injury has been reported for other immediate early genes including *c-jun* and *jun-D* (Jacobs et al., 1994). Similarly, photothrombotic injury acutely altered expression of c-Fos. C-Fos was expressed throughout the ipsilateral cortex. It seems that photothrombotic injury, like other focal lesions, triggered cell responses throughout the ipsilateral cortex, even in regions distant from the injury site, such as the ipsilateral piriform cortex.

## Hsp70 expression

The expression of *Hsp70* has been extensively used to characterize injured

neurons (Gonzalez et al., 1989). Hsp70 induction has been reported in the brain

following unilateral surgical wounding (Brown et al., 1989), ischemic episodes

(Gonzalez et al., 1991; Sharp et al., 1991b; Simon et al., 1991) and excitotoxic

treatments (Vass et al., 1989; Lowenstein et al., 1990; Gass et al., 1995; Armstrong et

al., 1996). After photothrombotic injury, Hsp70 protein has been localized in

microvessels bordering the lesion (Lindsberg et al., 1996). In the present study, *Hsp70*

was expressed in a zone adjacent and peripheral to the necrotic area in a manner similar

to that observed following surgical wounding of the cerebral cortex (Brown et al.,

1989). One hour after photothrombotic injury, the necrotic zone was relatively small

while the *Hsp70*-positive zone was larger and surrounded the necrotic zone. At 24

hours after the photothrombotic injury, the necrotic zone was relatively large and the

*Hsp70*-positive zone was narrow, surrounding the necrotic zone. This observation

suggests that there was a progressive increase in size of the necrotic zone and that the

*Hsp70*-positive zone seen at 1 hour approximates the penumbra. Interestingly, the area

of injury, i.e., combined areas of *Hsp70* expression and of necrosis, was approximately

equal in all the animals (see Figure 6.2 and Table 4). This suggests that even as early

as 1 hour after photothrombotic injury, *Hsp70* expression delineates the area of necrosis

at 24 hours after photothrombotic injury. In fact, it has been suggested that *Hsp70*

expression could be used to determine the extent of the injured area (Kinouchi et al., 1993).

## Hsp27 expression

In contrast to *Hsp70* expression, Hsp27 expression was not restricted to the region surrounding the injury site but was observed throughout the ipsilateral cortex, including the piriform cortex, parietal cortex and superficial layers of the cingulate cortex. Interestingly, Hsp27 was not expressed in the posterior cingulate cortex or in the retrosplenial cortex. The distribution of Hsp27 immunoreactivity was similar to glial fibrillary acidic protein (GFAP) immunoreactivity in reactive astrocytes observed 2 days after application of potassium chloride on the cerebral cortex (Herrera and Cuello, 1992). This result suggests that Hsp27 expression may play a role in reactive astrocytes. Recently, astrocytes have been shown to express Hsp27 immunoreactivity at 12 hours after kainic acid-induced status epilepticus in the rat (Plumier et al., 1996). Similarly, Hsp27 immunoreactivity was first detected 12 hours after photothrombotic injury. The induction of Hsp27 in both studies suggests that Hsp27 represents a component of the stress response specific to astrocytes.

Regulation of expression of *c-fos*, *Hsp70* and *Hsp27* are clearly different. The expression of *c-fos* is increased by many events that cause neuronal activation, and possibly long-term changes in cellular phenotype (Curran and Morgan, 1995). Expression of Hsp70 is induced by noxious stimuli, and the accumulation of coagulated, precipitated or denatured protein in the cells. Pre-existing heat shock

transcription factors are activated when Hsc70 releases the heat shock transcription

factors and binds denatured protein. The heat shock transcription factors trimerize,

bind to a heat shock element in the promoter region of heat shock genes and initiate

transcription (Sistonen et al., 1994). The expression of Hsp27 in astrocytes throughout

the ipsilateral cortex could result from spreading depression that rapidly triggers

neuronal and glial expression of c-fos in the entire cerebral cortex (Dragunow and

Robertson, 1988). However, only glial cells responded to the activation signal and

synthesized Hsp27 after injury. While expression of Hsp70 is regulated by at least two

heat shock transcription factors (Sistonen et al., 1994), it is unlikely that Hsp27

induction in astrocytes involves activation of these specific heat shock transcription

factors. Expression of Hsp70 was observed only adjacent to the photothrombotic injury

site and was not observed in the entire ipsilateral cortex as was Hsp27. However, it is

likely that Hsp27 was induced through a specific mechanism. For example, astrocytic

uptake of excitatory amino acids, such as glutamate, through the glutamate transporter

GLT-1 (Ginsberg et al., 1995), may be involved in the astrocytic expression of Hsp27.

Alternately, the astrocytic expression of Hsp27 could be induced via transduction

pathways related to specific trophic factors, such as ciliary neurotrophic factor that

induces astrogliosis (Winter et al., 1995). It is also possible that the induction of

Hsp27 was secondary to morphological changes occurring during astrogliosis, such as

hypertrophy or reorganization of the cytoskeleton. Indeed, Hsp27 has been

demonstrated to play a role in dynamics of actin filaments (Lavoie et al., 1993b;

Landry and Huot, 1996).

*Conclusions*

In conclusion, photothrombotic injury of the fronto-parietal cortex triggered the

expression of immediate early genes (*c-fos*) and heat shock genes (*Hsp70* and *Hsp27*) in

the ipsilateral hemisphere. However, each gene product had a specific regional

distribution. In addition, while both *c-fos* and *Hsp70* expressions have been reported in

neurons as well as glial cells following cortical injury (Dragunow and Robertson, 1988;

Brown et al., 1989), Hsp27 induction was only detected in astrocytes. After injury,

regions and cell types of the brain can have varying and specific responses as indicated

by the expression of *c-fos*, *Hsp70* and Hsp27.

# CHAPTER 7:

# INDUCTION OF Hsp27

# AFTER CORTICAL SPREADING DEPRESSION

# Introduction

Application of potassium chloride to the cerebral cortex induces neuronal depolarization at the application site. These neurons release glutamate that in turn, depolarizes adjacent neurons through N-methyl-D-Aspartate (NMDA)-receptor activation. This progressive wave of neuronal depolarization that eventually spreads through the entire cerebral cortex, is called cortical spreading depression (Kraig et al., 1991; Bonthius et al., 1995). Cortical spreading depression has recently been shown to protect against subsequent transient focal cerebral ischemia (Kobayashi et al., 1995; Matsushima et al., 1996). A similar resistance to ischemic injury has also been observed following a mild ischemic preconditioning treatment (Kitagawa et al., 1991a). A mild global ischemic insult reduced the extent of hippocampal damage after a subsequent severe global ischemic insult (Kitagawa et al., 1991a; Liu et al., 1992) and significantly decreased the infarct size after permanent middle cerebral artery occlusion (Simon et al., 1993). In addition, a brief focal ischemic episode has been shown to be protective against subsequent severe global ischemic injury (Glazier et al., 1994). This 'ischemic tolerance' phenomenon has been associated repeatedly with the synthesis of heat shock proteins (Kirino et al., 1991; Kitagawa et al., 1991a; Nishi et al., 1993; Simon et al., 1993; Glazier et al., 1994) but conclusive evidence for an association remains elusive.

Much of the attention in 'ischemic tolerance' and endogenous protective mechanisms has focused on the inducible 70-kDa heat shock protein. Hsp70 has been

suggested to participate in the protective mechanisms against ischemic injury to both the heart (Currie et al., 1988; Marber et al., 1995; Plumier and Currie, 1996) and brain (Kirino et al., 1991; Liu et al., 1992, 1993; Simon et al., 1993; Nishi et al., 1993; Glazier et al., 1994). While cortical spreading depression induced ischemic tolerance throughout the cerebral cortex, Hsp70 was only detected around the KCl application site (Kobayashi et al., 1995). It was concluded that Hsp70 was not involved in ischemic tolerance induced by cortical spreading depression. Similarly, brief repetitive middle cerebral artery occlusions decreased infarct size following a subsequent 100 minute-occlusion (Chen et al., 1996) and Hsp70 accumulation and degradation did not match exactly with the acquisition and decay of ischemic tolerance. These results did not exclude a role for other heat shock proteins such as Hsp27 whose expression is known to increase cell resistance to oxidative injury (Mehlen et al., 1995). In fact, Hsp27 has been shown to be expressed following cerebral ischemia (Kato et al., 1994; 1995; see chapter 6).

The purpose of this study was to examine and characterize the temporal and spatial distribution of Hsp27 expression following KCl-induced spreading depression. The effect of systemic administration of the NMDA receptor antagonist, MK-801, a compound known to inhibit spreading depression was also examined. It was concluded that KCl-induced cortical spreading depression triggered a complex astroglial response, i.e., Hsp27 immunoreactivity varied according to brain region and could be dissociated from neuronal activity as measured by Fos immunoreactivity.

## Material and methods

### Animals

All the animals were cared for in accordance with the *Guide to the Care and Use of Experimental animals* of the Canadian Council on Animal Care.

### Potassium chloride application

Eighteen adult male Sprague-Dawley rats (250-300 grams, Charles River, Montreal) were anesthetized with sodium pentobarbital (50 mg/kg ip). The surface of the skull was exposed through a longitudinal incision in the skin. A rectangle of bone 3 mm wide and 5 mm long was removed from the right side of the skull. The dura mater was exposed. A cotton tip soaked in KCl (3M) was applied to dura mater over the right parietal cortex for 5 minutes (n=6) or 20 minutes (n=9). Then, the cranial bone was glued back using dental cement and the skin was sutured. At 2 hours (n=3), 2 (n=3) or 4 (n=9) days after surgery, the rats were killed and perfused via the aorta with 100 mM phosphate buffer containing 2% paraformaldehyde and 0.2% glutaraldehyde (4°C). The brain was then removed and post-fixed in 100 mM phosphate buffer containing 2% paraformaldehyde. In three rats, the dura mater was exposed as described above but KCl was not applied. These sham-treated rats were killed 4 days after surgery and perfused as described above.

### MK-801 treatment

Adult rats were injected ip with 3 or 9 mg/kg of MK-801 (n=3 for each dose) and killed 2 days later in order to determine the effect of MK-801 on Hsp27 expression.

To reduce reactive gliosis, we used a dose of 3 mg/kg of MK-801 injected ip 30 minutes before a 20-minute cortical application of potassium chloride (Herrera and Cuello, 1992; Bonthius and Steward, 1993). At 2 days (n=5) after surgery, MK-801 treated rats were killed and perfused as described above.

## Fos and Hsp27 immunohistochemistry

Fos immunohistochemistry was performed as described in chapter 6.

Hsp27 immunohistochemistry was performed as described in chapter 5. Immunohistochemically stained sections were mounted onto coated slides, air dried overnight and coverslipped. Some immunostained sections were counter-stained with cresyl violet (0.1%).

## Immunofluorescence

For GFAP/Hsp25 double labeling, sections were incubated one hour in PBS containing 10% horse and 10% goat serum. After three PBS rinses, sections were incubated overnight in PBS containing the rabbit polyclonal Hsp25 antibody and the mouse monoclonal GFAP antibody. After three PBS washes, sections were incubated with fluorescein-conjugated horse antibody raised against mouse IgG (1:30; Vector Laboratories Inc.) and Texas Red-conjugated goat antibody raised against rabbit IgG (1:300; Vector Laboratories Inc.) to detect the primary antibodies. Immunofluorescent sections were examined using a Zeiss Axioplan microscope equipped with an incident-light fluorescence illuminator and filters suitable for viewing the fluorochromes fluorescein and Texas Red.

*Image processing*

Immunostained sections were digitalized as described in chapter 4.

*Semi-quantitative densitometry*

Digitalized images were analyzed using NIH Image 1.60 software.

Densitometry of Hsp27 immunostaining was measured on three sections for each

animal in the ipsilateral and contralateral parietal cortices and in the thalamus. Final

optical densities for the parietal cortex were obtained by subtraction of corresponding

densitometry measurements of the thalamus, used as background values and presented

as means ± SEM. Optical densities from MK-801 treated (3 mg/kg, ip, 30 minutes

before KCl cortical application for 20 minutes, 2 day-survival) and non-treated rats

were compared with one-way analysis of variance. Analyses were followed by

Newman-Keuls tests.

## Results

*Hsp27 immunoreactivity after application of KCl*

Unilateral cortical application of KCl induced Hsp27 immunoreactivity in the rat

ipsilateral cerebral cortex (Figure 7.1). Hsp27 immunoreactivity was observed in the

fronto-parietal cortex, entorhinal cortex and piriform cortex, but not in the retrosplenial

cortex or in the posterior cingulate cortex. No Hsp27 immunoreactivity was observed

in the contralateral cortex of KCl-treated rats or in the cerebral cortex of sham-operated

rats. In the ipsilateral KCl-treated cortex, most of the immunoreactivity for Hsp27

appeared to be in astrocytes. At the site of KCl application, a few Hsp27

immunoreactive microglial cells were detected. Occasionally neurons on the border of

the injured area showed Hsp27 immunoreactivity.

## Hsp27- and GFAP -double immunofluorescence

Four days after unilateral cortical application of KCl, Hsp27-immunopositive

cells in the fronto-parietal cortex (Figure 7.2A) were also GFAP-immunopositive

(Figure 7.2B). Similarly, all Hsp27-immunoreactive cells of the piriform cortex

(Figure 7.2C) were GFAP-immunoreactive (Figure 7.2D). However, Hsp27-

imunoreactivity distribution was restricted to the piriform cortex and was not detected

in the amygdala (Figure 7.2C) while GFAP-immunofluorescence was detected in both

the piriform cortex and the amygdala (Figure 7.2D). Hsp27 immunofluorescence

illustrated the brushy appearance of the astrocytes with their numerous branching

processes (Figure 7.2E) while GFAP immunoreactivity labeled mainly cell bodies and

major processes (Figure 7.2F).

## Effect of MK-801 on KCl-induced Hsp27 immunoreactivity.

Systemic administration of the NMDA-receptor antagonist MK-801 (3 mg/kg,

ip) 30 minutes before cortical application of KCl reduced the extent of Hsp27

immunoreactivity in the ipsilateral parietal cortex (Figure 7.3). Two days after cortical

application of KCl, Hsp27 immunoreactivity in non-MK-801-treated animals was

observed in all layers of the parietal cortex (Figure 7.3A). Numerous astrocytes were

Hsp27-immunoreactive (Figure 7.3B). Systemic administration of MK-801 reduced the

extent of Hsp27 immunoreactivity in the ipsilateral parietal cortex (Figure 7.3C) with

apparently fewer Hsp27-positive astrocytes (Figure 7.3D). Semi-quantitative analysis

of optical densities of Hsp27 immunoreactivity in the parietal cortex (Figure 7.3E)

revealed that 1) in non-MK-801-treated rats, KCl-induced Hsp27 immunoreactivity was

significantly different between the contralateral and ipsilateral parietal cortices

(16.5±2.3 versus 73.3±5.2 arbitrary units, respectively; $p < 0.05$); 2) in MK-801-

treated rats, KCl-induced Hsp27 immunoreactivity was significantly different between

the contralateral and ipsilateral parietal cortices (14.7±5.2 versus 42.8±6.6 arbitrary

units, respectively; $p < 0.05$); 3) Hsp27 immunoreactivity was not different between

contralateral cortices of non-MK-801-treated and MK-801-treated animals (16.5±2.3

versus 14.7±5.2 arbitrary units, respectively); 4) Hsp27 immunoreactivity was

significantly different between ipsilateral cortices of non-MK-801-treated and MK-801-

treated animals (73.3±5.2 versus 42.8±6.6 arbitrary units, respectively; $p < 0.05$).

## Regional distribution of Hsp27 immunoreactivity

Hsp27 immunoreactivity was not observed in the cingulate cortex, except

occasionally in layer I (see Figure 7.1) or in the retrosplenial cortex (Figure 7.4A).

Fos immunoreactivity, a marker of neuronal activation, was detected in the entire

ipsilateral cortex, including the cingulate cortex and retrosplenial cortex (Figure 7.4B).

High doses of the NMDA-receptor antagonist, MK-801, have been reported to

induce Hsp70 specifically in neurons of the posterior cingulate cortex and retrosplenial

cortex (Sharp et al., 1991a). Thus we examined the posterior cingulate cortex and

retrosplenial cortex for Hsp27 immunoreactivity after a higher dose of MK-801. As

shown above (Figure 7.1 and Figure 7.4A), two days after systemic administration of 3

mg/kg of MK-801, no Hsp27 immunoreactivity was observed in the cingulate cortex or

retrosplenial cortex. However, two days after systemic administration of 9 mg/kg of

MK-801, Hsp27 immunoreactivity was detected in the retrosplenial cortex and in the

posterior cingulate cortex (Figure 7.4C). Counterstaining of immunostained sections

revealed that the Hsp27-positive astrocytes were localized in layer III of the cingulate

cortex (Figure 7.4D).

*Modulation of Hsp27 distribution by reduction of cortical injury.*

Six animals were subjected to 5 minutes of cortical application of KCl. Four of

these animals had immunoreactivity for Hsp27 similar in intensity and distribution as

the animals treated with KCl for 20 minutes. However, two of six animals subjected to

5 minute-application of KCl showed a distribution of Hsp27 immunoreactivity different

from that observed in animals after 20 minute-application of KCl. In both cases, Hsp27

immunoreactivity was not observed in all layers of the ipsilateral cortex but was

observed only in the superficial layers (Figure 7.5). In one rat, Hsp27-immunoreactive

astrocytes were detected around the lesion site, in clusters in layers I - III throughout

the ipsilateral cortex, and in layers II and III of the piriform cortex (Figure 7.5A). In

the second rat, Hsp27 immunoreactivity was detected in layers I - III of the ipsilateral

cortex and in the entire piriform cortex (Figure 7.5B).

Top panel:

Figure 7.1. Hsp27 immunoreactivity in the rat cerebral cortex after potassium chloride

application. Four days after 20 minute-application of KCl onto the right cerebral cortex

(right side), Hsp27 immunoreactivity was observed in all cortical layers of the

ipsilateral parietal, perirhinal and piriform cortex. Note the absence of Hsp27

immunostaining in the ipsilateral retrosplenial cortex and in the contralateral cortex (left

side).

Bottom panel:

Figure 7.2. Hsp27 and glial fibrillary acidic protein (GFAP) immunoreactivity four

days after cortical application of potassium chloride. A Texas Red-conjugated antibody

was used to detect the rabbit polyclonal antibody immunoreacting with Hsp27 (A, C

and E). A fluorescein-conjugated antibody was used to detect the mouse monoclonal

antibody against GFAP (B, D and F). Double-labeled cells were revealed with

appropriate filters in the parietal cortex (A and B) and in the piriform cortex (C and D,

and E and F). Examples of double-labeled cells are shown by arrows (A, B, E and F).

The amygdala is indicated by the asterisks (C and D). An example of Hsp27-negative

and GFAP-positive astrocyte is indicated arrow heads (E and F). Note that fine

secondary processes of astrocytes are Hsp27-immunoreactive but not GFAP-positive

(compared E and F). Bar equals 50μm.

Figure 7.1
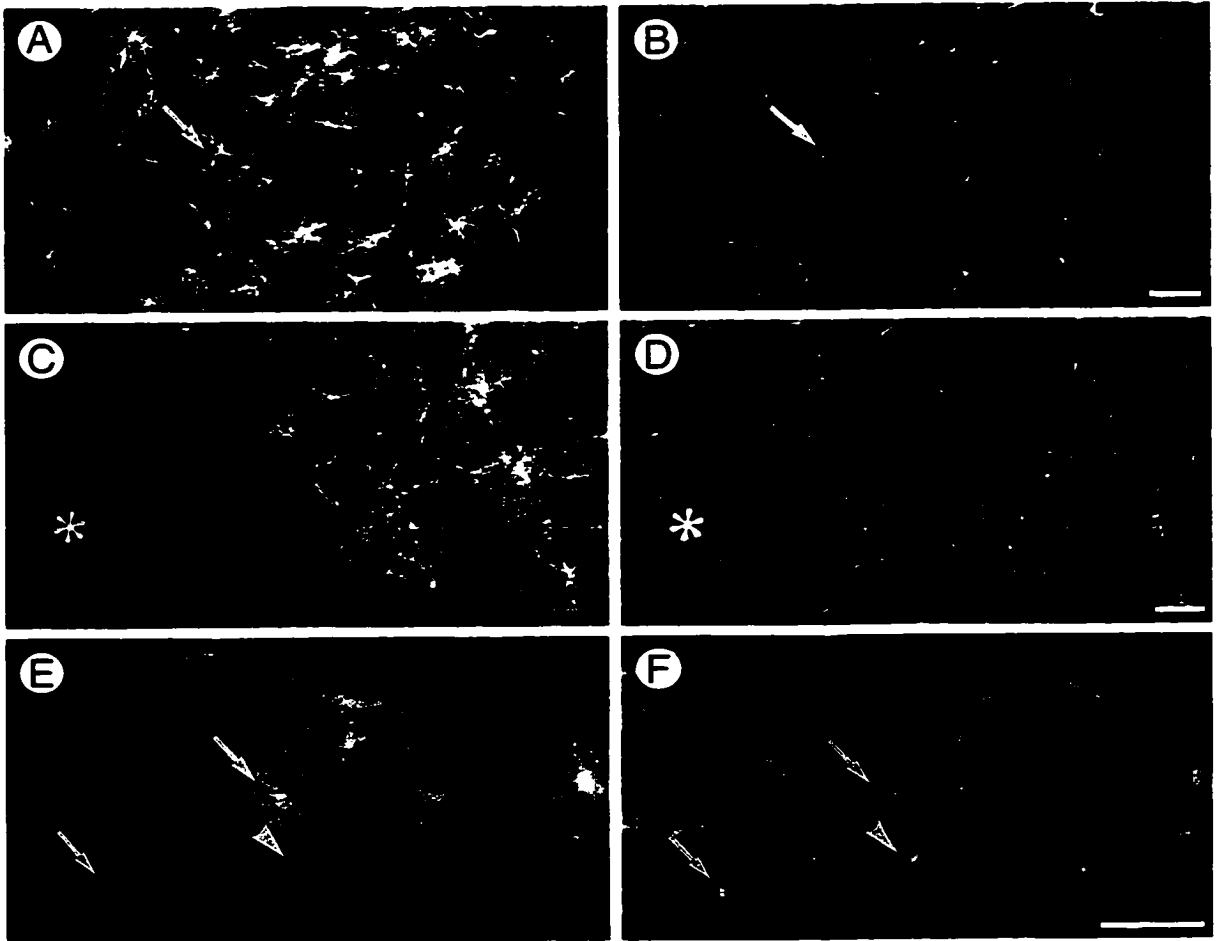


Figure 7.2

Figure 7.3. Effect of systemic administration of MK-801 on the induction of Hsp27

immunoreactivity following cortical application of potassium chloride. In non-MK-

801-treated rats, two days after 20 minute-cortical application of KCl, Hsp27

immunoreactivity was detected in all layers of the cortex, but not in the posterior

cingulate or retrosplenial cortex (A). Hsp27 immunoreactivity was still detected in

astrocytes (B). In MK-801-treated rats (3 mg/kg, ip), Hsp27 immunoreactivity

appeared to be attenuated in all layers of the cortex (C), two days after 20 minute-

cortical application of KCl. This Hsp27 immunoreactivity was detected in astrocytes

(D). Semi-quantitative analysis revealed that MK-801 treatment significantly reduced

the intensity of Hsp27 immunoreactivity (E). Values indicated are means ± SEM

(arbitrary units). C, contralateral parietal cortex. L, lesioned ipsilateral parietal

cortex. Asterisks indicate significant differences in Hsp27 immunoreactivity between

treatments using one-way analysis of variance and Newman-Keuls post hoc

comparisons ($p < 0.05$).
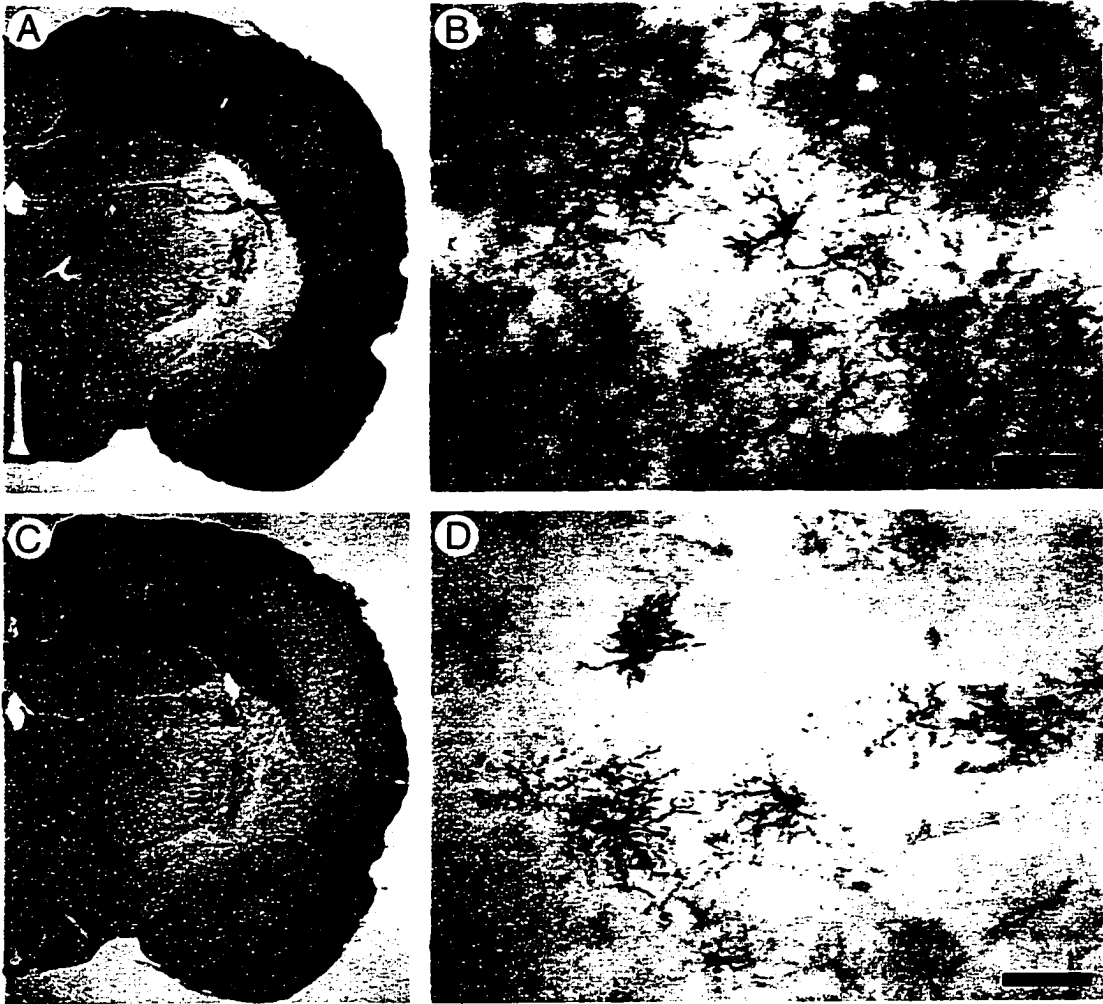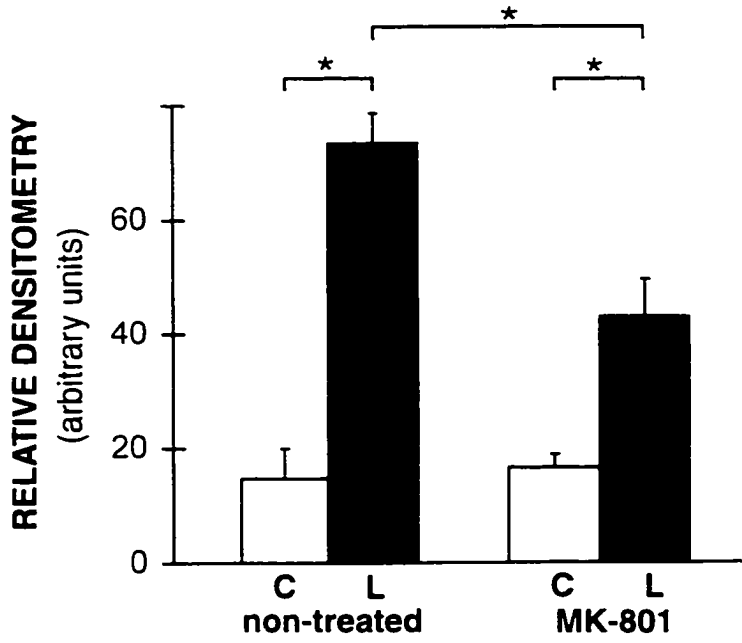
Figure 7.3

Figure 7.4. Hsp27 immunoreactivity in the granular retrosplenial cortex. At 2 or 4

days after cortical application of KCl, no Hsp27 immunoreactivity was observed in the

retrosplenial cortex, except in the glial limitans (A). Two hours after cortical

application of KCl, Fos immunoreactivity was observed in the entire ipsilateral cortex,

including the retrosplenial cortex (B). Two days after administration of MK-801 (9

mg/kg, ip), Hsp27 immunoreactive astrocytes were observed in the retrosplenial cortex

and the cingulate cortex (C). Cresyl violet counterstaining of Hsp27 immunoreacted

horizontal section revealed that Hsp27 positive astrocytes were located in layer III of

the retrosplenial cortex (D). Bar equals 100 μm.
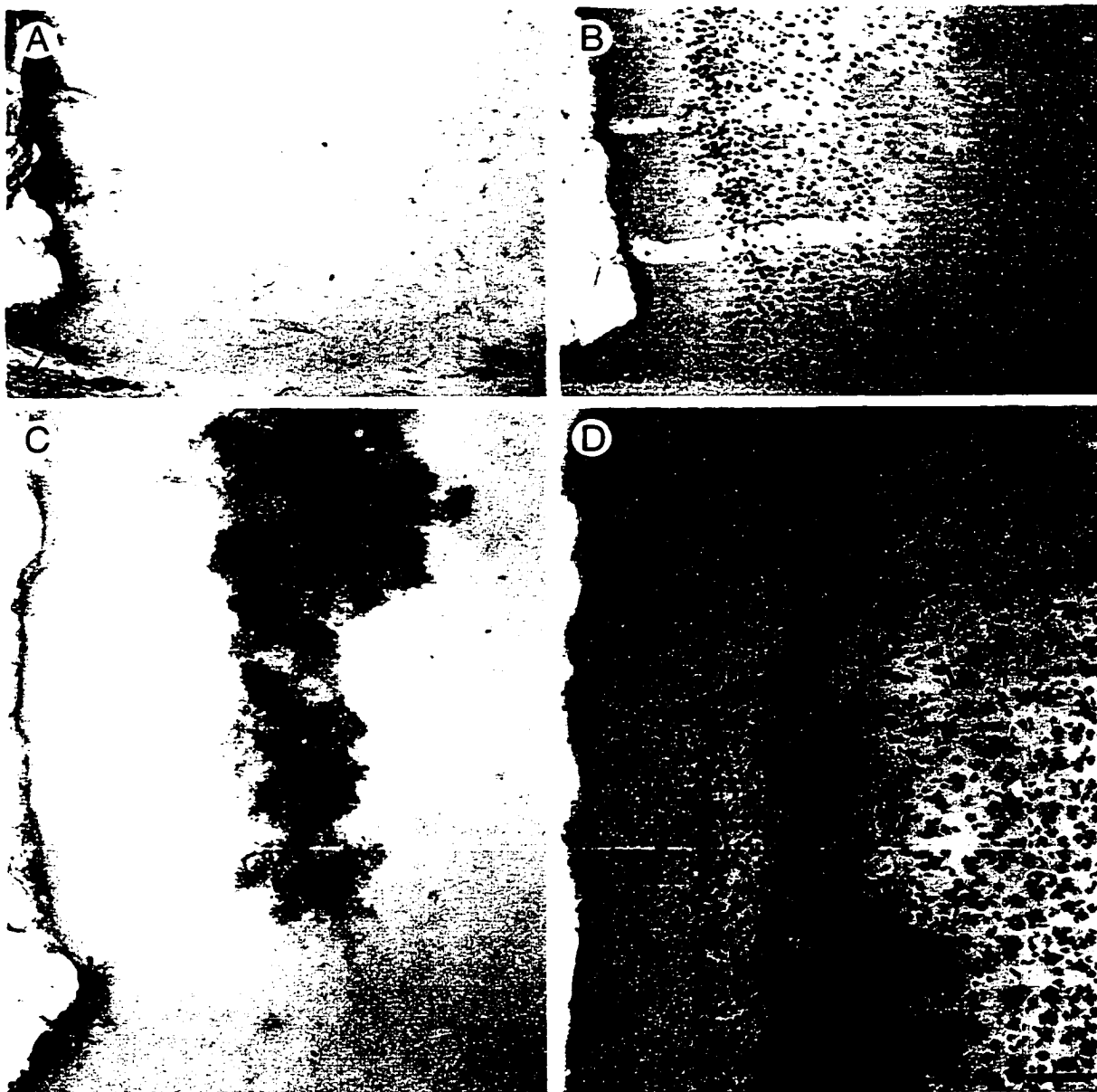
Figure 7.4

Figure 7.5. Hsp27 immunoreactivity in the rat cortex four days after 5 minute-cortical

application of potassium chloride. While 4 of 6 rats had Hsp27 immunoreactivity

similar to those with 20 minute-application of KCl, 2 of six rats showed less intense

Hsp27 immunoreactivity. In one rat, Hsp27 immunoreactivity was observed around the

lesion site, in clusters of astrocytes in layers I-III of the parietal cortex, and in layers II

and III of the piriform cortex (A). In the other rat, Hsp27 immunoreactivity was

observed around the lesion site, in cortical layers I, II, and III, throughout the parietal

cortex and in the entire piriform cortex (B). Clusters of Hsp27-immunoreactive

astrocytes are indicated by arrow heads (A). Note the absence of Hsp27

immunoreactivity even in layer I of the parietal cortex (arrows).
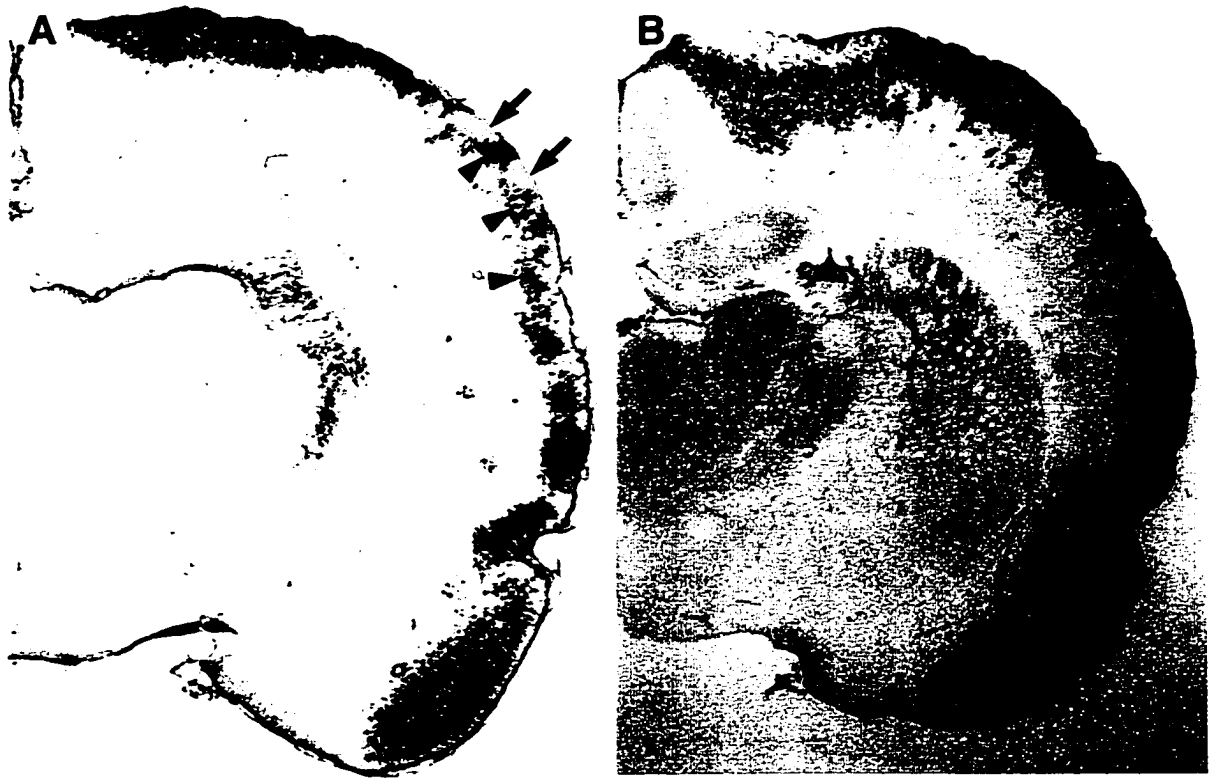
Figure 7.5

**Discussion**

Cortical application of KCl induced Hsp27 immunoreactivity in the rat ipsilateral cerebral cortex. Hsp27 immunoreactivity was localized in GFAP-positive astrocytes. Suppression of KCl-induced cortical spreading depression with systemic administration of the NMDA-receptor antagonist, MK-801 (3 mg/kg), significantly attenuated the expression of Hsp27. While cortical application of KCl induced Hsp27 immunoreactivity in most of the ipsilateral cerebral cortex, there was no Hsp27 immunoreactivity in the posterior cingulate cortex and retrosplenial cortex. However, astrocytes in the posterior cingulate and retrosplenial cortex did express Hsp27 after injury to adjacent neurons by systemic administration of MK-801 (9 mg/kg). Finally, brief (5 minutes) cortical application of KCl revealed a progressive recruitment of astrocytes expressing Hsp27, from cell clusters (Figure 7.5A), to superficial cortical layers (Figure 7.5B) to all cortical layers (Figure 7.1; as seen after 20 minutes of KCl application).

*Distribution of Hsp27 expression*

This study showed that cortical application of KCl and the subsequent cortical spreading depression induced Hsp27 expression in astrocytes. Similar treatment also induces Fos expression in neurons and the expression of GFAP in astrocytes throughout the ipsilateral cortex (Herrera and Robertson, 1990; Kraig et al., 1991; Herrera and Cuello, 1992; Bonthius and Steward, 1993; Herdegen et al., 1993; Bonthius et al., 1995).

## Hsp27 induction

To investigate the pathways for induction of Hsp27 after cortical application of KCl, MK-801, an NMDA-receptor antagonist was used to block cortical spreading depression (Marrannes et al., 1988). Similar MK-801 treatment prior to application of KCl to the cerebral cortex also blocked Fos expression (Herrera and Robertson, 1990; Jacobs et al., 1994) and the generation of astrogliosis measured by GFAP upregulation (Herrera and Cuello, 1992; Bonthius and Steward, 1993; Bonthius et al., 1995). In the present study, Hsp27 immunoreactivity was also affected by MK-801 treatment. A significant reduction in the intensity of Hsp27 immunoreactivity in the parietal cortex was observed. This suggests that Hsp27 is induced by a similar mechanism to that of GFAP. However, MK-801 systemic administration at a dose reported to block cortical spreading depression and subsequent GFAP increase did not completely inhibit Hsp27 expression. There was still a significant difference between contralateral and ipsilateral parietal cortices of MK-801 treated animals that were examined 2 days following cortical application of KCl. This result suggests that following cortical application of KCl, Hsp27 is also induced by a mechanism different from that of GFAP. This hypothesis is also supported by the observations that cortical application of sodium chloride (3M) induced Hsp27 expression (data not shown) but not spreading depression (Kraig et al., 1991). Thus it seems that Hsp27 may be induced through more than one pathway. One pathway involves spreading depression and neuronal activation and can be blocked by the NMDA-receptor antagonist, MK-801. The lack of complete MK-801

inhibition of Hsp27 astrocytic expression following cortical application of KCl suggests a second pathway that is independent of spreading depression. These results also demonstrated that a stress response can occur in astrocytes without GFAP induction. Therefore, GFAP induction does not correlate as closely as Hsp27 induction with activation of astrocytes. It seems that Hsp27 may be a more sensitive marker than GFAP to study reactive astrocytes.

A third alternative pathway triggered by necrosis is also possible. In this study, Hsp27 was expressed in astrocytes surrounding the necrotic cells at the site of application of KCl. Similarly, GFAP-positive astrocytes were reported around the necrotic area and GFAP expression was not decreased by MK-801 treatment (Bonthius and Steward, 1993). In a recent study, Hsp27 was abundant in astrocytes around necrotic neurons of the piriform cortex following status epilepticus in the rat (Plumier et al., 1996). It seems therefore that necrosis triggered Hsp27 and GFAP in a NMDA-receptor-independent fashion.

## Regional differences in Hsp27 expression

The posterior cingulate and retrosplenial cortex respond to cortical application of KCl and spreading depression much differently than other regions of the neocortex. As shown here, following cortical application of KCl, Hsp27 was not expressed in the posterior cingulate and retrosplenial cortex. In addition, GFAP was not expressed in the cingulate and retrosplenial cortex after cortical application of KCl (Bonthius and Steward, 1993; Bonthius et al., 1995). The absence of GFAP expression was attributed

to either a lack of propagation of spreading depression or an intrinsic difference of astrocytes in these specific regions (Bonthius et al., 1995). In the present study, Fos, whose induction has been shown to be triggered by cortical spreading depression through NMDA receptor activity (Dragunow and Robertson, 1988; Herrera and Robertson, 1990; Herdegen et al. 1993), was detected in neurons throughout the ipsilateral cerebral cortex, including the posterior cingulate and retrosplenial cortex. This suggests that there were at least some changes in neuronal activity and gene expression that resulted from spreading depression into the posterior cingulate and retrosplenial cortex. In addition, Hsp27 was induced in astrocytes in these specific regions after systemic administration of a high dose of MK-801 (9 mg/kg) but not after a low dose (3 mg/kg). Interestingly, MK-801 treatment has been shown to induce selective neuronal injury measured by Hsp70 immunoreactivity in the posterior cingulate and retrosplenial cortex (Olney et al., 1990; 1991). Neurons in rats treated with 1 mg/kg of MK-801 express higher levels of Hsp70 than neurons in rats treated with 5 mg/kg MK-801 (Allen and Iversen, 1990; Fix et al., 1993). It was concluded that 5 mg/kg dose of MK-801 was more toxic to neurons and resulted in rapid cell death (Sharp et al., 1994). The results presented in the present study suggest that, in the retrosplenial cortex, Hsp27 expression in astrocytes was not associated with an increase in neuronal activity following cortical spreading depression or even injury after low dose of MK-801, but was associated with neuronal death after a high dose of MK-801. This is in contrast to the expression of Hsp27 in astrocytes of the parietal or

piriform cortex where cell death or even injury of adjacent neurons was not detected after cortical application of KCl. Thus it seems that there is an intrinsic difference between astrocytes of the parietal cortex and those of the cingulate and retrosplenial cortex.

## Astrocyte activation following spreading depression

As mentioned earlier, cortical spreading depression induces expression of Fos and GFAP throughout the ipsilateral parietal cortex and piriform cortex (Dragunow and Robertson, 1988; Kraig et al., 1991; Herrera and Cuello, 1992; Bonthius and Steward, 1993; Herdegen et al., 1993; Bonthius et al., 1995), suggesting uniform activation of neurons. However in this study, in 2 of 6 animals, 5 minute-cortical application of KCl that is sufficient to trigger cortical spreading depression (Kraig et al., 1991; Herdegen et al., 1993) induced Hsp27 expression in clusters of astrocytes in layer II and III or in most astrocytes of layers I -III of the parietal cortex. This lower level expression of Hsp27 in these two animals suggested that the signal for Hsp27 expression in astrocytes did not progressively spread through the ipsilateral cortex, but rather appeared in small clusters of astrocytes throughout the superficial layers of the cortex that eventually joined, and recruited astrocytes from deeper cortical layers. It may be that KCl-induced cortical spreading depression has also a heterogeneous effect on neurons undetectable by Fos immunoreactivity.

*Hsp27 functions in astrocytes*

At least three functions for Hsp27 have been reported *in vitro* (see chapter 5). Firstly, Hsp27 has been implicated in the regulation of actin filament dynamics (reviewed by Landry and Huot, 1996). In astrocytes, Hsp27 might participate in the regulation of growth processes that have been shown to involve actin filament dynamics (Baorto et al., 1992). Secondly, Hsp27 has been related to antioxidative mechanisms via an increase in the total levels of glutathione (Mehlen et al., 1996a) that has been reported to be present in glial cells but not in neurons (Slivka et al., 1987; Raps et al., 1989). Finally, Hsp27 prevented protein aggregation and promoted refolding of denatured proteins (Jakob et al., 1993), suggesting that it may act as a molecular chaperone.

*Conclusions*

Whatever the specific role of Hsp27 may be (regulation of antioxidative enzymes, actin filaments or protein folding), it seems that Hsp27 can generally protect cells from injury and facilitate recovery of reversibly injured cells (Landry et al., 1989; Lavoie et al., 1993a; Mehlen et al., 1995). In the brain, this protective role may be even more interesting. After injury, cell-cell interactions may play an important role in the overall survival and function of the brain. In fact, astrocytes *in vitro* have been shown to increase neuronal survival against oxidative stress induced by hydrogen peroxide (Desagher et al., 1996). In the rat brain, cortical spreading depression induces Hsp27 in astrocytes (as shown here) and neuronal protection from ischemic

injury (Kobayashi et al., 1995; Matsushima et al., 1996). I suggest that expression of Hsp27 increases resistance of astrocytes to ischemic injury, maintains normal function of astrocytes during and after ischemic injury, and plays a role, through astrocytes, in neuronal protection. Finally, it may be that neuronal perturbation induces a stress response in the surrounding glia and that these stress-conditioned glia improve neuronal survival after injury.

**CHAPTER 8:**


**GENERAL DISCUSSION**

## Summary of the work

The most important findings of this work are that Hsp70 plays a role in protection of cells in the heart and brain from ischemic injury, that Hsp27 is constitutively expressed in select populations of neurons, and that Hsp27 is induced in cortical astrocytes after ischemia or cortical spreading depression. In addition, it has been shown that ischemic injury in the rat myocardium induces expression of stress genes, including Hsp70, in the ischemic area but not in the necrotic or infarcted area. This Hsp70 mRNA accumulation occurred in several cell types of the ischemic area, including myocytes and endothelial cells. While expression of Hsp70 is induced by mild ischemic injury and oxidative stress, Hsp70 has been suggested to play a protective role after ischemic injury (Currie et al., 1988, 1993) through cellular repair mechanisms. The role of Hsp70 in ischemic protection, was examined in transgenic mice overexpressing the human Hsp70. Following ischemic injury, hearts from Hsp70-transgenic mice had reduced release of creatine kinase indicating less cellular injury and improved myocardial contractile recovery during reperfusion. Since Hsp70 has been suggested to contribute to ischemic protection in the brain (Kirino et al., 1991; Kitagawa et al., 1991; Liu et al., 1992, 1993; Nishi et al., 1993; Simon et al., 1993; Glazier et al., 1994), Hsp70-transgenic mice were tested for resistance to cerebral ischemic injury. Following 24 hour occlusion of the middle cerebral artery, infarct areas were not different between non-transgenic and transgenic mice. However, hippocampal neurons in the Hsp70-transgenic mice were resistant to this ischemia-

related injury. Considerable evidence is accumulating that Hsp27 protects cells against oxidative stress and cell death (Landry et al., 1989; Lavoie et al., 1993a; Mehlen et al., 1995; Huot et al., 1996; Mehlen et al., 1996a, 1996b). Thus, a substantial part of this work explored the expression of Hsp27 in the brain. While Hsp27 was not present in the cerebral cortex of normal rats, surprisingly, it was constitutively expressed, often at high levels, in select populations of neurons of the brain stem and the spinal cord. Cortical focal ischemic injury induced the expression of Hsp27 in astrocytes throughout the injured cerebral cortex while Hsp70 was expressed only immediately adjacent to the injury. Thus the stress response varied according to cell type and brain region. Finally, the expression of Hsp27 was examined after cortical spreading depression, a known consequence of ischemic injury in the brain. Potassium chloride-induced cortical spreading depression induced expression of Hsp27 in astrocytes of the ipsilateral cortex. Inhibition of neuronal depolarization and cortical spreading depression with MK-801, blocked the astrocytic expression of Hsp27.

**Protection against ischemic injury by Hsp70 and Hsp27**

Cell culture experiments have demonstrated that overexpression of a single Hsp such as Hsp70 or Hsp27 was sufficient to increase cell resistance to several injuries, including heat shock (Landry et al., 1989; Angelidis et al., 1991; Li et al., 1991), oxidative stress (Mehlen et al., 1995; Huot et al., 1996; Mehlen et al., 1996a), stress mimicking ischemic conditions (Williams et al., 1993; Mestril et al., 1994), and TNF-

induced apoptosis (Mehlen et al., 1996b). In this thesis, evidence has been presented to support a role for Hsp70 in protection of cells in the heart and brain. Transgenic mice that were engineered to express constitutively high levels of the human inducible Hsp70 showed improved myocardial contractile recovery after ischemic injury. Similar myocardial protection against ischemic injury was also observed in other strains of Hsp70-transgenic mice (Marber et al., 1995; Radford et al., 1996). These studies suggest that constitutive expression of the inducible Hsp70 played a direct role in the protection of the myocardium from ischemia and reperfusion injury.

In the brain, the transgenic mice overexpressing Hsp70 had significantly less neuronal cell loss in the hippocampus after 24 hour occlusion of the middle cerebral artery as compared to the non-transgenic mice. In this model, the hippocampal neuronal cell loss may be related to the neuronal cell death in the cortex. Ischemia-induced neuronal cell death in the cortex and the subsequent release of glutamate may have triggered excitotoxic injury of the hippocampal neurons. The hippocampal neurons of the Hsp70-transgenic mice were resistant to this ischemia-related and possibly excitotoxic injury. In fact, heat shock has been shown to protect cortical neurons against glutamate excitotoxicity *in vitro* (Lowenstein et al., 1991; Rordorf et al., 1991). Thus, it may be that Hsp70 plays a protective role in ischemia-induced excitotoxicity occurring in the penumbra.

As mentioned above, there is considerable evidence for Hsp27 playing a protective role in injured cells (Landry et al., 1989; Mehlen et al., 1995; Huot et al.,

1996; Mehlen et al., 1996a, 1996b). In the heart, Hsp27 is expressed constitutively at high levels. However, its function is speculative. Hsp27 may contribute to myocardial protection against oxidative injury in the normal heart or *de novo* expression of Hsp27 after heat shock may contribute to the overall myocardial protection against ischemia. Hsp27 phosphorylation is important for cellular protection against oxidative stress (Huot et al., 1995), and may regulate Hsp27 function in ischemic protection. In the present studies, Hsp27 expression following ischemia was examined in the cerebral cortex since there is little or no Hsp27 present normally. After focal ischemia or after induction of cortical spreading depression, Hsp27 was expressed throughout the ipsilateral cerebral cortex, mainly in astrocytes and rarely in neurons. On initial consideration, such astrocytic expression of Hsp27 appears not to be related to protection of neurons during ischemic injury. However, cortical application of potassium chloride and the ensuing cortical spreading depression have been shown to reduce neuronal cell death after ischemic injury (Kobayashi et al., 1995; Matsushima et al., 1996). Together, these results suggest an intriguing possibility. Hsp27 may protect astrocyte function during and after ischemia and through astrocyte-neuron interaction, improve neuronal survival. In fact such a protective effect of astrocytes on the survival of neurons after oxidative injury has been demonstrated *in vitro* in mixed astrocyte-neuron cultures (Desagher et al., 1996). It may be that Hsp27 confers to astrocytes tolerance to ischemic injury and that, by delaying astrocyte injury and the

shut-down of astrocyte functions such as antioxidant activity or glutamate uptake, Hsp27 contributes to the reduction of injurious stress affecting neurons.

## Mechanisms of protection by Hsp70 and Hsp27

While the results of experiments using Hsp70-transgenic mice demonstrated a role for Hsp70 in organ protection against ischemic injury (Marber et al., 1995; Radford et al., 1996; see chapters 3 and 4), the cell types involved in this protective effect have still to be determined. In fact, in the transgenic mice the expression of the exogenous human Hsp70 was regulated by the β-actin promoter and thus the human Hsp70 was constitutively expressed in many cell types, including myocytes, endothelial cells, neurons and glial cells. By comparison with the results from Hsp70 transfection studies in cultured cells (Williams et al., 1993; Mestril et al., 1994), Hsp70 expression in myocytes seems sufficient to protect myocytes from ischemic injury. Since the role of Hsp70 in cellular protection against injury has been observed in numerous cell types, it is likely that expression of Hsp70 in neurons might also have a protective effect against ischemic injury. Although evidence for HSP70 neuronal protection against ischemic injury is still missing, in the present studies as discussed above, Hsp70 was shown to protect hippocampal neurons from the ischemia-related excitotoxicity. All this evidence suggests that Hsp70 can act as an intracellular protective mechanism against ischemic injury in the myocardium and that Hsp70 may function as a protective

mechanism against direct ischemic injury and ischemia-related excitotoxicity in the brain.

Interestingly, Hsp70 expression in other cell types than myocytes and neurons might also contribute to the overall resistance and better functional recovery of the heart and the brain after ischemia. For example, endothelial cells expressed Hsp70 in the ischemic area of the myocardium (see chapter 2) and in the brain (Kinouchi et al., 1993; Lindsberg et al., 1996). In Hsp70-transgenic mice, Hsp70 expression in endothelial cells could increase resistance of endothelial cells to ischemia and oxidative injury and could contribute to the maintenance of the structural integrity of the microvasculature. In this case, injury to myocytes or neurons would be delayed, reduced or even prevented and Hsp70 would protect myocytes and neurons against ischemic injury through indirect mechanisms. Of course, combination of both intracellular and extracellular protective mechanisms maximizes the protection against ischemic injury.

In the cerebral cortex, as discussed above, protection by Hsp27 may involve cooperation of different cell-types since Hsp27 was rarely observed in neurons but was expressed rapidly and at high levels in astrocytes. This expression of Hsp27 in astrocytes is likely to preserve astrocyte function during ischemic injury, and improve astrocyte-neuron interaction that contributes to reduced injury to neurons.

## Intracellular sites of actions of Hsp70 and Hsp27

While Hsp70 expression protects cells against ischemic injury, the site of action and the precise molecular mechanism of how Hsp70 protects cells from injury are still unclear. One suggestion is that Hsp70 plays a role in the renaturation or refolding of denatured, misfolded or aggregated proteins. During ischemic injury with decreased intracellular pH, ATP depletion, and calcium overload, it may be that proteins denature or precipitate and become non-functional and that Hsp70 chaperones these denatured proteins (Figures 1.1 and 1.2). Similarly, Hsp70 may also interact with the cytoskeletal components and prevent collapse of the cytoskeleton following ischemic injury (Ganote and Armstrong 1993; Tsang, 1993). Indeed, heat-induced disruption of the intermediate filaments did not occur in thermotolerant cells (Welch and Mizzen, 1988). Another possibility is that Hsp70, like Hsc70, may facilitate mitochondrial enzyme translocation from the site of translation into the mitochondria (Pfanner et al 1994; Langer and Neupert 1994; Marber et al 1994; Ungermann et al 1994). Increased ability to import newly synthesized protein into the mitochondria may contribute to the recovery of mitochondrial functions after ischemic injury. Whatever the exact mechanism of action of Hsp70 following ischemic injury, the functional state of Hsp70 seems to be important. For example, in the myocardium, while heat shock treatment induced an increase of Hsp70 that lasts for days and even weeks (Currie and White, 1983; Karmazyn et al., 1990), the protective effect of heat shock pre-treatment against ischemia was only detected after 24 hours and was already lost by 40 hours (Currie et

al., 1993). These results suggest that by 40 hours after heat shock, while Hsp70 was present, it may not have been functional. In fact, abundant but unnecessary protein in cells may be sequestered in non-functional form prior to degradation (Feder et al., 1992). On the other hand, in transfection or transgenic experiments, expression of Hsp70 was continuous and the pool of functional Hsp70 was always replenished, giving engineered cells or animals a constant level of ischemic protection.

Similarly to Hsp70, the site and the mechanism of action of Hsp27 in cellular protection are unknown. Hsp27 might participate in protein renaturation (Jakob et al., 1993; Jakob and Buchner, 1994), in cytoskeleton dynamics (Landry and Huot, 1996) and in antioxidant enzyme regulation (Mehlen et al., 1996a).

## Are Hsp70 and Hsp27 the only protective mechanisms?

While it seems clear that Hsp70 plays a fundamental role in the protection of the myocardium and the brain against ischemic injury, it is also clear that cells have other mechanisms to protect themselves from changes in their environment. Other heat shock proteins or any other gene products induced or altered by thermal stress or even ischemic injury are likely to play a role in recovery of organs from metabolic injury. For example, antioxidative enzymes have elevated activity after heat shock treatment (Currie et al., 1988; Karmazyn et al., 1990; Yellon, et al 1992). Hearts showed elevation in catalase activity at 24 and 48 hours after heat shock treatment (Karmazyn et al., 1990). This increased catalase activity corresponded to the time of greatest

recovery of the myocardium from ischemic injury and inhibition of catalase reduced the contractile recovery to control values (Karmazyn et al., 1990; Kingma et al., 1996). In other experiments, elevation of body temperature with amphetamine in pigs resulted in a marked increase in antioxidative enzyme activity of copper/zinc-superoxide dismutase and catalase 48 hours later (Maulik et al., 1994). Thus, antioxidants appear to contribute to hyperthermia-induced myocardial protection.

Increase in the blood supply to the organ is also a possible mechanism of organ protection against ischemic injury. For example, the collateral flow can be increased by either angiogenesis or vasodilation. In fact, modification in vascular resistance and perfusion pressure may contribute to the overall protection against ischemic injury by heat shock treatment (Karmazyn et al., 1990; Currie et al., 1993). Heat shock also decreases neutrophil activation and chemotaxis after ischemia (Stojadinovic et al., 1995) and reduction of neutrophil infiltration has been associated with improvement of myocardial function (Arai et al., 1996; Fukuda et al., 1995; Pabla et al., 1996) and with cerebral protection against ischemia (Connolly et al., 1996; Jiang et al., 1995).

## Endogenous protective mechanisms

Multi-cellular organisms clearly have many ways of recovering from injury. For example, some vertebrates (amphibians) have the ability to regenerate lost appendages, some organs (liver) can replace lost segments, and some cells (epithelium) undergo continual replacement. One general strategy is to replace dead or injured cells

by new functional cells. However, in the heart and in the brain, the functional cells, i.e., the myocytes and the neurons, are post-mitotic and cannot re-enter the cell cycle to replace lost cells. Thus, for post-mitotic cells, the heat shock or stress response may be of paramount importance for survival of the organism to changes in environmental conditions. In the heart and brain there are several strategies to protect against ischemia. Firstly, there are cellular protective mechanisms within myocytes and neurons. These cellular protection mechanisms include synthesis of new proteins, such as Hsps, that will facilitate recovery, or activation or increase in the activity of constitutive enzymes, such as antioxidants. These changes reduce intracellular damage and contribute to a more rapid recovery of cellular function. Secondly, protective mechanisms can originate from cooperation of myocytes or neurons with other cells. For example, increased resistance of the small blood vessels to ischemic injury or up-regulation of other supporting cells, could be an important component of such protective mechanisms. In fact, it may be that both strategies occur simultaneously in order to protect organ function. In this thesis, evidence is provided for the up-regulation of Hsp70 and its contribution to endogenous cellular protection. In addition, expression of Hsp27 after ischemia or spreading depression was localized in astrocytes and not in cortical neurons. Most interesting is the possibility that Hsp27 while upregulated in astrocytes and presumably playing a role in astrocyte function, protects neurons from ischemic injury through cell-cell interactions.

**Future perspectives**

Although strong evidence suggests that Hsp70 is involved in myocardial and cerebral protection against ischemia, additional experiments are required to determine how this protection is achieved. Although transgenic mice constitutively overexpressing the rat or human exogenous Hsp70 showed normal growth and development (Marber et al., 1995; Radford et al.,1996; chapter 3), one cannot rule out the possibility that a long-term effect of Hsp70 expression throughout the life of the animal, including development and adulthood, might radically change the characteristics of the parental strain. For example, in Hsp70-transgenic mice, the constitutive expression of Hsp70 might have had some effects on the overall physiology or anatomy of the transgenic mice such as decrease in normal blood pressure or increase in collateral irrigation. To eliminate these possibilities, the expression of the transgene could be regulated by an inducible promoter rather than a constitutive promoter. Under these conditions, control mice would be the same as transgenic mice but without the induced expression of the transgene. The only technical limitation in such a study of heat shock proteins is to be sure that the inducer of the transgene expression does not also induce a general stress response and the concomitant synthesis of several heat shock proteins.

The role of Hsp27 in the nervous system in normal conditions or after ischemia has still to be determined. In glia, Hsp27 expression could be related to cell division or de-differentiation while in neurons, Hsp27 is more likely involved in cytoskeleton

regulation or protein chaperoning. One way to examine the role of Hsp27 would be to generate transgenic mouse models. Transgenic mice expressing Hsp27 and transgenic mice expressing a non-functional (non-phosphorylatable) mutant Hsp27 could provide insights into Hsp27 function in the normal and ischemic nervous system. Several groups of investigators are attempting to generate such transgenic mice.

A major line of research that remains to be studied is the mechanisms involved in cell-cell interactions in order to increase organ protection against stress such as ischemia. Since endothelial cells represent easy targets for therapeutic drugs, it would be exciting to examine whether endothelial cells could be altered to confer tolerance to ischemic injury in the heart or the brain. An interesting experiment would be to induce phosphorylation of the constitutive Hsp27 in endothelial cells and determine the level of protection after ischemia.

Of course, the ultimate goal is to find ways to induce protective mechanisms against ischemia and other pathological stresses. Understanding how Hsp70 and Hsp27 protect the myocardium and the brain will lead to the development of new strategies for prevention and treatment of myocardial infarction, stroke and other pathological diseases.

BIBLIOGRAPHY

Abe K, Tanzi RE, Kogure K (1991) Induction of HSP70 mRNA after transient ischemia in gerbil brain. *Neurosci Lett* 125: 166-168

Aldes LD (1995) Subcompartmental organization of the ventral (protusor) compartment in the hypoglossal nucleus of the rat. *J Comp Neurol* 353: 89-108

Allen HL, Iversen LL (1990) Phencyclidine, dizocilipine, and cerebrocortical neurons. *Science* 247: 221

Altschuler SM, Bao X, Bieger D, Hopkins DA, Miselis RR (1989) Viscerotopic representation of the upper alimentary tract in the rat: Sensory ganglia and nuclei of the solitary and spinal trigeminal tracts. *J Comp Neurol* 283: 248-268

Altschuler SM, Bao X, Miselis RR (1991) Dendritic architecture of nucleus ambiguus motoneurons projecting to the upper alimentary tract. *J Comp Neurol* 309: 402-414

Altschuler SM, Bao X, Miselis RR (1994) Dendritic architecture of hypoglossal motoneurons projecting to extrinsic tongue musculature in the rat. *J Comp Neurol* 342: 538-550

Andres J, Sharma HS, Knoll R, Stahl J, Sassen LM, Verdouw PD, Schaper W (1993) Expression of heat shock proteins in the normal and stunned porcine myocardium. *Cardiovasc Res* 27: 1421-1429

Angelidis CE, Lazaridis I, Pagoulatos GN (1991) Constitutive expression of heat-shock protein 70 in mammalian cells confers thermotolerance. *Eur J Biochem* 199: 35-39

Aquino DA, Padin C, Perez JM, Peng D, Lyman WD, Chiu F-C (1996) Analysis of glial fibrillary acidic protein, neurofilament protein, actin and heat shock proteins in human fetal brain during the second trimester. *Dev Brain Res* 91: 1-10

Arai M, Lefer DJ, So T, DiPaula A, Aversano T, Becker LC (1996) An anti-CD18 antibody limits infarct size and preserves left ventricular function in dogs with ischemia and 48-hour reperfusion. *J Am Coll Cardiol* 27: 1278-1285

Armstrong JN, Plumier J-CL, Robertson HA, Currie RW (1996) The inducible 70,000 mol. wt heat shock protein is expressed in degenerating dentate hilus and piriform cortex after systemic administration of kainic acid in the rat. *Neuroscience* (in press)

Arrigo A-P (1990) The monovalent ionophore monensin maintains the nuclear localization of the human stress protein hsp28 during heat shock recovery. *J Cell Sci* 96: 419-427

Arrigo A-P, Landry J (1994) Expression and function of the low-molecular-weight heat-shock proteins. In: *The biology of heat shock proteins and molecular chaperones* (Morimoto RI, Tissières A, Georgopoulos C, eds), Cold Spring Harbor, Cold Spring Harbor Laboratory Press, 335-373

Arrigo A-P, Mehlen P (1994) Expression, cellular location and function of low molecular weight heat shock proteins (Hsp20s) during development of the nervous system. In: *Heat shock proteins in the nervous system* (Mayer RJ, Brown IR, eds), San Diego, Academic Press, 145-167

Arrigo A-P, Suhan JP, Welch WJ (1988) Dynamic changes in the structure and intracellular locale of the mammalian low-molecular-weight heat shock protein. *Mol Cell Biol* 8: 5059-5071

Baorto MD, Mellado W, Shelanski ML (1992) Astrocyte process growth induction by actin breakdown. *J Cell Biol* 117: 357-367

Barone FC, Knudsen DJ, Nelson AH, Feuerstein GZ, Willette RN (1993) Mouse strain differences in susceptibility to cerebral ischemia are related to cerebral vascular anatomy. *J Cereb Blood Flow Metab* 13: 683-692

Becker J, Craig EA (1994) Heat-shock proteins as molecular chaperones. *Eur J Biochem* 219: 11-23

Beckmann RP, Mizzen LE, Welch WJ (1990) Interaction of Hsp 70 with newly synthesized proteins: implications for protein folding and assembly. *Science* 248: 850-854

Beers RF, Sizer IW (1952) A spectrophotometric method for measuring the breakdown of hydrogen peroxide by catalase. *J Biol Chem* 195: 133-140

Bennardini F, Wrzosek A, Chiesi M (1992) Alpha B-crystallin in cardiac tissue. Association with actin and desmin filaments. *Circ Res* 71: 288-294

Benndorf R, Haye K, Ryazantsev S, Wieske M, Behlke J, Lutsch G (1994) Phosphorylation and supramolecular organization of murine small heat-shock protein HSP25 abolish its actin polymerization-inhibiting activity. *J Biol Chem* 269: 20780-20784

Berger EM, Woodward MP (1983) Small heat shock proteins in Drosophila may confer thermal tolerance. *Exp Cell Res* 147: 437-442

Bieger D, Hopkins DA (1987) Viscerotopic representation of the upper alimentary tract in the medulla oblongata in the rat: The nucleus ambiguus. *J Comp Neurol* 262: 546-562

Bonthius DJ, Lothman EW, Steward O (1995) The role of extracellular ionic changes in upregulating the mRNA for glial fibrillary acidic protein following spreading depression. *Brain Res* 674: 314-328

Bonthius DJ, Steward O (1993) Induction of cortical spreading depression with potassium chloride upregulates levels of messenger RNA for glial fibrillary acidic protein in cortex and hippocampus: Inhibition by MK-801. *Brain Res* 618: 83-94

Boorstein WR, Ziegelhoffer T, Craig EA (1994) Molecular evolution of the HSP70 multigene family. *J Mol Evol* 38: 1-17

Brand T, Sharma HS, Fleischmann KE, Dunker DJ, McFalls EO, Verdouw PD, Schaper W (1992) Proto-oncogene expression in porcine myocardium subjected to ischemia and reperfusion. *Circ Res* 71: 1351-1360

Bras H, Destombes J, Gogan P, Tyc-Dumont S (1987) The dendrites of single brain-stem motoneurons intracellularly labeled with horseradish peroxidase in the cat.

An ultrastructural analysis of the synaptic covering and the microenvironment. *Neuroscience* 22: 971-981

Brodsky JL (1996) Post-translational protein translocation: Not all hsc70s are created equal. *Trends Biochem Sci* 21: 122-126

Brodsky JL, Hamamoto S, Feldheim D, Schekman R (1993) Reconstitution of protein translocation from solubilized yeast membranes reveals topologically distinct roles for BiP and cytosolic Hsc70. *J Cell Biol* 120: 95-102

Brosnan CF, Battistini L, Gao Y-L, Raine CS, Aquino DA (1996) Heat shock proteins and multiple sclerosis: A review. *J Neuropathol Exp Neurol* 55: 389-402

Brown IR (1983) Hyperthermia induces the synthesis of a heat shock protein by polysomes isolated from the faetal and neonatal mammalian brain. *J Neurochem* 40: 1490-1493

Brown IR, Rush S, Ivy GO (1989) Induction of a heat shock gene at the site of tissue injury in the rat brain. *Neuron* 2: 1559-1564

Brown RHJr (1995) Superoxide dismutase in familial amyolotrophic lateral sclerosis: Model for gain of function. *Curr Opin Neurobiol* 5: 841-846

Buzin CH, Bournias-Vardiabasis N (1982) Teratogens induce a subset of small heat shock proteins in Drosophila primary embryonic cell cultures. *Proc Natl Acad Sci USA* 81: 4075-4079

Chappell TG, Konforti BB, Schmid SL, Rothman JE (1987) The ATPase core of a clathrin uncoating protein. *J Biol Chem* 262: 746-751

Chappell TG, Welch WJ, Schlossmann DM, Palter KB, Schlesinger MJ, Rothman JE (1986) Uncoating ATPase is a member of the 70 kilodalton family of stress proteins. *Cell* 45: 3-13

Chen J, Graham SH, Zhu RL, Simon RP (1996) Stress proteins and tolerance to focal cerebral ischemia. *J Cereb Blood Flow Metab* 16: 566-577

Cheney CM, Shearn A (1983) Developmental regulation of Drosophila imaginal disc proteins: synthesis of a heat shock protein under non-heat-shock conditions. *Dev Biol* 95: 325-330

Chiang H-L, Terlecky SR, Plant CP, Dice JF (1989) A role for a 70-kilodalton heat shock protein in lysosomal degradation of intracellular proteins. *Science* 246: 382-385.

Chirico WJ, Waters MG, Blobel G (1988) 70K heat shock related proteins stimulate protein translocation into microsomes. *Nature* 332: 805-810

Chiu R, Boyle WJ, Meek, J, Smeal T, Hunter T, Karin M (1988) The c-Fos protein interacts with c-Jun/AP-1 to stimulate transcription of AP-1 responsive genes. *Cell* 54: 541-552

Chopp M, Chen H, Ho KL, Dereski MO, Brown E, Hetzel FW, Welch KM (1989) Transient hyperthermia protects against subsequent forebrain ischemic cell damage in the rat. *Neurology* 39: 1396-1398

Chrétien P, Landry J (1988) Enhanced constitutive expression of the 27-kDa heat shock proteins in heat-resistant variants from Chinese hamster cells. *J Cell Physiol* 137: 157-166

Ciocca DR, Dams DJ, Edwards DP, Bjercke RJ, McGuire WL (1983) Distribution of an estrogen-induced protein with a molecular weight of 24,000 in normal and malignant tissues and cells. *Cancer Res* 43: 1204-1210

Ciocca DR, Oesterreich S, Chamness GC, McGuire WL, Fuqua SA (1993) Biological and clinical implications of heat shock protein 27,000 (Hsp27): A review. *J Natl Cancer Inst* 85: 1558-1570

Cleveland DW (1996) Neuronal growth and death: Order and disorder in the axoplasm. *Cell* 84: 663-666

Cohen G, Dembiec D, Marcus J (1970) Measurement of catalase activity in tissue extracts. *Analytical Biochem* 34: 30-38

Collard J-F, Côté F, Julien J-P (1995) Defective axonal transport in a transgenic mouse model of amyotrophic lateral sclerosis. *Nature* 375: 61-64

Comelli MC, Guidolin D, Seren MS, Zanoni R, Canella R, Rubini R, Manev H (1993) Time course, localization and pharmacological modulation of immediate early inducible genes, brain-derived neurotrophic factor and trkB messenger RNAs in the rat brain following photochemical stroke. *Neuroscience* 55: 473-490

Connolly ESJr, Winfree CJ, Springer TA, Naka Y, Liao H, Yan SD, Stern DM, Solomon RA, Gutierrez-Ramos JC, Pinsky DJ (1996) Cerebral protection in homozygous null ICAM-1 mice after middle cerebral artery occlusion. Role of neutrophil adhesion in the pathogenesis of stroke. *J Clin Invest* 97: 209-216

Coppo A, Manzi A, Pulitzer JF, Takahashi H (1973) Abortive bacteriophage T4 head assembly in mutants of Escherichia coli. *J Mol Biol* 76: 61-87

Coyle P (1976) Vascular patterns of the rat hippocampal formation. *Exp Neurol* 52: 447-458

Craig EA, Baxter BK, Becker J, Halladay J, Ziegelhoffer T (1994) Cytosolic hsp70s of *Saccharomyces cerevisiae*: Roles in protein synthesis, protein translocation, proteolysis, and regulation. In: *The biology of heat shock proteins and molecular chaperones* (Morimoto RI, Tissières A, Georgopoulos C, eds), Cold Spring Harbor, Cold Spring Harbor Laboratory Press, 31-52

Crête P, Landry J (1990) Induction of HSP27 phosphorylation and thermoresistance in Chinese hamster cells by arsenite, cycloheximide, A23187, and EGTA. *Radiat Res* 121: 320-327

Curran T, Franza BRJr (1988) Fos and Jun: The AP-1 connection. *Cell* 55: 395-397

Curran T, Morgan JI (1995) Fos: An immediate-early transcription factor in neurons. *J Neurobiol* 26: 403-412

Currie RW (1986) Synthesis of stress-induced protein in isolated and perfused rat hearts. *Biochem Cell Biol* 64: 418-426

Currie RW (1987) Effects of ischemia and perfusion temperature on the synthesis of stress-induced (heat shock) proteins in isolated and perfused rat hearts. *J Mol Cell Cardiol* 19: 795-808

Currie RW (1988) Protein synthesis in perfused rat hearts after *in vivo* hyperthermia and *in vitro* cold ischemia. *Biochem Cell Biol* 66: 13-19

Currie RW, Karmazyn M, Kloc M, Mailer K (1988) Heat-shock response is associated with enhanced post-ischemic ventricular recovery. *Circulation Res* 63: 543-549

Currie RW, Sharma VK, Stepkowski SM, Payce RF (1987) Effects of ischaemia and perfusion temperature on the synthesis of stress induced (heat shock) proteins in isolated and perfused rat hearts. *J Mol Cell Cardiol* 19: 795-808

Currie RW, Tanguay RM, Kingma JGJr (1993) Heat-shock response and limitation of tissue necrosis during occlusion/reperfusion in rabbit hearts. *Circulation* 87: 963-971

Currie RW, White FP (1981) Trauma-induced protein in rat tissues: A physiological role for a "heat shock" protein? *Science* 214: 72-73

Das DK, Engelman RM, Kimura Y (1993) Molecular adaptation of cellular defences following preconditioning of the heart by repeated ischaemia. *Cardiovasc Res* 27: 578-584

Das DK, Maulik N, Moraru II (1995) Gene expression in acute myocardial stress. Induction by hypoxia, ischemia, reperfusion, hyperthermia and oxidative stress. *J Mol Cell Cardiol* 27: 181-193

David J-C, Currie RW, Robertson HA (1994) Expression and distribution of Hsp70 and hsc73 messenger RNAs in rat brain following heat shock: Effect of dizocilpine maleate. *Neuroscience* 62: 945-954

228

de Jong WW, Leunissen JA, Voorter CE (1993) Evolution of the alpha-crystallin/small heat-shock protein family. *Mol Biol Evol* 10: 103-126

de Waegh S, Brady ST (1990) Altered slow axonal transport and regeneration in a myelin-deficient mutant mice: The Trembler as an *in vivo* model for schwann cell-axon interactions. *J Neurosci* 10: 1855-1865

DeLuca-Flaherty C, McKay BB, Parham P, Hill BL (1990) Uncoating protein (hsc70) binds a conformationally labile domain of clathrin light chain LCa to stimulate ATP hydrolysis. *Cell* 62: 875-887.

Deng T, Karin M (1993) Jun B differs from c-Jun in its DNA binding and dimerization domains, and represses c-jun by formation of inactive heterodimers. *Gene Dev* 7: 479-490

Desagher S, Glowinski J, Premont J (1996) Astrocytes protect neurons from hydrogen peroxide toxicity. *J Neurosci* 16: 2553-2562

Deshaies RJ, Koch BD, Werner-Washburne M, Craig EA, Schekman R (1988) A subfamily of stress proteins facilitates translocation of secretory and mitochondrial precursor polypeptides. *Nature* 332: 800-805

DiDomenico BJ, Bugaisky GE, Lindquist S (1982) Heat shock and recovery are mediated by different translational mechanisms. *Proc Natl Acad Sci USA* 79: 6181-6185

Dienel GA, Kiessling M, Jacewicz M, Pulsinelli WA (1986) Synthesis of heat shock proteins in rat brain cortex after transient ischemia. *J Cereb Blood Flow Metab* 6: 505-10

Dillmann WH, Mehta HB, Barrieux A, Guth BD, Neeley WE, Ross JJr (1986) Ischemia of the dog heart induces the appearance of a cardiac mRNA coding for a protein with migration characteristics similar to heat-shock/stress protein 71. *Circ Res* 59: 110-114

Dingwall C, Laskey R (1992) The nuclear membrane. *Science* 258: 942-947

Discroll M (1992) Molecular genetics of cell death in the nematode *Caenorhabditis elegans*. *J Neurobiol* 23: 1327-1351

Donnelly TJ, Sievers RE, Vissern FLJ, Welch WJ, Wolfe CL (1992) Heat shock protein induction in rat hearts. A role for improved myocardial salvage after ischemia and reperfusion? *Circulation* 85: 769-778

Dragunow M, Robertson HA (1988) Brain injury induces c-fos protein(s) in nerve and glial-like cells in adult mammalian brain. *Brain Res* 455: 295-299

Estus S, Zaks WJ, Frereman RS, Gruda M, Bravo R, Johnson EM (1994) Altered gene expression in neurons during programmed cell death: Identification of *c-jun* as necessary for neuronal apoptosis. *J Cell Biol* 127: 1717-1727

Everitt BJ, Meister B, Hökfelt T, Melander T, Terenius L, Rökaeus A, Theodorsson-Norheim E, Dockray G, Edwardson J, Cuello C, Elde R, Goldstein M, Hemmings H, Ouimet C, Walaas I, Greengard P, Vale W, Weber E, Wu J-Y, Chang K-J (1986) The hypothalamic arcuate nucleus-median eminence complex: Immunohistochemistry of transmitters, peptides and DARPP-32 with reference to coexistence in dopamine neurons. *Brain Res Rev* 11: 97-155

Ewing JF, Haber SN, Maines MD (1992) Normal and heat-induced patterns of expression of heme oxygenase-1 (Hsp32) in rat brain: Hyperthermia causes rapid induction of mRNA and protein. *J Neurochem* 58: 1140-1149

Fath KR, Lasek RJ (1988) Two classes of actin microfilaments are associated with the inner cytoskeleton of axons. *J Cell Biol* 107: 613-621

Feder JH, Rossi JM, Solomon J, Solomon N, Lindquist S (1992) The consequences of expressing hsp70 in Drosophila cells at normal temperatures. *Genes Dev* 6: 1402-1413

Fix AS, Horn JW, Wightman KA, Johnson CA, Long GG, Storts RW, Farber N, Wozniak DF, Olney JW (1993) Neuronal vacuolization and necrosis induced by the noncompetitive N-methyl-D-aspartate (NMDA) antagonist MK(+)801

(dizocilpine maleate): A light and electron microscopic evaluation of the rat retrosplenial cortex. *Exp Neurol* 123: 204-215

Flynn GC, Pohl J, Flocco MT, Rothman JE (1991) Peptide-binding specificity of the molecular chaperone BiP. *Nature* 353: 726-730

Fox EA, Powley TL (1992) Morphology of identified preganglionic neurons in the dorsal motor nucleus of the vagus. *J Comp Neurol* 322: 79-98

Freedman MS, Clarke BD, Cruz TF, Gurd JW, Brown IR (1981) Selective effect of LSD and hyperthermia on the synthesis of synaptic proteins and glycoproteins. *Brain Res* 207: 129-145

Frydman J, Hartl FU (1996) Principles of chaperone-assisted protein folding: Differences between *in vitro* and *in vivo* mechanisms. *Science* 272: 1497-1502

Fukuda H, Sawa Y, Kadoba K, Taniguchi K, Shimazaki Y, Matsuda H (1995) Supplement of nitric oxide attenuates neutrophil-mediated reperfusion injury. *Circulation* 92: II413-II416

Fuqua SA, Blum-Salingaros M, McGuire WL (1989) Induction of the estrogen-regulated "24K" protein by heat shock. *Cancer Res* 49: 4126-4129

Gagliardini V, Fernandez P-A, Lee RKK, Drexler HCA, Rotello RJ, Fishman MC, Yuan J (1994) Prevention of vertebrate neuronal death by the *crmA* gene. *Science* 263: 826-828

Ganote C, Armstrong S (1993) Ischaemia and the myocyte cytoskeleton: Review and speculation. *Cardiovasc Res* 27: 1387-1403

Gass P, Prior P, Kiessling M (1995) Correlation between seizure intensity and stress protein expression after limbic epilepsy in the rat brain. *Neuroscience* 65: 27-36

Georgopoulos CP, Hendrix RW, Casjens SR, Kaiser AD (1973) Host participation in bacteriophage lambda head assembly. *J Mol Biol* 76: 45-60

Gernold M, Knauf U, Gaestel M, Stahl J, Kloetzel P-M (1993) Development and tissue-specific distribution of mouse small heat shock protein hsp25. *Dev Genet* 14: 103-111

Ginsberg SD, Martin LJ, Rothstein JD (1995) Regional deafferentation down-regulates subtypes of glutamate transporter proteins. *J Neurochem* 65: 2800-2803

Glaser RL, Wolfner MF, Lis JT (1986) Spatial and temporal pattern of hsp26 expression during normal development. *EMBO J* 5: 747-754

Glazier SS, O'Rourke DM, Graham DI, Welsh FA (1994) Induction of ischemic tolerance following brief focal ischemia in rat brain. *J Cereb Blood Flow Metab* 14: 545-553

Gonzalez MF, Lowenstein D, Fernyak S, Hisanaga K, Simon R, Sharp FR (1991) Induction of heat shock protein 72-like immunoreactivity in the hippocampal formation following transient global ischemia. *Brain Res Bull* 26: 241-250

Gonzalez MF, Shiraishi K, Kisanaga K, Sagar SM, Mandabach M, Sharp FR (1989) Heat shock proteins as markers of neural injury. *Mol Brain Res* 6: 93-100

Graeme RG, Cairns J, Bee Ng S, Tan YH (1993) Inactivation of a Redox-sensitive phosphatase during the early events of tumor necrosis factor/interleukin-1 signal transduction. *J Biol Chem* 268: 2141-2148

Grant G (1965) Degenerative changes in dendrites following axonal transection. *Experientia* 21: 722-723

Haas IG, Wabl M (1983) Immunoglobulin heavy chain binding protein. *Nature* 306: 387-389

Ham J, Babij C, Whitfield J, Pfarr CM, Lallemand D, Yaniv M, Rubin LL (1995) A c-jun dominant negative mutant protects sympathetic neurons against programmed cell death. *Neuron* 14: 927-939

Handler AM (1982) Ecdysteroid titers during pupal and adult development in Drosophila melanogaster. *Dev Biol* 93: 73-82

Hartl FU (1996) Molecular chaperones in cellular protein folding. *Nature* 381: 571-580

Hass C, Klein U, Kloetzel P-M (1990) Developmental expression of Drosophila melanogaster small heat shock proteins. *J Cell Sci* 96: 413-418

Head MW, Corbin E, Goldman JE (1993) Overexpression and abnormal modification of the stress proteins αB-crystallin and Hsp27 in Alexander disease. *Am J Pathol* 143: 1743-1753

Head MW, Corbin E, Goldman JE (1994) Coordinate and independent regulation of αB-crystallin and HSP27 expression in response to physiological stress. *J Cell Physiol* 159: 41-50

Heads RJ, Latchman DS, Yellon DM (1994) Stable high level expression of a transfected human HSP70 gene protects a heart-derived muscle cell line against thermal stress. *J Mol Cell Cardiol* 26: 695-699

Herdegen T, Sandkuhler J, Gass P, Kiessling M, Bravo R, Zimmermann M (1993) JUN, FOS, KROX, and CREB transcription factor proteins in the rat cortex: Basal expression and induction by spreading depression and epileptic seizures. *J Comp Neurol* 333: 271-288

Herrera DG, Cuello AC (1992) MK-801 affects the potassium-induced increase of glial fibrillary acidic protein immunoreactivity in rat brain. *Brain Res* 598: 286-293

Herrera DG, Robertson HA (1989) Unilateral induction of c-fos protein in cortex following cortical devascularization. *Brain Res* 503: 205-213

Herrera DG, Robertson HA (1990) Application of potassium chloride to the brain surface induces the c-fos proto-oncogene: Reversal by MK-801. *Brain Res* 510: 166-170

Hightower LE (1980) Cultured animal cells exposed to amino acid analogues or puromycin rapidly synthesise several polypeptides. *J Cell Physiol* 102: 407-427

Hightower LE, Li T (1994) Structure and function of the mammalian hsp70 family. In: *Heat shock proteins in the nervous system* (Mayer RJ, Brown IR, eds), San Diego, Academic Press, 1-30

Hitotsumatsu T, Iwaki T, Fukui M, Tateishi J (1996) Distinctive immunohistochemical profiles of small heat shock proteins (heat shock protein 27 and alpha B-crystallin) in human brain tumors. *Cancer* 77: 352-361

Höhfeld J, Minami Y, Hartl F-U (1995) Hip, a novel cochaperone involved in the eukaryotic Hsc70/hsp40 reaction cycle. *Cell* 83: 589-598

Hortwiz J (1992) α-crystallin can function as a molecular chaperone. *Proc Natl Acad Sci USA* 89: 10449-10453

Hunt SP, Rossi J (1985) Peptide- and non-peptide-containing unmyelinated primary afferents: The parallel processing of nociceptive information. *Phil Trans R Soc Lond B* 308: 283-289

Huot J, Houle F, Spitz DR, Landry J (1996) Hsp27 phosphorylation-mediated resistance against actin fragmentation and cell death induced oxidative stress. *Cancer Res* 56: 273-279

Huot J, Lambert H, Lavoie JN, Guimond A, Houle F, Landry J (1995) Characterization of 45-kDa/54-kDa Hsp27 kinase, a stress-sensitive kinase which may activate the phosphorylation-dependent protective function of mammalian 27-kDa heat-shock protein Hsp27. *Eur J Biochem* 227: 416-427

Hutter MM, Sievers RE, Barbosa V, Wolfe CL (1994) Heat-shock protein induction in rat hearts: A direct correlation between the amount of heat-shock protein induced and the degree of myocardial protection. *Circulation* 89: 355-360

Ireland RC, Berger E, Sirotkin K, Yund MA, Osterbur D, Fristrom J (1982) Ecdysterone induces the transcription of four heat-shock genes in Drosophila S3 cells and imaginal discs. *Dev Biol* 93: 498-507

Ireland RC, Berger EM (1982) Synthesis of low molecular weight heat shock peptides stimulated by ecdysterone in a cultured Drosophila cell line. *Proc Natl Acad Sci USA* 79: 855-859

Iwaki T, Iwaki A, Tateishi J, Sakaki Y, Goldman JE (1993) αB-crystallin and 27-kd heat shock protein are regulated by stress conditions in the central nervous system and accumulate in Rosenthal fibers. *Am J Pathol* 143: 487-495

Iwaki T, Kume-Iwaki A, Liem RKH, Goldman JE (1989) αB-crystallin is expressed in non-lentillar tissues and accumulates in Alexander's disease brain. *Cell* 57: 71-78

Iwaki T, Kume-Iwaki A, Liem RKH, Goldman JE (1990) Cellular distibution of αB-crystallin in non-lenticular tissues. *J Histochem Cytochem* 38: 31-39

Iwaki T, Wisniewski T, Iwaki A, Corbin E, Tomokane N, Tateishi J, Goldman JE (1992) Accumulation of αB-crystallin in central nervous system glia and neurons in pathologic conditions. *Am J Pathol* 140: 345-356

Jacobs O, Van Bree L, Mailleux P, Zhang F, Schiffmann SN, Halleux P, Albala N, Vanderhaeghen J-J (1994) Homolateral cerebrocortical increase of immediate early gene and neurotransmitter messenger RNAs after minimal cortical lesion: Blockade by N-methyl-D-aspartate antagonist. *Neuroscience* 59: 827-836

Jacquin MF, Semba K, Rhoades RW, Egger MD (1982) Trigeminal primary afferents project bilaterally to dorsal horn and ipsilaterally to cerebellum, reticular formation, and cuneate, solitary, supratrigeminal and vagal nuclei. *Brain Res* 246: 285-291

Jakob U, Buchner J (1994) Assisting spontaneity: The role of Hsp90 and small Hsps as molecular chaperones. *Trends Biochem Sci* 19: 205-211

Jakob U, Gaestel M, Engel K, Buchner J (1993) Small heat shock proteins are molecular chaperones. *J Biol Chem* 268: 1517-1520

Jiang N, Moyle M, Soule HR, Rote WE, Chopp M (1995) Neutrophil inhibitory factor is neuroprotective after focal ischemia in rats. *Ann Neurol* 38: 935-942

Johnson DA, Gautsch JW, Sportsman JR, Elder JH (1984) Improved technique utilizing nonfat dry milk for analysis of proteins and nucleic acids transferred to nitrocellulose. *Gene Anal Tech* 1: 3-8

Kamii H, Kinouchi H, Sharp FR, Koistinaho J, Epstein CJ, Chan PH (1994) Prolonged expression of *hsp70* mRNA following transient focal cerebral ischemia in transgenic mice overexpressing CuZn-superoxide dismutase. *J Cereb Blood Flow Metab* 14: 478-486

Karmazyn M, Mailer K, Currie RW (1990) Acquisition and decay of heat-shock-enhanced post-ischemic ventricular recovery. *Am J Physiol* 259: H424-H431

Kato H, Kogure K, Liu X-H, Araki T, Kato K, Itoyama Y (1995) Immunohistochemical localization of the low molecular weight stress protein Hsp27 following focal cerebral ischemia in the rat. *Brain Res* 679: 1-7

Kato H, Liu Y, Kogure K, Kato K (1994) Induction of 27-kDa heat shock protein following cerebral ischemia in a rat model of ischemic tolerance. *Brain Res* 634: 235-244

Kato M, Herz F, Kato S, Hirano A (1992a) Expression of stress-response (heat-shock) protein 27 in human brain tumors: An immunohistochemical study. *Acta Neuropathol* 83: 420-422

Kato S, Hirano A, Herz F, Ohama E (1993) Comparative study on the expression of stress-response protein (srp) 72, srp27, αB-crystallin and ubiquitin in brain tumours. An immunohistochemical investigation. *Neuropathol Applied Neurobiol* 19: 436-442

Kato S, Hirano A, Umahara T, Kato M, Herz F, Ohama E (1992b) Comparative immunohistochemical study on the expression of αB crystalllin, ubiquitin and stress-response protein 27 in ballooned neurons in various disorders. *Neuropathol Applied Neurobiol* 18: 335-340

Khalid H, Tsutsumi K, Yamashita H, Kishikawa M, Yasunaga A, Shibata S (1995) Expression of the small heat shock protein (hsp) 27 in human astrocytomas correlates with histologic grades and tumor growth fractions. *Cell Mol Neurobiol* 15: 257-268

Kingma JGJr, Simard D, Rouleau JR, Tanguay RM, Currie RW (1996) Contribution of catalase to hyperthermia-mediated cardioprotection after ischemia-reperfusion in rabbits. *Am J Physiol* (in press)

Kinouchi H, Sharp FR, Chan PH, Koistinaho J, Sagar SM, Yoshimoto T (1994) Induction of c-fos, junB, c-jun, and hsp70 mRNA in cortex, thalamus, basal ganglia, and hippocampus following middle cerebral artery occlusion. *J Cereb Blood Flow Metab* 14: 808-817

Kinouchi H, Sharp FR, Koistinaho J, Hicks K, Kamii H, Chan PH (1993) Induction of heat shock Hsp70 mRNA and HSP70 kDa protein in neurons in the 'penumbra' following focal cerebral ischemia in the rat. *Brain Res* 619: 334-338

Kirino T, Tsujita Y, Tamura A (1991) Induced tolerance to ischemia in gerbil hippocampal neurons. *J Cereb Blood Flow Metab* 11: 299-307

Kitagawa K, Matsumoto M, Kuwabara K, Tagaya M, Ohtsuki T, Hata R, Ueda H, Handa N, Kimura K, Kamada T (1991a) 'Ischemic tolerance' phenomenon detected in various brain regions. *Brain Res* 561: 203-211

Kitagawa K, Matsumoto M, Tagaya M, Hata R, Ueda H, Niinobe M, Handa N, Fukunaga R, Kimura K, Mikoshiba K, Kamada T (1990) 'Ischemic tolerance' phenomenon found in the brain. *Brain Res* 528: 21-24

Kitagawa K, Matsumoto M, Tagaya M, Kuwabara K, Hata R, Handa N, Fukunaga R, Kimura K, Kamada T (1991b) Hyperthermia-induced neuronal protection against ischemic injury in gerbils. *J Cereb Blood Flow Metab* 11: 449-452

Klemenz R, Andres A-C, Fröhli E, Schäfer R, Ayoama A (1993) Expression of the murine small heat shock proteins hsp25 and αB-crystallin in the absence of stress. *J Cell Biol* 120: 639-645

Klemenz R, Frohli E, Steiger RH, Schafer R, Aoyama A (1991) Alpha B-crystallin is a small heat shock protein. *Proc Natl Acad Sci USA* 88: 3652-3656

Knowlton AA (1995) The role of heat shock proteins in the heart. *J Mol Cell Cardiol* 27: 121-131

Knowlton AA, Brecher P, Apstein C, Ngoy S, Romo GM (1991) Rapid expression of heat shock protein in the rabbit after brief cardiac ischemia. *J Clin Invest* 87: 139-147

Knyihár E, Csillik B (1977) Regional distribution of acid phosphatase-positive axonal systems in the rat spinal cord and medulla, representing central terminals of cutaneous and visceral nociceptive neurons. *J Neurol Transm* 40: 227-234

Kobayashi S, Harris VA, Welsh FA (1995) Spreading depression induces tolerance of cortical neurons to ischemia in rat brain. *J Cereb Blood Flow Metab* 15: 721-727

Kogure K, Kato H (1993) Altered gene expression in cerebral ischemia. *Stroke* 24: 2121-2127

Kraig RP, Dong LM, Thisted R, Jaeger CB (1991) Spreading depression increases immunohistochemical staining of glial fibrillary acidic protein. *J Neurosci* 11: 2187-2198

Kuznetsov SA, Langford GM, Weiss DG (1992) Actin-dependent organelle movement in squid axoplasm. *Nature* 356: 722-725

Landry J, Chrétien P (1983) Relationship between hyperthermia induced heat shock proteins and thermotolerance in Morris hepatoma cells. *Can J Biochem* 61: 428-437

Landry J, Chrétien P, Lambert H, Hickey E, Weber LA (1989) Heat shock resistance conferred by expression of the human HSP27 gene in rodent cells. *J Cell Biol* 109: 7-15

Landry J, Chrétien P, Laszlo A, Lambert H (1991) Phosphorylation of Hsp27 during development and decay of thermotolerance in Chinese hamster cells. *J Cell Physiol* 147: 93-101

Landry J, Huot J (1995) Modulation of actin dynamics during stress and physiological stimulation by signaling pathway involving p38 map kinase and heat-shock protein 27. *Biochem Cell Biol* 73: 703-707

Landry J, Huot J (1996) Modulation of actin dynamics during stress and physiological stimulation by a signaling pathway involving p38 MAP kinase and heat-shock protein 27. *Biochem Cell Biol* 73: 703-707

Langer T, Neupert W (1994) Chaperoning mitochondrial biogenesis. In: *The biology of heat shock proteins and molecular chaperones* (Morimoto RI, Tissières A, Georgopoulos C, eds), Cold Spring Harbor, Cold Spring Harbor Laboratory Press, pp. 53-83

Lavoie JN, Gingras-Breton G, Tanguay RM, Landry J (1993a) Induction of Chinese hamster HSP27 gene expression in mouse cells confers resistance to heat shock. HSP27 stabilization of the microfilament organization. *J Biol Chem* 268: 3420-3429

Lavoie JN, Hickey E, Weber LA, Landry J (1993b) Modulation of actin microfilament dynamics and fluid phase pinocytosis by phosphorylation of heat shock protein 27. *J Biol Chem* 268: 24210-24214

Lavoie JN, Lambert H, Hickey E, Weber LA, Landry J (1995) Modulation of cellular thermoresistance and actin filament stability accompanies phosphorylation-

induced changes in the oligomeric structure of heat shock protein 27. *Mol Cell Biol* 15: 505-516

Lee MK, Marszalek JR, Cleveland DW (1994) A mutant neurofilament subunit causes massive, selective motor neuron death: Implications for the pathogenesis of human motor neuron disease. *Neuron* 13: 975-988

Li GC, Li LG, Liu YK, Mak JY, Chen LL, Lee WM (1991) Thermal response of rat fibroblasts stably transfected with the human 70-kDa heat shock protein-encoding gene. *Proc Natl Acad Sci USA* 88: 1681-1685

Li GC, Werb Z (1982) Correlation between the synthesis of heat shock proteins and the development of thermotolerance in Chinese hamster fibroblats. *Proc Natl Acad Sci USA* 79: 3918-3922

Lindquist S (1986) The heat-shock response. *Annu Rev Biochem* 55: 1151-1191

Lindsberg PJ, Frerichs KU, Sirén A-L, Hallenbeck JM, Nowak TSJr (1996) Heat-shock protein and C-fos expression in focal microvascular brain damage. *J Cereb Blood Flow Metab* 16: 82-91

Lingenhöhl K, Friauf E (1991) Sensory neurons and motoneurons of the jaw-closing reflex pathway in rats: A combined morphological and physiological study using the intracellular horseradish peroxidase technique. *Exp Brain Res* 83: 385-396

Liu Y, Kato H, Nakata N, Kogure K (1992) Protection of rat hippocampus against ischemic neuronal damage by pre-treatment with sublethal ischemia. *Brain Res* 586: 121-124

Liu Y, Kato H, Nakata N, Kogure K (1993) Temporal profile of heat shock protein 70 synthesis in ischemic tolerance induced by preconditioning ischemia in rat hippocampus. *Neuroscience* 56: 921-927

Longoni S, James P, Chiesi M (1990a) Cardiac alpha-crystallin. I. Isolation and identification. *Mol Cell Biochem* 97: 113-20

240

Longoni S, Lattonen S, Bullock G, Chiesi M (1990b) Cardiac alpha-crystallin. II. Intracellular localization. *Mol Cell Biochem* 97: 121-128

Loomis WF, Wheeler SA (1982) The physiological role of heat-shock proteins in *Dictyostelium*. In: *Heat shock: From bacteria to man* (Schlesinger MJ, Ashburner M, Tissières A, eds), ), Cold Spring Harbor, Cold Spring Harbor Laboratory Press, 353-359

Lowenstein DH, Chan PH, Miles MF (1991) The stress protein response in cultured neurons: Characterization and evidence for a protective role in excitotoxicity. *Neuron* 7: 1053-1060

Lowenstein DH, Simon RP, Sharp FR (1990) The pattern of 72-kDa heat shock protein-like immunoreactivity in the rat brain following flurothyl-induced status epilepticus. *Brain Res* 531: 173-182

Löw-Friedrich I, Weisensee D, Mitrou P, Schoeppe W (1992) Cytokines induce stress protein formation in cultured cardiac myocytes. *Basic Res Cardiol* 87: 12-18

Lowry OH, Rosebrough MJ, Farr AL, Randall RJ (1951) Protein measurement with the Folin phenol reagent. *J Biochem* 193: 265-272

MacMillan V, Judge D, Wiseman A, Settles D, Swain J, Davis J (1993) Mice expressing a bovine basic fibroblast growth factor transgene in the brain show increased resistance to hypoxemic-ischemic cerebral damage. *Stroke* 24: 1735-1739

Mannen H (1960) "Noyau fermé" et "noyau ouvert". Contribution à l'étude cytoarchitectonique du tronc cérébral envisagée du point de vue du mode d'arborisation dendritique. *Arch Ital Biol* 98: 333-350

Manzerra P, Brown IR (1992a) Expression of heat shock genes (hsp70) in the rat spinal cord: Localization of constitutive- and hyperthermia-inducible mRNA species. *J Neurosci Res* 31: 606-615

Manzerra P, Brown IR (1992b) Distribution of constitutive- and hyperthermia-inducible heat shock mRNA species (hsp70) in the Purkinje layer of the rabbit cerebellum. *Neurochem Res* 17: 559-564

Marber MS, Latchman DS, Walker JM, Yellon DM (1993) Cardiac stress protein elevation 24 hours after brief ischemia or heat stress is associated with resistance to myocardial infarction. *Circulation* 88: 1264-1272

Marber MS, Mestril R, Chi SH, Sayen MR, Yellon DM, Dillmann WH (1995) Overexpression of the rat inducible 70-kD heat stress protein in a transgenic mouse increases the resistance of the heart to ischemic injury. *J Clin Invest* 95: 1446-1456

Marber MS, Walker JM, Latchman DS, Yellon DM (1994) Myocardial protection after whole body heat stress in the rabbit is dependent on metabolic substrate and is related to the amount of the inducible 70-kD heat stress protein. *J Clin Invest* 93: 1087-1094

Marin R, Valet JP, Tanguay RM (1993) hsp23 and hsp26 exhibit distinct spatial and temporal patterns of constitutive expression in Drosophila adults. *Dev Genet* 14: 69-77

Marrannes R, Willems R, DePrins E, Wauquier A (1988) Evidence for a role of the N-methyl-D-aspartate (NMDA) receptor in cortical spreading depression in the rat. *Brain Res* 457: 226-240

Mason PJ, Hall LMC, Gausz J (1984) The expression of heat shock genes during normal development in Drosophila melanogaster. *Mol Gen Genet* 194: 73-78

Matsushima K, Hogan MJ, Hakim AM (1996) Cortical spreading depression protects against subsequent focal cerebral ischemia in rats. *J Cereb Blood Flow Metab* 16: 221-226

Maulik N, Wei Z, Liu X, Engelman RM, Rousou JA, Das DK (1994) Improved postischemic ventricular functional recovery by amphetamine is linked with its ability to induce heat shock. *Mol Cell Biochem* 137:17-24

McKay DB, Wilbanks SM, Flaherty KM, Ha J-H, O'Brien MC, Shirvanee LL (1994) Stress-70 proteins and their interaction with nucleotides. In: *The biology of heat shock proteins and molecular chaperones* (Morimoto RI, Tissières A, Georgopoulos C, eds), Cold Spring Harbor, Cold Spring Harbor Laboratory Press, 153-177

Mehlen P, Kretz-Remy C, Préville X, Arrigo A-P (1996a) Human hsp27, Drosophila hsp27 and human αB-crystallin expression-mediated increase in glutathione is essential for the protective activity of these proteins against TNFα-induced cell death. *EMBO J* 15: 2695-2706

Mehlen P, Préville X, Chareyron P, Briolay J, Klementz R, Arrigo A-P (1995) Constitutive expression of human Hsp27, Drosophila Hsp27, or human alpha B-crystallin confer resistance to TNF- and oxidative stress-induced cytotoxicity in stably transfected murine L929 fibroblasts. *J Immunol* 154: 363-74

Mehlen P, Schulze-Osthoff K, Arrigo A-P (1996b) Small stress proteins as novel regulators of apoptosis. Heat shock protein 27 blocks Fas/APO-1- and staurosporine-induced cell death. *J Biol Chem* 271: 16510-16514

Mehta HB, Popovitch BK, Dillman WH (1988) Ischemia induces changes in the level of mRNAs coding for stress protein 71 and creatine kinase M. *Circ Res* 63: 512-517

Merck KB, Groenen PJTA, Voorter CEM, de Haard-Hoekman WA, Horwitz J, Bloemendal H, de Jong WW (1994) Structural and functional similarities of bovine α-crytallin and mouse small heat-shock protein. A family of chaperones. *J Biol Chem* 268: 1046-1052

Mestril R, Chi S-H, Sayen MR, O'Reilly K, Dillmann WH (1994) Expression of inducible stress protein 70 in rat heart myogenic cells confers protection against stimulated ischemia-induced injury. *J Clin Invest* 93: 759-767

Mestril R, Dillmann WH (1995) Heat shock proteins and protection against myocardial ischemia. *J Mol Cell Cardiol* 27: 45-52

Mestril R, Schiller P, Amin J, Klapper H, Ananthan J, Voellmy R (1986) Heat shock and ecdysterone activation of the Drosophila melanogaster hsp23 gene: A sequence element implied in developmental regulation. *EMBO J* 5: 1667-1673

Mezger V, Bensaude O, Morange M (1989) Unusual levels of heat shock element-binding activity in embryonal carcinoma cells. *Mol Cell Biol* 9: 3888-3896

Milano CA, Allen LF, Rockman HA, Dolber PC, McMinn TR, Chien KR, Johnson TD, Bond RA, Lefkowitz RJ (1994) Enhanced myocardial function in transgenic mice overexpressing the ß$_2$-adrenergic receptor. *Science* 264: 582-586

Miron T, Vancompernolle K, Vandekerckhove J, Wilchek M, Geiger B (1991) A 25-kD inhibitor of actin polymerization is a low molecular mass heat-shock protein. *J Cell Biol* 114: 255-261

Miron T, Wilchek M, Geiger B (1988) Characterization of an inhibitor of actin polymerization in vinculin-rich fraction of turkey gizzard smooth muscle. *Eur J Biochem* 178: 543-553

Mitchell HK, Moller G, Petersen NS, Lipps-Sarmento L (1979) Specific protection from phenocopy induction by heat shock. *Dev Genet* 1: 181-192

Morimoto RI (1993) Cells in stress: Transcriptional activation of heat shock genes. *Science* 259: 1409-1410

Morimoto RI, Jurivich DA, Kroeger PE, Mathur SK, Murphy SP, Nakai A, Sarge KD, Abravaya K, Sistonen LT (1994) Regulation of heat shock gene transcription by a family of heat shock factors. In: *The biology of heat shock proteins and molecular chaperones* (Morimoto RI, Tissières A, Georgopoulos C, eds), Cold Spring Harbor, Cold Spring Harbor Laboratory Press, 417-455

Morimoto RI, Sarge KD, Abravaya K (1992) Transcriptional regulation of heat shock genes. *J Biol Chem* 267: 21987-21990

Morimoto RI, Tissières A, Georgopoulos C (1990) The stresss response, function of the proteins, and perspectives. In: *Stress proteins in biology and medicine*

(Morimoto RI, Tissières A, Georgopoulos C, eds), Cold Spring Harbor, Cold Spring Harbor Laboratory Press, 1-36

Myrmel T, McCully JD, Malikin L, Krukenkamp IB, Levitsky S (1994) Heat-shock protein 70 mRNA is induced by anaerobic metabolism in rat hearts. *Circulation* 90: II-299-II-305

Nagy JI, Hunt SP (1983) The termination of primary afferents within the rat dorsal horn: Evidence for rearrangement following capsaicin treatment. *J Comp Neurol* 218: 145-148

Nakai A, Morimoto RI (1993) Characterization of a novel chicken heat shock transcription factor, heat shock factor 3, suggests a new regulatory pathway. *Mol Cell Biol* 13: 1983-1997

Nakata N, Kato H, Kogure K (1993) Inhibition of ischaemic tolerance in the gerbil hippocampus by quercetin and anti-heat shock protein-70 antibody. *NeuroReport* 4: 695-698

Newman DB (1985a) Distinguishing rat brainstem reticulospinal nuclei by their neuronal morphology. I. Medullary nuclei. *J Hirnforsch* 26: 187-226

Newman DB (1985b) Distinguishing rat brainstem reticulospinal nuclei by their neuronal morphology. II. Pontine and mesencephalic nuclei. *J Hirnforsch* 26: 385-418

Ng WA, Grupp IL, Subramaniam A, Robbins J (1991) Cardiac myosin heavy chain mRNA expression and myocardial function in the mouse heart. *Cir Res* 69: 1742-1750

Nilges RG (1944) The arteries of the mammalian cornu ammonis. *J Comp Neurol* 80: 177-190

Nishi S, Taki W, Uemura Y, Higashi T, Kikuchi H, Kudoh H, Satoh M, Nagata K (1993) Ischemic tolerance due to the induction of HSP70 in a rat ischemic recirculation model. *Brain Res* 615: 281-288

Nover L (1991) Inducers of HSP synthesis: Heat shock and chemical stressors. In: *Heat shock response* (Nover L, ed), Florida, CRC Press, 5-40

Nover L, Scharf KD (1984) Synthesis, modification and structural binding of heat-shock proteins in tomato cell cultures. *Eur J Biochem* 139: 303-313

Nowak TSJr (1985) Synthesis of a stress protein following transient ischemia in the gerbil. *J Neurochem* 45: 1635-1641

Nowak TSJr (1990) Protein synthesis and the heart shock/stress response after ischemia. *Cerebrovasc Brain Metab Rev* 2: 345-366

Nowak TSJr (1991) Localization of 70 kDa stress protein mRNA induction in gerbil brain after ischemia. *J Cereb Blood Flow Metab* 11: 432-439

Odutola AK (1976) Cell groupings and Golgi architecture of the hypoglossal nucleus of the rat. *Exp Neurol* 52: 356-371

O'Farrell PH (1975) High resolution two-dimensional electrophoresis of proteins. *J Biol Chem* 250: 4007-4021

Olney JW, Labruyere J, Price MT (1990) Pathological changes induced in cerebrocortical neurons by phencyclidine and related drugs. *Science* 244: 1360-1362

Olney JW, Labruyere J, Wang G, Wozniak DF, Price MT, Sesma MA (1991) NMDA antagonist neurotoxicity: Mechanism and prevention. *Science* 254: 1515-1518

Pabla R, Buda AJ, Flynn DM, Blesse SA, Shin AM, Curtis MJ, Lefer DJ (1996) Nitric oxide attenuates neutrophil-mediated myocardial contractile dysfunction after ischemia and reperfusion. *Circ Res* 78: 65-72

Paul ML, Currie RW, Robertson HA (1995) Priming of a $D_1$ dopamine receptor behavioural response is dissociated from striatal immediate-early gene activity. *Neuroscience* 66: 347-359

Pechan PM (1991) Heat shock proteins and cell proliferation. *FEBS Lett* 280: 1-4.

Pelham HR (1990) The retention signal for soluble proteins of the endoplasmic reticulum. *Trends Biochem Sci* 15: 483-486

Pelham HRB (1986) Speculations on the functions of the major heat shock and glucose regulated proteins. *Cell* 46: 959-961

Pfaller K, Arvidsson J (1988) Central distribution of trigeminal and upper cervical primary afferents in the rat studied by anterograde transport of horseradish peroxidase conjugated to wheat germ agglutinin. *J Comp Neurol* 268: 91-108

Pfanner N, Craig EA, Meijer M (1994) The protein import machinery of the mitochondrial inner membrane. *Trends Biochem Sci* 19: 368-372

Plumier J-CL, Armstrong JN, Landry J, Babity JM, Robertson HA, Currie RW (1996) Expression of the 27,000 mol. wt heat shock protein following kainic acid-induced status epilepticus in the rat. *Neuroscience* (in press)

Plumier J-CL, Currie RW (1996) Heat-shock induced myocardial protection against ischemic injury: A role for Hsp70? *Cell Stress & Chaperones* 1: 13-17

Radford NB, Fina M, Benjamin IJ, Moreadith RW, Graves KH, Zhao P, Gavva S, Wiethoff A, Sherry AD, Malloy CR, Williams RS (1996) Cardioprotective effects of 70-kDa heat shock protein in transgenic mice. *Proc Natl Acad Sci USA* 93: 2339-2342

Raps SP, Lai JCK, Hertz L, Cooper AJL (1989) Glutathione is present in high concentrations in cultured astrocytes but not in cultured neurons. *Brain Res* 493: 398-401

Renhawek K, Bosman GJCGM, de Jong WW (1994) Expression of small heat-shock protein hsp27 in reactive gliosis in Alzheimer disease and other types of dementia. *Acta Neuropathol* 87: 511-519

Riabowol KT, Mizzen LA, Welch WJ (1988) Heat shock is lethal to fibroblasts injected with antibodies against hsp70. *Science* 242: 433-436.

Ribeiro-da-Silva A (1995) Substantia gelatinosa of spinal cord. In: *The Rat Nervous System* (Paxinos G, ed), San Diego, Academic Press, 47-59

Riddihough G, Pelham HRB (1986) Activation of the *Drosophila* hsp27 promoter by heat shock and by ecdysone involves independent and remote regulatory sequences. *EMBO J* 5: 1653-1658

Riddihough G, Pelham HRB (1987) An ecdysone response element in the *Drosophila* hsp27 promoter. *EMBO J* 6: 3729-3734

Ritossa F (1962) A new puffing pattern induced by temperature shock and DNP in *Drosophila*. *Experientia* 18: 571-573

Romanes GJ (1964) The motor nuclei of the spinal cord. *Prog Brain Res* 11: 93-116

Rordorf G, Koroshetz WJ, Bonventre JV (1991) Heat shock protects cultured neurons from glutamate toxicity. *Neuron* 7: 1043-1051

Rosalki SB (1967) An improved procedure for serum creatine phosphokinase determination. *J Lab Clin Med* 69: 696-705

Ryan KR, Jensen RE (1995) Protein translocation across mitochondrial membranes: what a long, strange trip it is. *Cell* 83: 517-519

Sakai K, Akima M, Tsuyama K (1983) Evaluation of the isolated perfused heart of mice, with special reference to vasoconstriction caused by intracoronary acetylcholine. *J Pharmacol Methods* 10: 263-270

Sanchez Y, Parsell DA, Taulien J, Vogel JL, Craig EA, Lindquist S (1993) Genetic evidence for a functional relationship between Hsp104 and Hsp70. *J Bacteriol* 175: 6484-6491

Sarge KD, Park-Sarge OK, Kirby JD, Mayo KE, Morimoto RI (1994) Expression of heat shock factor 2 in mouse testis: Potential role as a regulator of heat-shock protein gene expression during spermatogenesis. *Biol Reprod* 50: 1334-1343

Sarge KD, Zimarino V, Holm K, Wu C, Morimoto RI (1991) Cloning and characterization of two mouse heat shock factors with distinct inducible and constitutive DNA-binding ability. *Gene Dev* 5: 1902-1911

Satoh J-I, Kim SU (1995) Cytokines and growth factors induce Hsp27 phosphorylation in human astrocytes. *J Neuropathol Exp Neurol* 54: 504-512

Schatz G, Dobberstein B (1996) Common principles of protein translocation across membranes. *Science* 271: 1519-1526

Schlesinger MJ, Ashburner M, Tissière A (eds) 1982 Heat shock. From bacteria to man, Cold Spring Harbor, Cold Spring Harbor Press, 440 p

Schuetz TJ, Gallo GJ, Sheldon L, Tempst P, Kingston RE (1991) Isolation for a cDNA for HSF2: Evidence for two heat shock factor genes in humans. *Proc Natl Acad Sci USA* 88: 6911-6915

Schütte J, Viallet J, Nau M, Segal S, Fedorko J, Minna J (1989) *Jun*-B inhibits and *c-fos* stimulates the transforming and trans-activating activities of *c-jun*. *Cell* 59: 987-997

Semba K, Egger MD (1986) The facial "motor" nerve of the rat: Control of vibrissal movement and examination of motor and sensory components. *J Comp Neurol* 247: 144-158

Seymour L, Bezwoda WR, Meyer K, Behr C (1990) Detection of P24 protein in human breast cancer: Influence of receptor status and oestrogen exposure. *Br J Cancer* 61: 886-890

Sharp FR, Butman M, Aardalen K, Nickolenko J, Nakki R, Massa SM, Swanson RA, Sagar SM (1994) Neuronal injury produced by NMDA antagonists can be

detected using heat shock proteins and can be blocked with antipsychotics. *Psychopharmacol Bull* 30: 555-560

Sharp FR, Jasper P, Hall J, Noble L, Sagar SM (1991a) MK-801 and ketamine induce heat shock protein HSP72 in injured neurons in posterior cingulate and retrosplenial cortex. *Ann Neurol* 30: 801-809

Sharp FR, Lowenstein D, Simon R, Hisanaga K (1991b) Heat shock protein Hsp72 induction in cortical and striatal astrocytes and neurons following infarction. *J Cereb Blood Flow Metab* 11: 621-627

Shibanuma M, Kuroki T, Nose K (1992) Cell-cycle dependent phosphorylation of HSP28 by TGF beta 1 and H2O2 in normal mouse osteoblastic cells (MC3T3-E1), but not in their ras-transformants. *Biochem Biophys Res Commun* 187: 1418-1425

Simon RP, Cho H, Gwinn R, Lowenstein DH (1991) The temporal profile of 72-kDa heat-shock protein expression following global ischemia. *J Neurosci* 11: 881-889

Simon RP, Niiro M, Gwinn R (1993) Prior ischemic stress protects against experimental stroke. *Neurosci Lett* 163: 135-7

Sirokin K, Davison N (1982) Developmentally regulated transcription from *Drosophila melanogaster* site 67B. *Dev Biol* 89: 196-210

Sistonen L, Sarge KD, Morimoto RI (1994) Human heat shock factors 1 and 2 are differentially activated and can synergistically induce HSP70 gene transcription. *Mol Cell Biol* 14: 2087-2099

Sistonen L, Sarge KD, Phillips B, Abravaya K, Morimoto RI (1992) Activation of heat shock factor 2 during hemin-induced differentiation of human erythroleukemia cells. *Mol Cell Biol* 12: 4104-4111

Slivka A, Mytilineou C, Cohen G (1987) Histochemical evaluation of glutathione in brain. *Brain Res* 409: 275-284

Steare SE, Yellon DM (1993) The protective effect of heat stress against reperfusion arrhythmias in the rat. *J Mol Cell Cardiol* 25: 1471-1481

Stojadinovic A, Kiang J, Smallridge R, Galloway R, Shea-Donohue T (1995) Induction of heat-shock protein 72 protects against ischemia/reperfusion in rat small intestine. *Gastroenterology* 109: 505-515

Tanguay RM (1989) Localized expression of a small heat shock protein, hsp39, in specific cells of the central nervous system during early embryogenesis in *Drosophila*. *J Cell Biol* 9: 5265-5271

Tanguay RM, Wu Y, Khandjian EW (1993) Tissue-specific expression of heat shock proteins of the mouse in the absence of stress. *Dev Genet* 14: 112-118

Taubes G (1996) Misfolding the way to disease. *Science* 271: 1493-1495

Têtu B, Lacasse B, Bouchard HL, Lagace R, Huot J, Landry J (1992) Prognostic influence of HSP-27 expression in malignant fibrous histiocytoma: A clinicopathological and immunohistochemical study. *Cancer Res* 52: 2325-2328

Thorne SA, Winrow VR, Blake DR (1992) Stress proteins, self defence, and the myocardium. *Br Heart J* 67: 279-280

Tissières A, Mitchell HK, Tracy U (1974) Protein synthesis in salivary glands of *Drosophila melanogaster*. Relation to chromosome puffs. *J Mol Biol* 84: 389-398

Tomoika C, Nishioka K, Kogure K (1993) A comparison of induced-heat-shock protein in neurons destined to survive and those destined to die after transient ischemia in rats. *Brain Res* 612: 216-220

Towbin H, Staeheln T, Gordon J (1979) Electrophoretic transfer of proteins from polyacrylamide gels to nitrocellulose sheets: Procedure and some applications. *Proc Natl Acad Sci USA* 76: 4350-4354

Tsang TC (1993) New model for 70 kDa heat-shock proteins' potential mechanisms of function. *FEBS Lett* 323: 1-3

Ulloa L, Avila J (1996) Involvement of γ and β actin isoforms in mouse neuroblastoma differentiation. *Eur J Neurosci* 8: 1441-1451

Ungermann C, Neupert W, Cyr DM (1994) The role of Hsp70 in conferring unidirectionality on protein translocation into mitochondria. *Science* 266: 1250-1253

Vass K, Berger ML, Nowak TSJr, Welch WJ, Lassmann H (1989) Induction of stress protein HSP70 in nerve cells after status epilepticus in the rat. *Neurosci Lett* 100: 259-264

Vass K, Welch WJ, Nowak TSJr (1988) Localization of 70-kDa stress protein induction in gerbil brain after ischemia. *Acta Neuropathol* (Berlin) 77: 128-135

Vitek MP, Berger EM (1984) Steroid and high-temperature induction of the small heat-shock protein genes in Drosophila. *J Mol Biol* 178: 173-189

Voorter CE, Wintjes L, Bloemendal H, de Jong WW (1992) Relocalization of alpha B-crystallin by heat shock in ovarian carcinoma cells. *FEBS Lett* 309: 111-114

Wan XST, Trojanowski JQ, Gonatas JO, Liu CN (1982) Cytoarchitecture of the extranuclear and commissural dendrites of hypoglossal nucleus neurons as revealed by conjugates of horseradish peroxidase with cholera toxin. *Exp Neurol* 78: 167-175

Watson BD, Dietrich WD, Busto R, Wachtel MS, Ginsberg MD (1984) Induction of reproducible brain infarction by photochemically initiated thrombosis. *Ann Neurol* 17: 497-504

Webster KA, Discher DJ, Bishopric NH (1994) Regulation of fos and jun immediate-early genes by Redox or metabolic stress in cardiac myocytes. *Circ Res* 74: 679-686

Welch WJ (1990) The mammalian stress response: Cell physiology and biochemistry of stress proteins. In: *Stress proteins in biology and medicine* (Morimoto RI, Tissières A, Georgopoulos C, eds), Cold Spring Harbor, Cold Spring Harbor Press, 223-278

Welch WJ (1992) Mammalian stress response: Cell physiology, structure/function of stress proteins, and implications for medicine and disease. *Physiol Rev* 72: 1063-1081

Welch WJ, Feramisco JR (1984) Nuclear and nucleolar localization of the 72,000-dalton heat shock protein in heat-shocked mammalian cells. *J Biol Chem* 259: 4501-4513

Welch WJ, Mizzen LA (1988) Characterization of the thermotolerant cell. II. Effects on the intracellular distribution of heat-shock protein 70, intermediate filaments, and small nuclear ribonucleoprotein complexes. *J Cell Biol* 106: 1117-1130

Welsh FA, Moyer DJ, Harris VA (1992) Regional expression of heat shock protein-70 mRNA and c-fos mRNA following focal ischemia in rat brain. *J Cereb Blood Flow Metab* 12: 204-212

White FP (1980) Differences in protein synthesised *in vivo* and *in vitro* by cells associated with the cerebral microvasculature. A protein synthesised in response to trauma? *Neuroscience* 5: 1793-1799

Wilkinson JM, Pollard I (1993) Immunochemical localization of the 25 kDa heat shock protein in unstressed rats: Possible functional implications. *Anat Rec* 237: 453-457

Williams RS, Thomas JA, Fina M, German Z, Benjamin IJ (1993) Human heat shock protein 70 (Hsp70) protects murine cells from injury during metabolic stress. *J Clin Invest* 92: 503-508

Winter CG, Saotome Y, Levison SW, Hirsh D (1995) A role for ciliary neurotrophic factor as an inducer of reactive gliosis, the glial response to central nervous system injury. *Proc Natl Acad Sci USA* 92: 5865-5869

Wisden W, Morris BJ, Hunt SP (1991) *In situ* hybridization with synthetic DNA probes. In: *Molecular Neurobiology - a practical approach* (Chad J, Wheal H, eds), Oxford, IRL, Vol. 2

Wistow G (1985) Domain structure and evolution in alpha-crystallins and small heat-shock proteins. *FEBS Lett* 181: 1-6

Wong PC, Brochelt DR (1995) Motor neuron disease caused by mutations in superoxide dismutase 1. *Curr Opin Neurol* 8: 294-301

Wu C, Clos J, Giogi G, Haroun RI, Kim S-J, Rabindran SK, Westwood JT, Wisniewski J, Yim G (1994) Structure and regulation of heat shock transcription factor. In: *The biology of heat shock proteins and molecular chaperones* (Morimoto RI, Tissières A, Georgopoulos C, eds), Cold Spring Harbor, Cold Spring Harbor Laboratory Press, 395-416

Xu Z, Dong DL-Y, Cleveland DW (1994) Neuronal intermediate filaments: New progress on an old subject. *Curr Opin Neurobiol* 4: 655-661

Yang G, Chan PH, Chen J, Carlson E, Chen SF, Weinstein P, Epstein CJ, Kamii H (1994) Human copper-zinc superoxide dismutase transgenic mice are highly resistant to reperfusion injury after focal cerebral ischemia. *Stroke* 25: 165-170

Yellon DM, Latchman DS (1992) Stress proteins and myocardial protection. *J Mol Cell Cardiol* 24: 113-124

Yellon DM, Latchman DS, Marber MS (1993) Stress proteins and endogenous route to myocardial protection: Fact or fiction? *Cardiovasc Res* 27: 158-161

Yellon DM, Pasini E, Cargnoni A, Marber MS, Latchman DS, Ferrari R (1992) The protective role of heat stress in the ischaemic and reperfused rabbit myocardium. *J Mol Cell Cardiol* 24: 895-907

Zantema A, Verlaan De Vries M, Maasdam D, Bol S, van der Eb A (1992) Heat shock protein 27 and alpha B-crystallin can form a complex, which dissociates by heat shock. *J Biol Chem* 267: 12936-12941
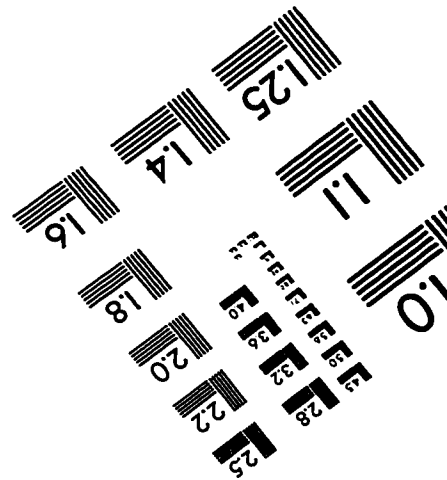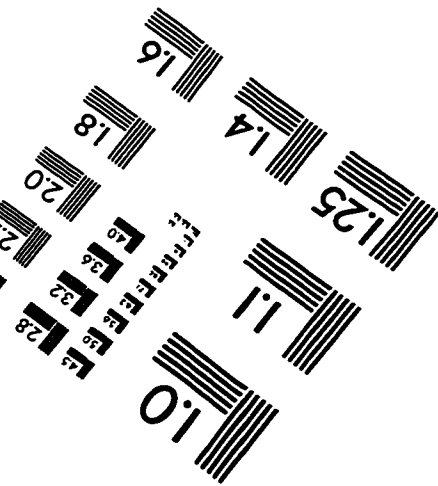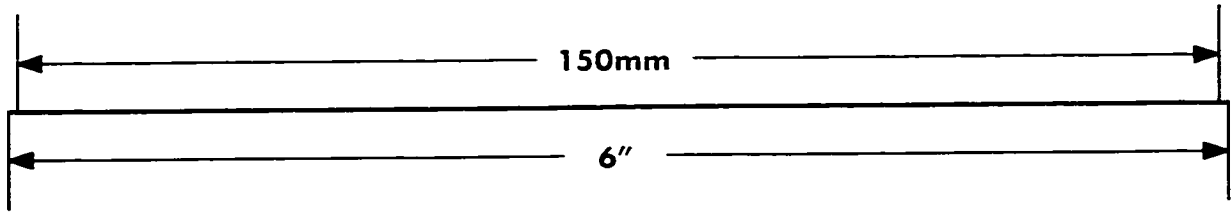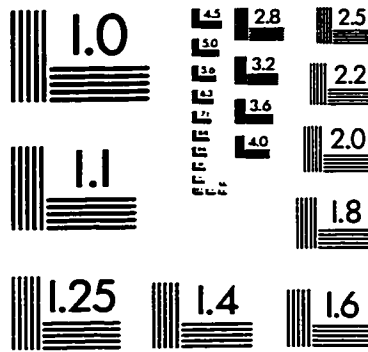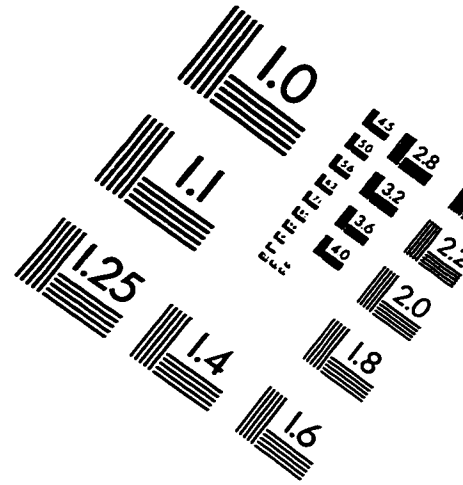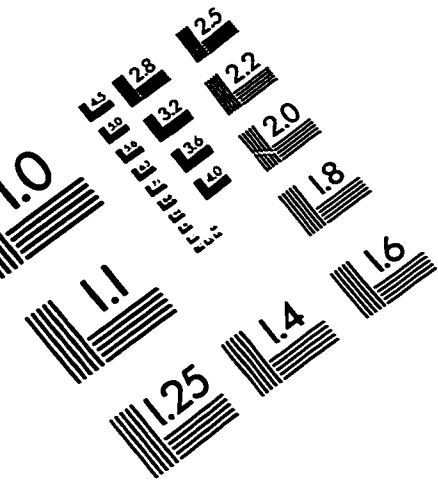
254

Zea Longa E, Weinstein PR, Carlson S, Cummins R (1989) Reversible middle cerebral artery occlusion without craniectomy in rats. *Stroke* 20: 84-91

Zheng JS, Boluyt MO, O'Neill L, Crow MT, Lakatta EG (1994) Extracellular ATP induces immediate-early gene expression but not cellular hypertrophy in neonatal cardiac myocytes. *Circ Res* 74: 1034-1041

Zimmerman JL, Petri W, Meselson M (1983) Accumulation of a specific subset of D. melanogaster heat shock mRNAs in normal development without heat shock. *Cell* 32: 1161-1170

Zimmermann R, Sagstetter M, Lewis MJ, Pelham HRB (1988) Seventy-kilodalton heat-shock proteins and an additional component from reticulocyte lysate stimulate import of M13 procoat protein into microsomes. *EMBO J* 7: 2875-2880

# IMAGE EVALUATION
## TEST TARGET (QA-3)

150mm

6"